



---

REPORT NO. RN-S-0099 (REVISED)

TO  
AEC-NASA SPACE NUCLEAR PROPULSION OFFICE  
PERFORMANCE CHARACTERISTICS OF ETS-1  
NUCLEAR EXHAUST SYSTEM



ROCKET ENGINE OPERATIONS - NUCLEAR

NERVA PROGRAM    OCTOBER 1964    CONTRACT SNP-1

---

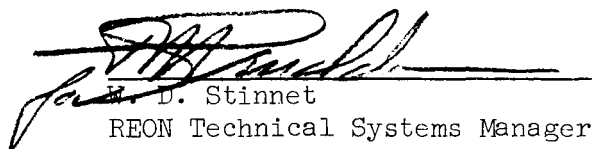
**AEROJET-GENERAL CORPORATION**  
A SUBSIDIARY OF THE GENERAL TIRE & RUBBER COMPANY

ABSTRACT

An ejector system for ETS-1 at NRDS was selected at the completion of the testing and analysis program of CY '63. During the CY '64 program, this selected ejector system was subjected to a series of system performance analysis tests for the purpose of providing an operational map, as well as a high level of confidence in the prediction of operation of the NES at NRDS.

Ejector system performance analysis tests were first conducted with a 1/8 scale model system. The full-scale prediction of performance and operation was made, covering design and off-design operation. This was reported in REON Report RN-S-0099, "Performance Characteristics of ETS-1 Nuclear Exhaust System, June 1964.

A 1/4-scale model ejector system was built and tested to verify the scaling parameters used and, consequently, to increase the confidence level of the performance predictions of the full-scale ejector system. The data was analysed and compared to the 1/8-scale data. Data agreement was considered to be very good in all areas, therefore, there is high confidence in the prediction of performance and operation of the NES at NRDS.

  
H. D. Stinnet  
REON Technical Systems Manager

FOREWORD

This report is presented in partial fulfillment of SNP-1 Contract Task Item 3.1.3, which states in part: "Provide the engineering effort to plan and conduct a 1/4-scale model gas dynamics program to verify the operation of the ETS-1 NES."

## INTRODUCTION

This report is the final presentation of the results of the ejector scale model test program, for Contract Year 1964, as they apply to the full-scale Nuclear Exhaust System (NES) for Engine Test Stand Number One (ETS-1).

Section I of this report is devoted to the presentation of the design, the expected operational performance and the necessary facility requirements as determined by the operation of the NES.

Section II of this report is a presentation of the results of the scale-model test programs and how these results were used to design the NES, to predict its operational performance, and to determine the necessary facility requirements. The major significance of this section is that it presents a comparison of results from identical ejector scale-model test programs carried out for two different scale sizes ( $1/8$  and  $1/4$ ). Comparison of results between these two systems increases the confidence of predictions of performance for the full-scale NES.

This report is one of four reports which define the operation, performance and handling of the ETS-1 NES. The other reports are:

- A. Use and Operational Analysis for NES, REON Report RN-S-0174
- B. Malfunction Analysis for NES, REON Report RN-S-0103
- C. Assembly and Installation Plan of NES Duct at ETS-1, REON Report RN-S-0097.

SYSTEM DESCRIPTION

Figure 1 shows the ejector configuration tested. The ejector system consists of an entrance cone (to station 52.3), a second throat (to station 364.3), a subsonic diffuser (to station 468.1), a 90° elbow, a contraction section, and a secondary safety purge system. The purpose of the secondary safety purge system is to act as an aerodynamic check valve in case of an engine malfunction. Certain types of engine malfunctions would cause an instantaneous stoppage of propellant to the engine which would result in a large pressure differential between the atmosphere and the engine compartment. The pressure differential would cause a flow of air into the ejector, resulting in either an engine-compartment overpressurization or an explosive hydrogen-air mixture in the system. The steam flow from the secondary safety purge system prevents this by maintaining a controlled inert atmosphere.

The engine nozzles tested and reported herein are the 10:1 conical Aerojet nozzle and the 12:1 contoured RN-6 Rocketdyne nozzle. The shape and location of the tested and recommended turbine exhaust nozzles are shown in Figure 2.

The dimensions and tolerances concerned with the location of the XE-1 engine with respect to the ETS-1 duct entrance are:

1. Nozzle exit plane to duct entrance plane  
13  $\pm 0$ " / -4" at minimum distance between planes  
(consistent with plug shield clearance)
2. Nozzle centerline lateral misalignment at nozzle exit plane  
 $\pm 1$ " from duct entrance centerline
3. Nozzle centerline angularity misalignment  
 $\pm 1^\circ$  at the nozzle exit plane, providing tolerance  
No. 2 is not exceeded

Although all 1/8- and 1/4-scale model tests were performed simulating a 9-inch clearance, it is believed that increasing this to a maximum of 13 inches, which is now required for properly installing and removing the engine, will not adversely affect the aerodynamic performance of the ejector system. The degree of aerodynamic stability might be altered but damping functions, such as the large engine compartment volume and seal leakage fluid surrounding the engine working fluid, will probably prevent any noticeable increase in instability.

CONTENTS

	<u>Page</u>
I. FULL-SCALE OPERATION _____	I-1
A. Aerodynamic _____	I-1
B. Heat Transfer _____	I-2
C. Safety Purge _____	I-3
D. Pre-Fire Purge _____	I-5
E. Exhaust Plume _____	I-5
F. Engine Compartment Temperature Survey _____	I-6
II. METHOD AND CONFIDENCE OF PREDICTIONS _____	II-1
A. Aerodynamics _____	II-1
B. Heat Transfer _____	II-6
C. Safety Purge _____	II-8
D. Pre-Fire Purge _____	II-9
E. Engine Compartment Temperature Survey _____	II-9
	<u>Figure</u>
Engine Compartment Pressure vs 10:1 Conical NERVA Nozzle Chamber Pressure _____	I-1
Engine Compartment Pressure vs 12:1 Contoured NERVA Nozzle Chamber Pressure _____	I-2
Ejector Wall Pressure When Testing the 10:1 Nozzle, 40% $P_c$ _____	I-3
Ejector Wall Pressures When Testing the 10:1 Nozzle, 100% $P_c$ _____	I-4
Ejector Wall Pressures When Testing the 12:1 Nozzle, 40% $P_c$ _____	I-5
Ejector Wall Pressures When Testing the 12:1 Nozzle, 100% $P_c$ _____	I-6
Mach Numbers When Testing the 10:1 Nozzle, 40% $P_c$ _____	I-7

CONTENTS (cont.)

	<u>Figure</u>
Mach Numbers When Testing the 10:1 Nozzle, 100% $P_c$ _____	I-8
Mach Numbers When Testing the 12:1 Nozzle, 40% $P_c$ _____	I-9
Mach Numbers When Testing the 12:1 Nozzle, 100% $P_c$ _____	I-10
Nozzle Exit and Engine Compartment Pressures vs Turbine Exhaust Flow Rate When Testing the 10:1 Nozzle, 40% $P_c$ _____	I-11
Nozzle Exit and Engine Compartment Pressure vs Turbine Exhaust Flow Rate When Testing the 10:1 Nozzle, 100% $P_c$ _____	I-12
Nozzle Exit and Engine Compartment Pressures vs Seal Leakage Flow Rate When Testing the 10:1 Nozzle, 40% $P_c$ _____	I-13
Nozzle Exit and Engine Compartment Pressures vs Seal Leakage Flow Rate When Testing the 10:1 Nozzle, 100% $P_c$ _____	I-14
Nozzle Exit and Engine Compartment Pressures vs Turbine Exhaust Flow Rate When Testing the 12:1 Nozzle, 40% $P_c$ _____	I-15
Nozzle Exit and Engine Compartment Pressures vs Turbine Exhaust Flow Rate When Testing the 12:1 Nozzle, 100% _____	I-16
Nozzle Exit and Engine Compartment Pressures vs Seal Leakage Flow Rate When Testing the 12:1 Nozzle, 40% $P_c$ _____	I-17
Nozzle Exit and Engine Compartment Pressure vs Seal Leakage Flow Rate When Testing the 12:1 Nozzle, 100% $P_c$ _____	I-18
Coolant Passage Configuration and Flow Conditions _____	I-19
Gas-Side Heat Transfer Coefficient vs Duct Station _____	I-20
Heat Flux vs Duct Station _____	I-21
Gas-Side Wall Temperature vs Duct Station _____	I-22
Wall Temperature Change vs Duct Station _____	I-23
Liquid-Side Heat Transfer Coefficient vs Duct Station _____	I-24
Coolant Bulk Temperature vs Duct Station _____	I-25
Effect of Off-Design Safety Purge on Starting Pressure _____	I-26

CONTENTS (cont.)

	<u>Figure</u>
Predicted Hydrogen Exhausted Plume Size and Shape _____	I-27
Predicted Maximum Thermal Radiation Flux ( $Q$ , Btu/ft <sup>2</sup> ) from Full-Scale NERVA Exhaust Plume at Selected Locations _____	I-28
Comparison of Performance Between 1/8- and 1/4-Scale Ejector Systems (10/1 Nozzle) _____	II-1
Comparison of Performance Between 1/8- and 1/4-Scale Ejector Systems (12/1 Nozzle) _____	II-2
Pressure Profile, Comparison of 1/8- and 1/4-Scale Data (10:1 Nozzle - 40% $P_c$ ) _____	II-3
Pressure Profile, Comparison of 1/8- and 1/4-Scale Data (10:1 Nozzle - 100% $P_c$ ) _____	II-4
Pressure Profile, Comparison of 1/8- and 1/4-Scale Data (12:1 Nozzle - 40% $P_c$ ) _____	II-5
Pressure Profile, Comparison of 1/8- and 1/4-Scale Data (12:1 Nozzle - 100%) _____	II-6
Mach No. Profile, Comparison of 1/8- and 1/4-Scale Data (10:1 Nozzle - 40% $P_c$ ) _____	II-7
Mach No. Profile, Comparison of 1/8- and 1/4-Scale Data (10:1 Nozzle - 100% $P_c$ ) _____	II-8
Mach No. Profile, Comparison of 1/8- and 1/4-Scale Data (12:1 Nozzle - 40% $P_c$ ) _____	II-9
Mach No. Profile, Comparison of 1/8- and 1/4-Scale Data (12:1 Nozzle - 100% $P_c$ ) _____	II-10
Pressure Tap Locations _____	II-11
Nozzle Exit Pressure vs Turbine Exhaust Flow Rate When Testing the 10/1 Nozzle, 40% $P_c$ _____	II-12
Engine Compartment Pressure vs Turbine Exhaust Flow Rate When Testing the 10/1 Nozzle _____	II-13
Testing the 10/1 Nozzle - 100% $P_c$ _____	II-14



CONTENTS (cont.)

	<u>Figure</u>
Engine Compartment Pressure vs Turbine Exhaust Flow Rate When Testing the 10/1 Nozzle 100% $P_c$ _____	II-15
Nozzle Exit Pressure vs Seal Leakage Flow Rate When Testing the 10/1 Nozzle - 40% $P_c$ _____	II-16
Engine Compartment Pressure vs Seal Leakage Flow Rate When Testing the 10/1 Nozzle - 40% $P_c$ _____	II-17
Nozzle Exit Pressure vs Seal Leakage Flow Rate When Testing the 10/1 Nozzle - 100% $P_c$ _____	II-18
Engine Compartment Pressure vs Seal Leakage Flow Rate When Testing the 10/1 Nozzle - 100% $P_c$ _____	II-19
Nozzle Exit Pressure vs Turbine Exhaust Flow Rate When Testing the 12/1 Nozzle - 40% $P_c$ _____	II-20
Engine Compartment Pressure vs Turbine Exhaust Flow Rate When Testing the 12/1 Nozzle - 40% $P_c$ _____	II-21
Nozzle Exit Pressure vs Seal Leakage Flow Rate When Testing the 12/1 Nozzle - 40% $P_c$ _____	II-22
Engine Compartment Pressure vs Seal Leakage Flow Rate When Testing the 12/1 Nozzle - 40% $P_c$ _____	II-23
Nozzle Exit Pressure vs Seal Leakage Flow Rate When Testing the 12/1 Nozzle - 100% $P_c$ _____	II-24
Engine Compartment Pressure vs Seal Leakage Flow Rate When Testing the 12/1 Nozzle - 100% $P_c$ _____	II-25
Thermocouple Locations _____	II-26
Normalized Heat Transfer Coefficients, Comparison of 1/8- and 1/4-Scale Data _____	II-27
Effect of Chamber Pressure on 1/4-Scale Normalized Heat Transfer Coefficients _____	II-28
Off Design Safety Purge Scale Model Test Data (1/8- and 1/4-Comparison) _____	II-29
Thermocouple Location and Dimensions of 1/4-Scale Engine Compartment _____	II-30

## I. FULL-SCALE OPERATION

### A. AERODYNAMIC

#### 1. Performance

The expected engine compartment pressure when testing the 10:1 area ratio, conical NERVA nozzle in the Nuclear Exhaust System at ETS-1 is shown in Figure I-1. Figure I-2 shows the expected engine compartment pressure when testing the 12:1 area ratio, contoured Rocketdyne (RN-6) nozzle.

#### 2. Wall Pressures and Mach Numbers

The internal wall-pressure profiles are illustrated in the graphs in Figures I-3 through I-6. The internal Mach numbers, based on the pressure profiles and one dimensional flow, are given in Figures I-7 through I-10.

#### 3. Off-Design Turbine Exhaust and Seal Leakage Flow

The effect of various turbine exhaust and seal leakage flow rates on the nozzle exit and the engine compartment pressures are shown in Figures I-11 through I-18. The seal leakage and turbine exhaust flow rates needed to cause flow separation in the nozzle are well above the expected 1.5 lb/sec of  $N_2$  seal leakage and the previously reported values of turbine flow rate. It should be emphasized that flow rates significantly greater than those expected increase the engine compartment pressure and should be avoided.

#### 4. Required Flow Into Engine Compartment

To eliminate inherent instability in the engine compartment pressure just prior to pull in it is necessary that some gas be introduced into the engine compartment during a test firing. If the amount of side shield seal leakage, and actuator bleed is as expected there is no problem. However, there is a possibility of no side shield seal leakage in which case it will be

necessary to add nitrogen to the engine compartment to make the total flow rate of nitrogen at least 1 lb/sec. Since the system can adequately handle this flow plus the expected seal leakage, it is recommended that this gas flow be added.

#### B. HEAT TRANSFER

The full-scale thermal performance of the duct was computed by a steady state, full power heat balance between the hot gas and the coolant. The hot side heat transfer coefficients were obtained by proper scaling of experimental results. The test data obtained from the impingement side of the ejector were assumed to apply completely around the ejector and were used to obtain the full-scale data presented in this report. The hot-gas side resistance will control the heat flux to the duct wall and will determine the required coolant velocity, coolant passage geometry and pressure drop such that safe levels of wall temperature and the desired levels of coolant pressure and outlet temperature will be maintained. The water manifolds are so located that the pressure drop is not excessive and the coolant water does not become saturated. This allows minimum water consumption. The coolant passage configuration, flow conditions, and results of the thermal analysis for full-scale operation are shown in Figures I-19 through I-25.

The design condition for the hot side of the duct wall was assumed to be NERVA engine full power operating conditions. In addition, an engine malfunction condition was considered. This condition results from reactor core "break-up," with resulting small particles of hot, solid material transverse the duct. This added heat flux (in addition to convection from the hot gases) was assumed to be the maximum obtainable; i.e., black-body radiation and all radiant energy emitted falling on the inside surface of the duct (FEFV = 1.0).

The following design limits were used in the heat-balance calculations for the coolant passage design:

1. Maximum wall temperature not to exceed 1150°F during normal operation (stress limit)

2. Maximum design coolant side wall temperature =  $320^{\circ}\text{F}$ . This insures no nucleate boiling in the coolant passage at design pressure. During the malfunction condition, the majority of the duct cooling surface will operate in the nucleate boiling regime; thus this restriction at design allows a margin of safety during the malfunction conditions.

3. Maximum outlet bulk temperature at malfunction conditions =  $180^{\circ}\text{F}$ . This restriction prevents "flashing" at the outlet.

A coolant-passage wall thickness of .095 in. was used throughout the ejector system. This was arrived at for safe operation during normal operating conditions by a stress analysis with input temperatures and temperature gradients obtained from the heat transfer analysis.

Burn-out heat flux is a function of coolant velocity and subcooling. An increase in either or both increases the maximum heat flux attainable with nucleate boiling. The burn-out flux was computed from two different correlations reported in the literature<sup>1,2</sup> and determined to be a factor of two higher than the maximum flux calculated for the assumed malfunction operation. The condition of minimum velocity and subcooling were used for the calculation (exit of Section 1). Therefore, from a thermal standpoint only, the duct will operate satisfactorily during the assumed malfunction condition.

#### C. SAFETY PURGE

The ejector system must, at all times, exhaust the hydrogen gas so that it can be safely disposed of by burning. Air must not be allowed to mix with the hydrogen inside the duct. While the engine is running, the primary ejector accomplishes this separation of air and hydrogen; prior to start-up, the air is replaced by nitrogen from the pre-fire ejector purge system located in the environmental cell. During engine cooldown with hydrogen, the steam flow is maintained to preclude the air.

<sup>1</sup>F. C. Gunther, Transactions of the ASME, 73, (1951).

<sup>2</sup>Louis Bernath, "Predictions of Heat Transfer Burnout," Preprint No. 8, AICHE, Heat-Transfer Symposium, National Meeting, Louisville, Ky, March 1955.

A major malfunction (e.g., rupture of a main propellant or seizure of a turbine) can cause an instantaneous cessation of flow to the engine and, in turn, collapse the established shock structure in the duct. Upon collapse of the shock structure, a large pressure differential exists between the engine compartment ( $P_v \leq 2$  psia) and the atmosphere ( $P_a = 12.8$  psia at NTS). This pressure gradient would force in air, mix it with the residual hydrogen in the duct, and create an explosive mixture. This surge of gas would also cause over-pressurization of the engine compartment and separate the side shields. A secondary purge system is located aft of the elbow to introduce the safety purge fluid. This inert fluid will fill the engine compartment and prevent air from entering the ejector and will prevent over-pressurization in the event of a malfunction, as described.

The required secondary safety-purge fluid for the ejector system is primarily steam, with the following properties:

Ratio of specific heats	1.25
Molecular weight	18-21
Nozzle stagnation pressure	100-115 psia
Nozzle stagnation temperature	1600-1700°R
Flow rate	115-130 lb/sec
Nozzle throat area	119 in. <sup>2</sup>

The secondary safety purge flow rate is equal to the sum of the choked flow rate (97 lb/sec) required to fill the engine compartment without allowing air to enter the ejector in the event of an instantaneous termination of the reactor working fluid, and the flow rate (23 lb/sec) required to prevent penetration of 35-mph air into the ejector (see Section I,C).

As pointed out in the past, the operation of the ejector system, as a whole, is affected to a great degree by the parameters of the secondary safety purge fluid. No analytical or empirical analysis is currently available to predict the effects of purge fluid parameters. Scale-model test data indicates that the secondary purge fluid mass flow rate and the system  $\Omega^*$  are the main influencing parameters.\* During the initial period of startup, or prior

---

\* 
$$\Omega = \frac{(T/m)^{1/2}_{\text{primary}}}{(T/m)^{1/2}_{\text{secondary}}}$$

to pull-in, the secondary mass flow rate exerts a very marked effect on performance. A larger than normal secondary mass flow rate will result in a lower initial value of engine compartment pressure. A smaller than normal mass flow will cause an increase in the engine compartment pressure and, if engine operation is dependent upon compartment pressure, this area might be one of major concern. Reference 1 also indicates that a high value of  $\Omega$  could be injurious to performance during the initial startup transients.

The major effect of  $\Omega$  is felt, however, at the start point of the ejector system, as shown in Figure I-26. An  $\Omega$  value beyond 5.5 will prevent the ejector system from starting. At the start point minor variations in secondary flow rate will not effect the system operation. A large increase in secondary flow will, however, act as an aerodynamic block to the primary flow and could prevent the ejector from starting.

#### D. PRE-FIRE PURGE

The engine compartment and the ejector must be purged with an inert gas prior to operation. The purge gas should be introduced through many orifices, located at the top of the engine compartment and at points where air could possibly be trapped. It is recommended that the purging process take place over at least a 100-sec period to allow thorough mixing to take place. A checkout run at NTS to determine the  $O_2$  content in different locations (corners, thrust structure, etc.) in the engine compartment as a function of pre-fire purge flow duration, is required for safety considerations. The safe  $O_2$  content is 4% or less by volume.

#### E. EXHAUST PLUME

The predicted exhaust plume size and shape, based on test data as well as analysis, is illustrated in Figure I-27, and the predicted thermal radiation from the exhaust plume to proximate surfaces is illustrated in Figure I-28.

---

<sup>1</sup> Experimental Evaluation of Secondary Pumping Systems for ETS-2, REON Report 2680, December 1963.

The accuracy of the predicted flame length is estimated to be +20% and -0%; that is, the flame can be up to 20% longer but it is not expected to be any shorter.

It is estimated that the full-scale thermal radiation from the exhaust plume will not be much higher (within 10%) than the higher values presented in Figure I-28, but it is possible that the radiation flux could be much lower (possibly 50%) than the values presented in Figure I-28.

Temperature rise-time data were calculated for the concrete drainage ditch, floor, walls and the aluminum radiation shields. The analysis and calculations are presented in REON Report RN-S-0168. The temperature rise-time reported is for an uncooled ditch however, it is recognized that the bottom of the ditch will have water in it and therefore concrete damage should be non-existent.

It is recommended that thermocouples, calorimeters and/or radiometers be used to measure the local thermal radiation flux during the checkout and preliminary tests (ambient hydrogen and low-power) at ETS-1. It is recommended to position calorimeters (1) on the south drainage ditch wall (near top of the wall and about 90 ft below duct exit), (2) on the vault door (5  $D_s$  above, and 10  $D_s$  to the side of the duct exit<sup>\*</sup>), and (3) on the superstructure above the concrete vault (in line with centerline of duct and 30 to 60 ft above the vault roof). Data obtained from these preliminary tests would serve as a check in predicting the thermal radiation flux during full power tests.

#### F. ENGINE COMPARTMENT TEMPERATURE SURVEY

An investigation was conducted of the temperature effects of engine assembly radiation and of the effects of possible "spill back" of hydrogen gas on equipment located in the engine compartment. This consisted of monitoring several thermocouples located in the 1/4-scale engine compartment during a low level (40%  $P_c$ ) and high level (100%  $P_c$ ) engine firing. The results of these tests show that the only effects are from thermal radiation from the uncooled test hardware.

<sup>\*</sup> $D_s$  = 4.33 ft = internal diameter of duct exit.

The surface temperature during full-scale engine tests are relatively low; therefore, the heating rates to equipment located in the cell should be relatively low. Consequently, it is believed that no special coolant need be provided to engine instrumentation and other exterior equipment.



NOTES.

1. DIMENSIONS ARE IN INCHES.
2. DIAMETERS ARE INTERNAL

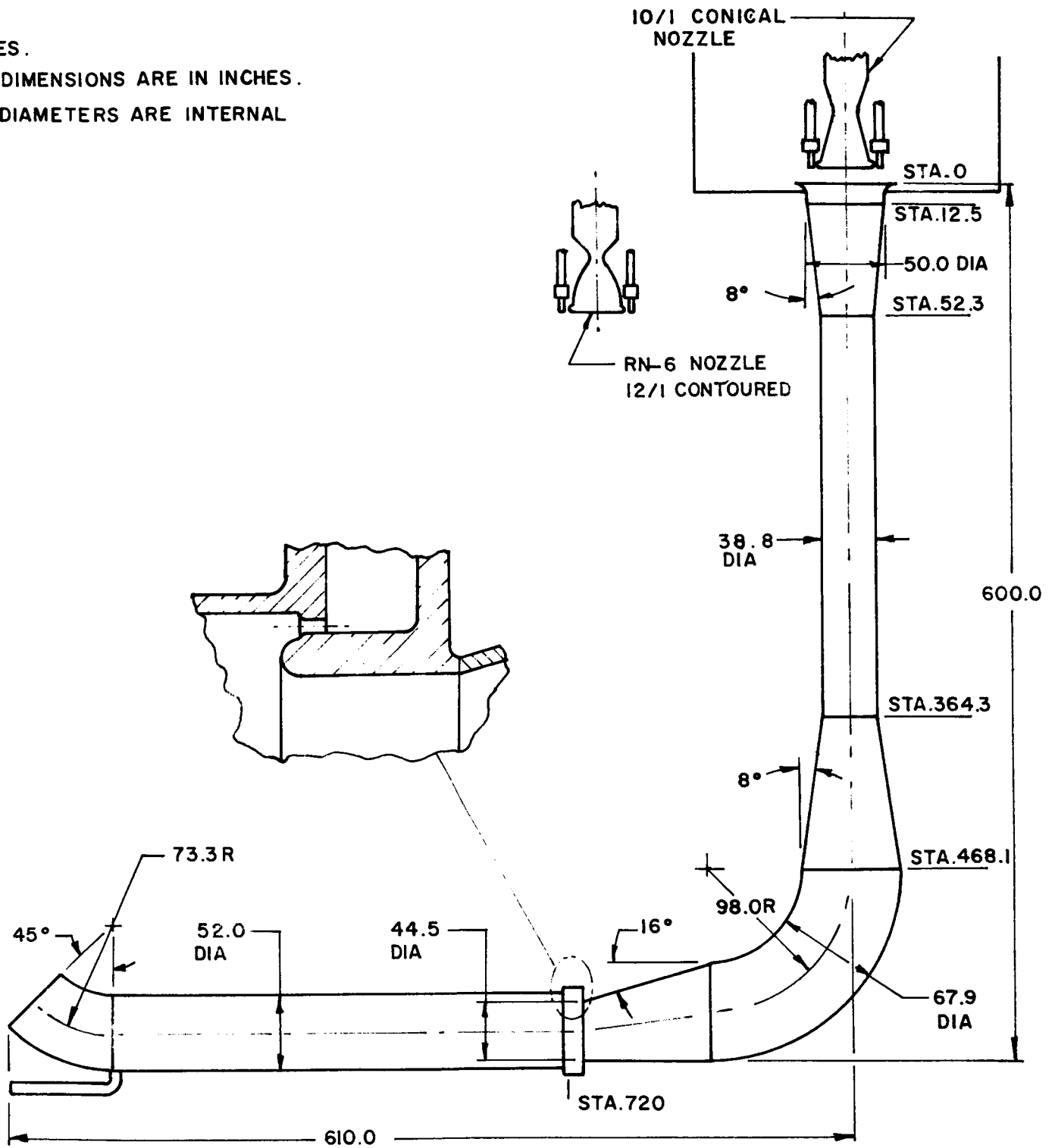


Figure 1

NES Subsonic Turn Ejector  
System for Use at ETS-1

- NOTES. 1. TURBINE EXHAUST FLOW AT DESIGN VALUE  
 2. SAFETY PURGE -  $P_{sc}=100-115$  psia,  $T_{sc}=1600-1700$  °R,  $\dot{W}_s=115-130$  lb/sec,  $\dot{M}_s=18-21$   
 3. SEAL LEAKAGE FLOW = 0-2 lb/sec AMBIENT  $N_2$   
 4.  $P_a = 12.8$  psia

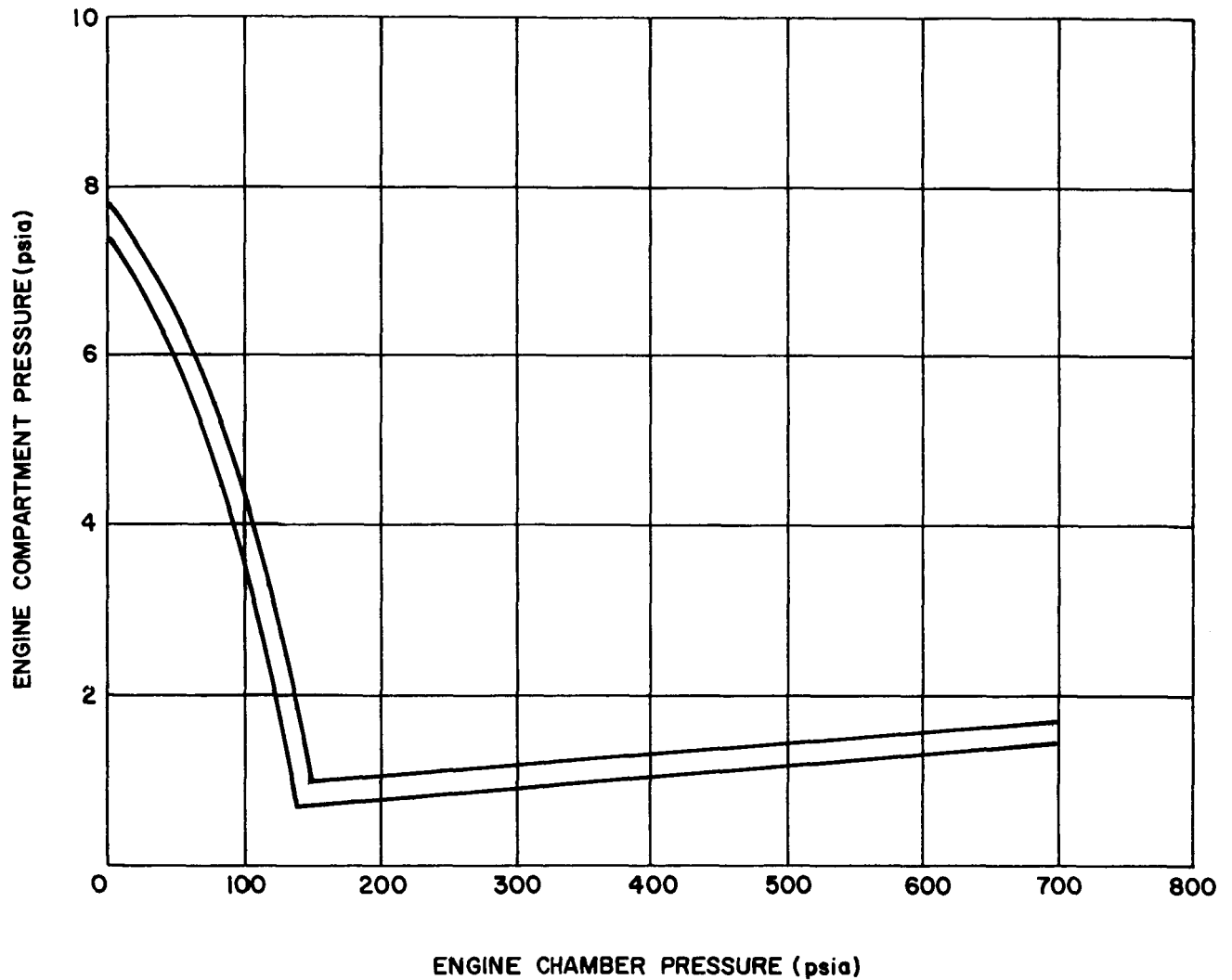


Figure I-1

Engine Compartment Pressure  
 vs 10:1 Conical NERVA Nozzle  
 Chamber Pressure

- NOTES. 1. TURBINE EXHAUST FLOW AT DESIGN VALUE  
 2. SAFETY PURGE -  $P_{sc} = 100 - 115$  psia,  $T_{sc} = 1600 - 1700$  °R,  $\dot{W}_s = 115 - 130$  lb/sec,  $\dot{m}_s = 18 - 21$   
 3. SEAL LEAKAGE FLOW =  $0 - 2$  lb/sec AMBIENT  $N_2$   
 4.  $P_a = 12.8$  psia

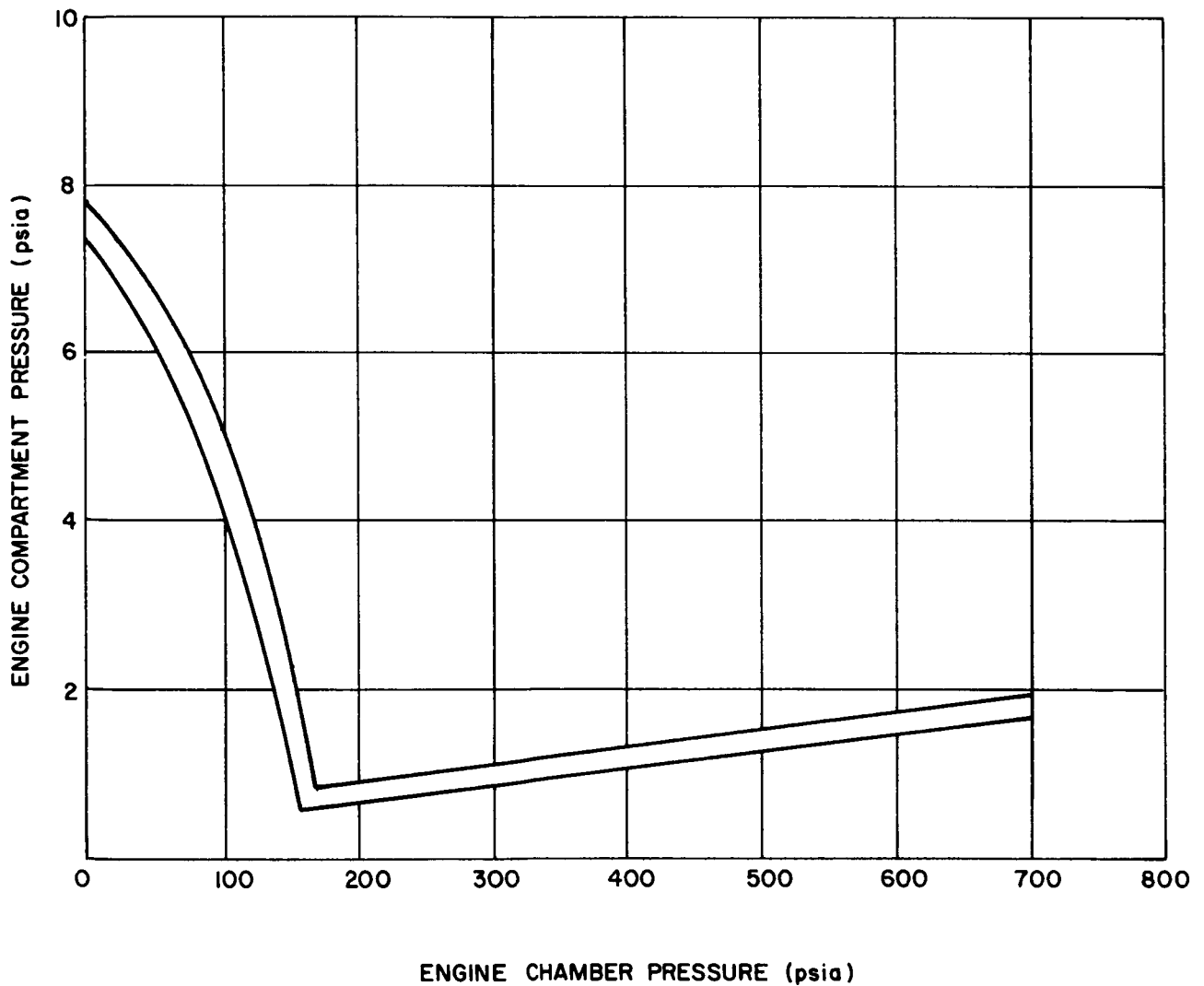


Figure I-2

Engine Compartment Pressure  
 vs 12:1 Contoured NERVA Nozzle  
 Chamber Pressure

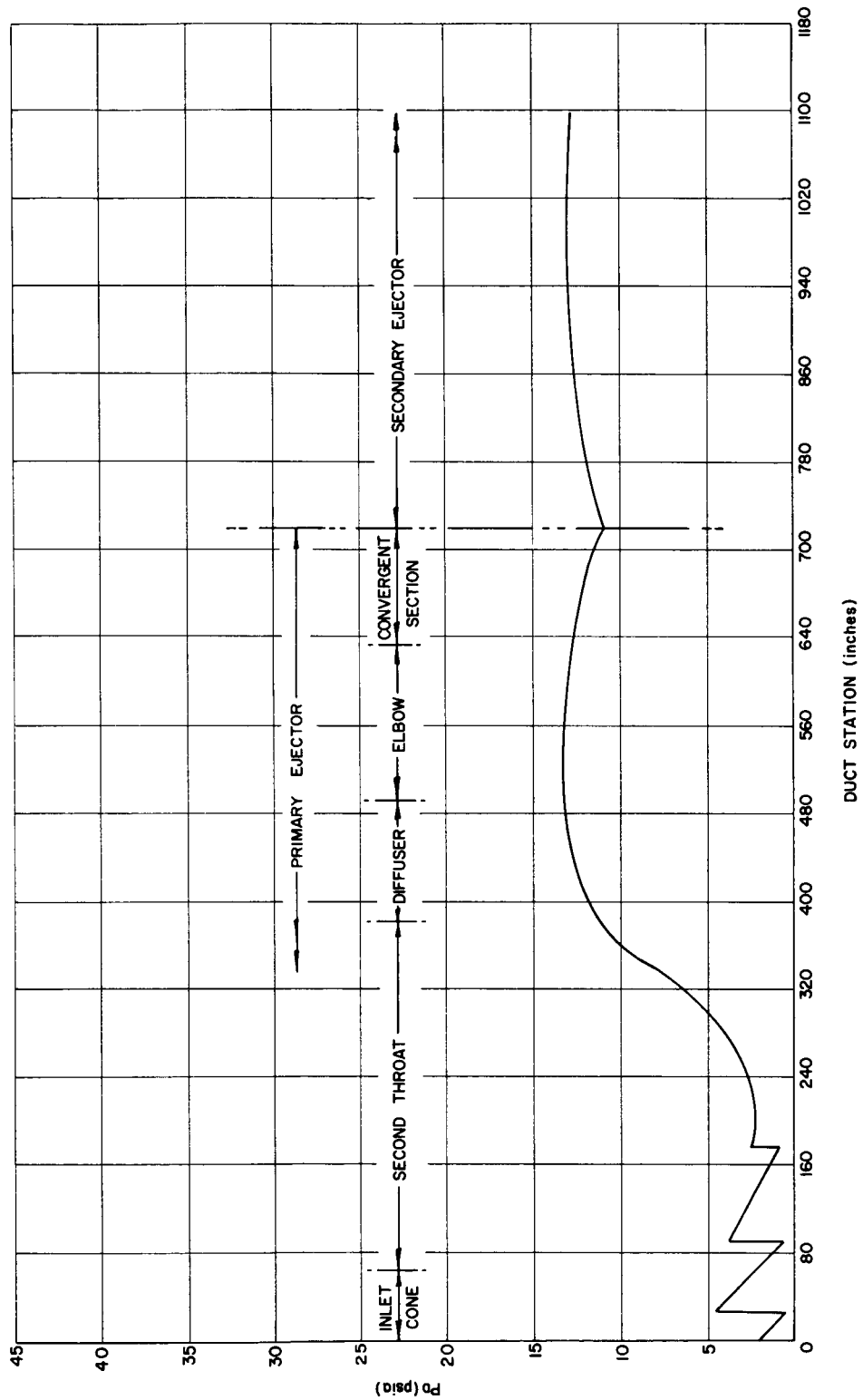


Figure I-3

Ejector Wall Pressures when Test-  
ing the 10:1 Nozzle,  $40\% P_c$

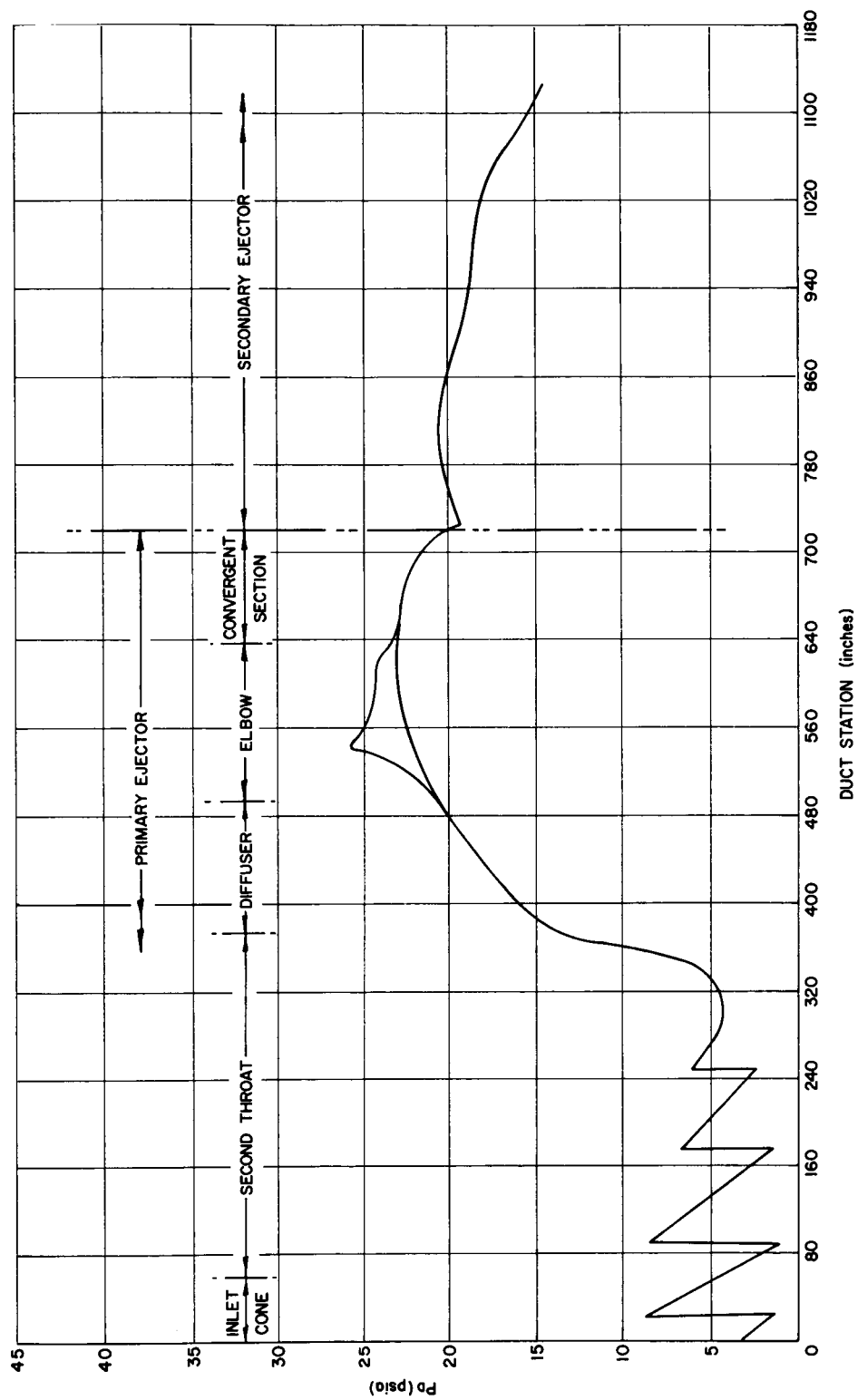


Figure I-4

Ejector Wall Pressures when  
Testing the 10:1 Nozzle, 100%  $P_c$

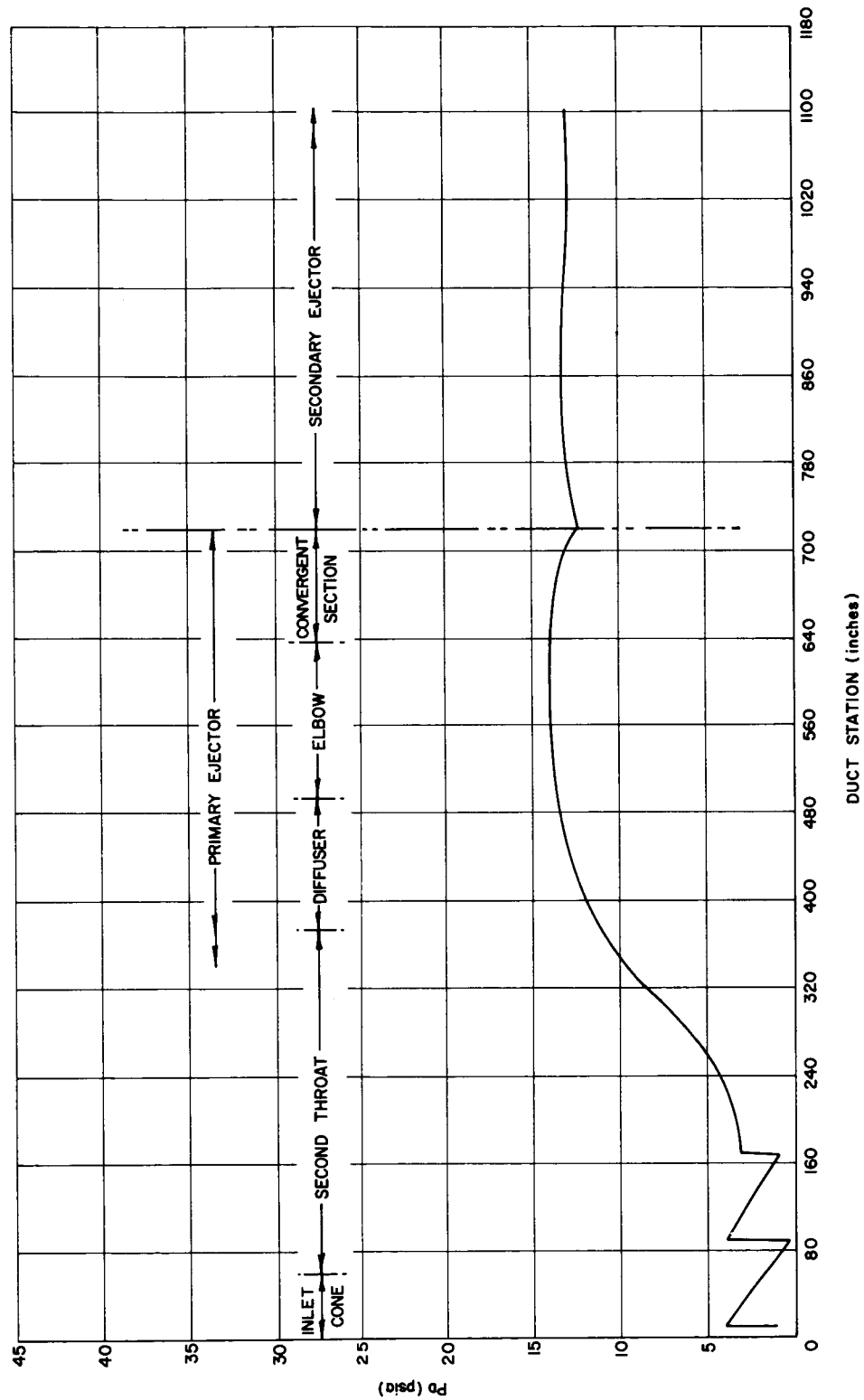


Figure I-5

Ejector Wall Pressures when  
Testing the 12:1 Nozzle, 40%  $P_c$

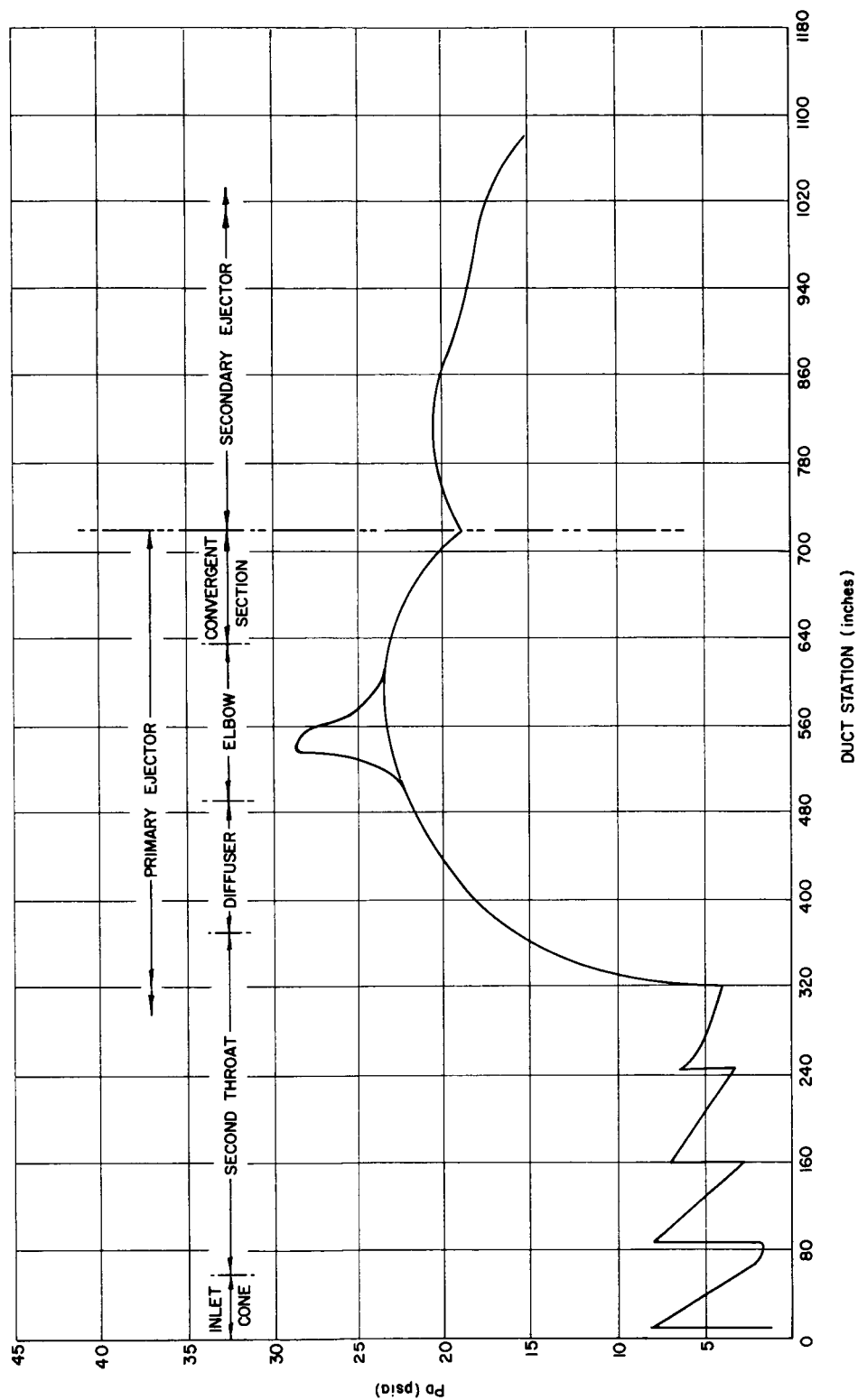


Figure I-6

Ejector Wall Pressures when  
Testing the 12:1 Nozzle, 100%  $P_c$

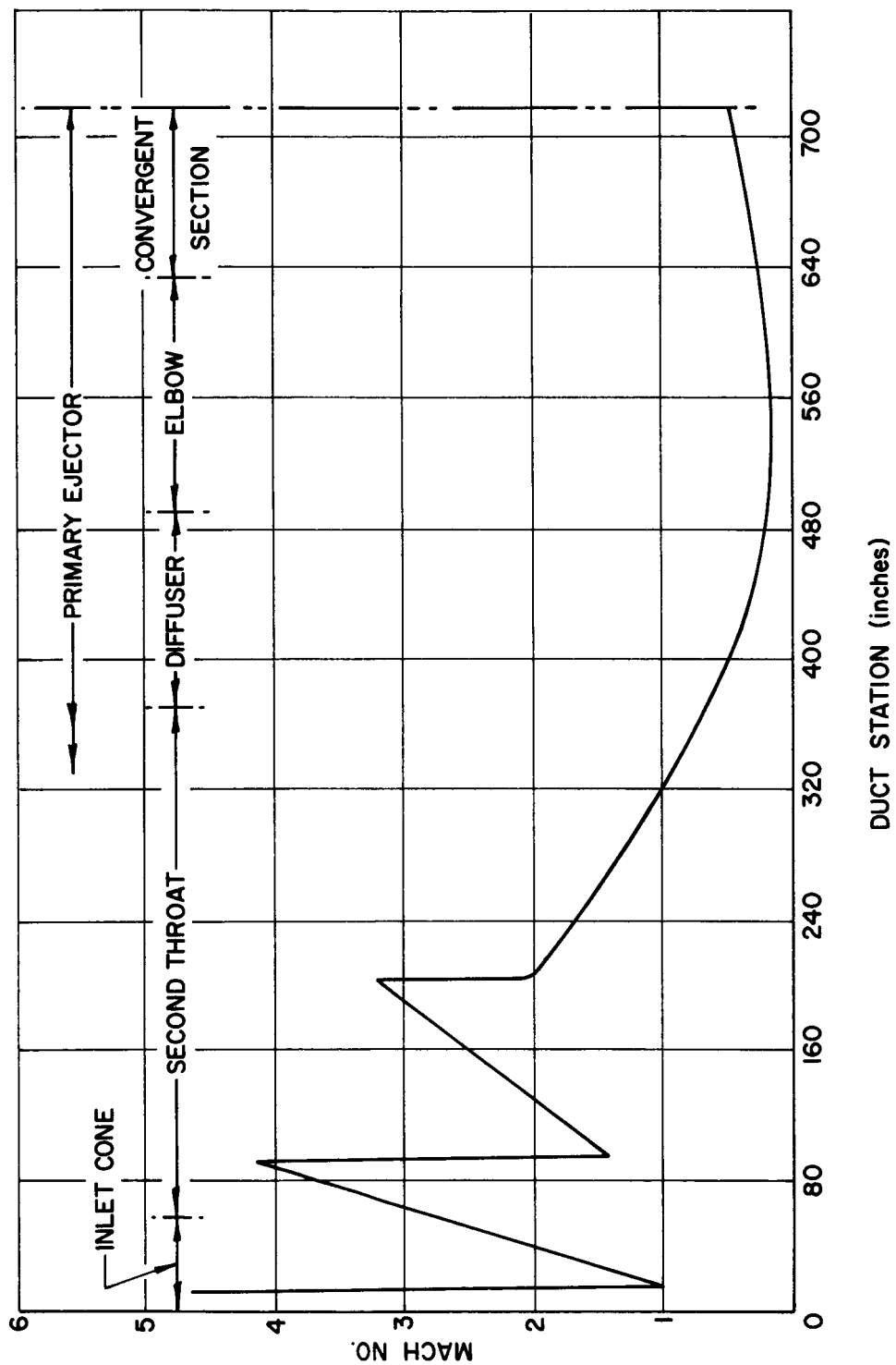


Figure I-7

Mach Numbers when Testing  
the 10:1 Nozzle, 40%  $P_c$



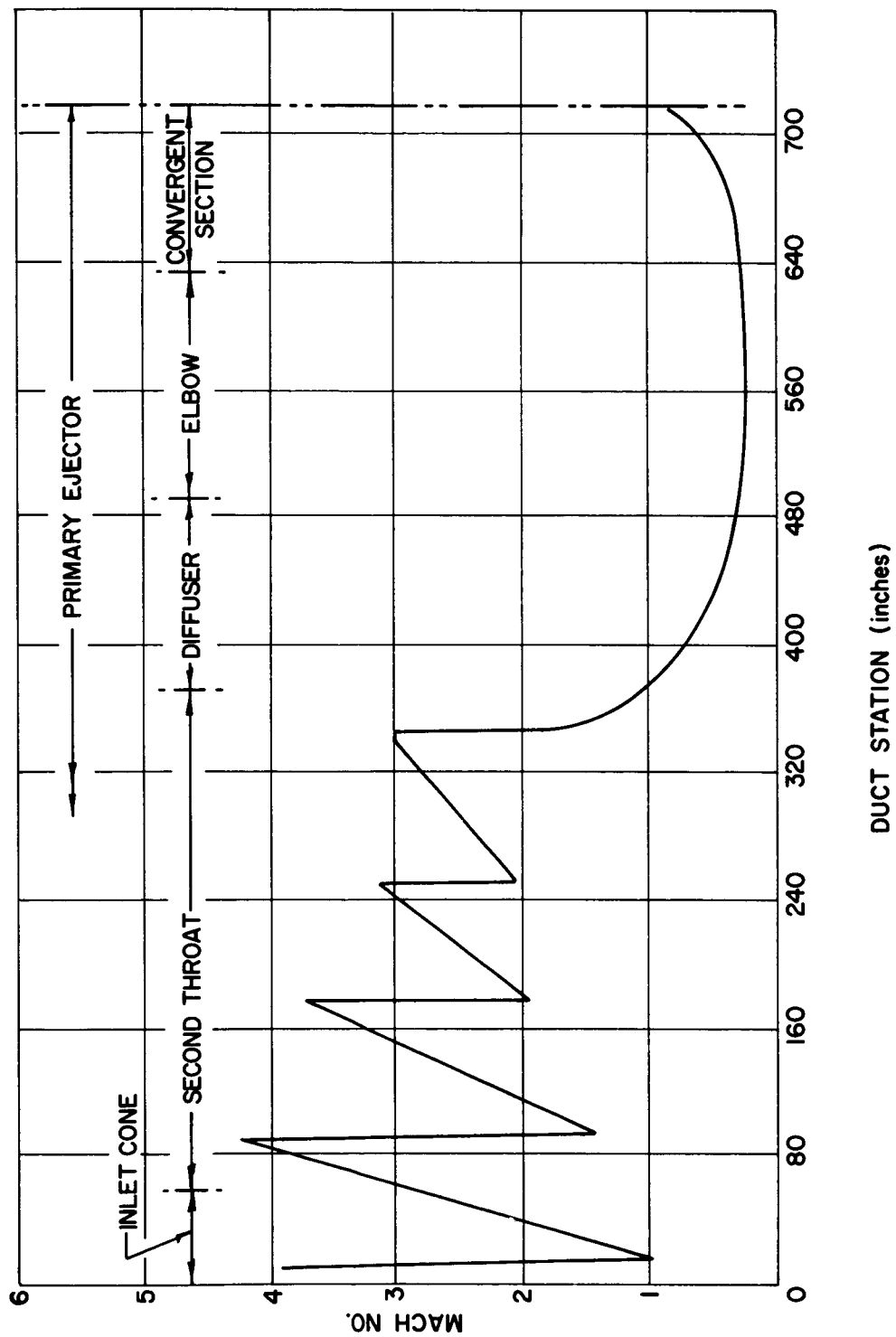


Figure I-8

Mach Numbers when Testing  
the 10:1 Nozzle, 100%  $P_c$

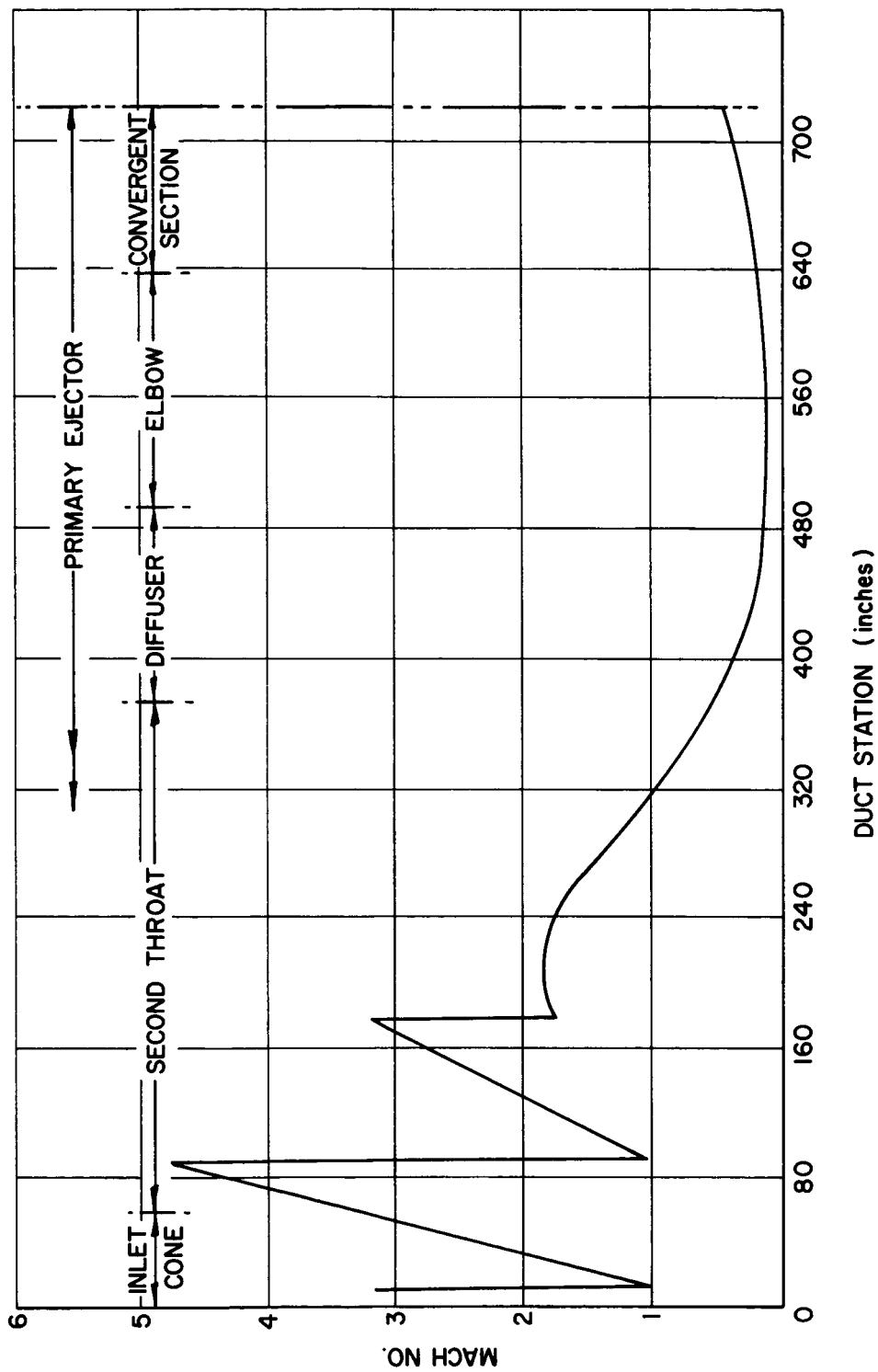


Figure I-9

Mach Numbers when Testing  
the 12:1 Nozzle, 40%  $P_c$

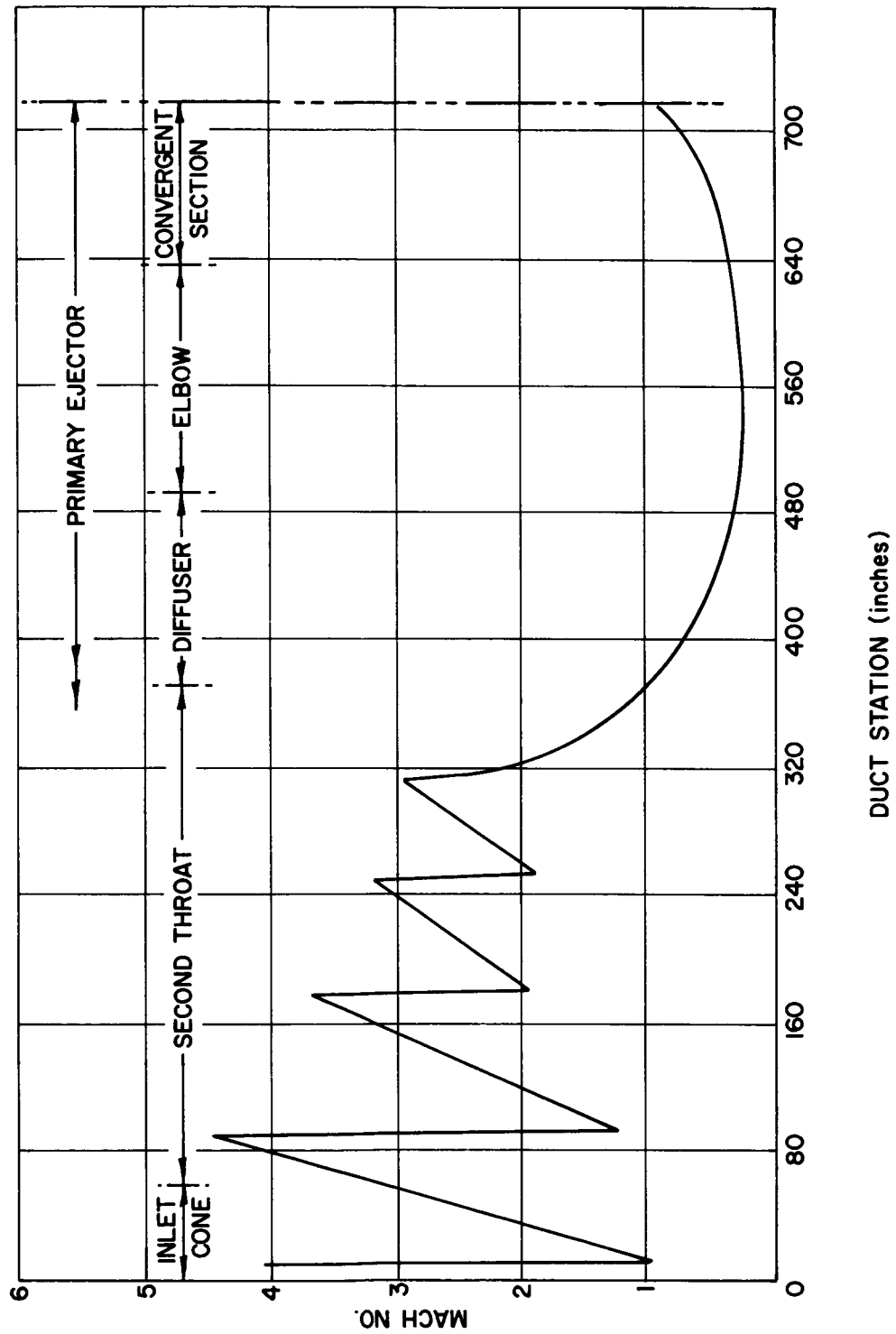


Figure I-10

Mach Numbers when Testing  
the 12:1 Nozzle, 100%  $P_c$

## NOTES.

1.  $P_e$  = NOZZLE EXIT PRESSURE,  $P_v$  = ENGINE COMPARTMENT PRESSURE
2.  $N_2$  SEAL LEAKAGE = 1.5 lb/sec
3. SAFETY PURGE AT DESIGN VALUE
4.  $P_a$  = 12.8 psia

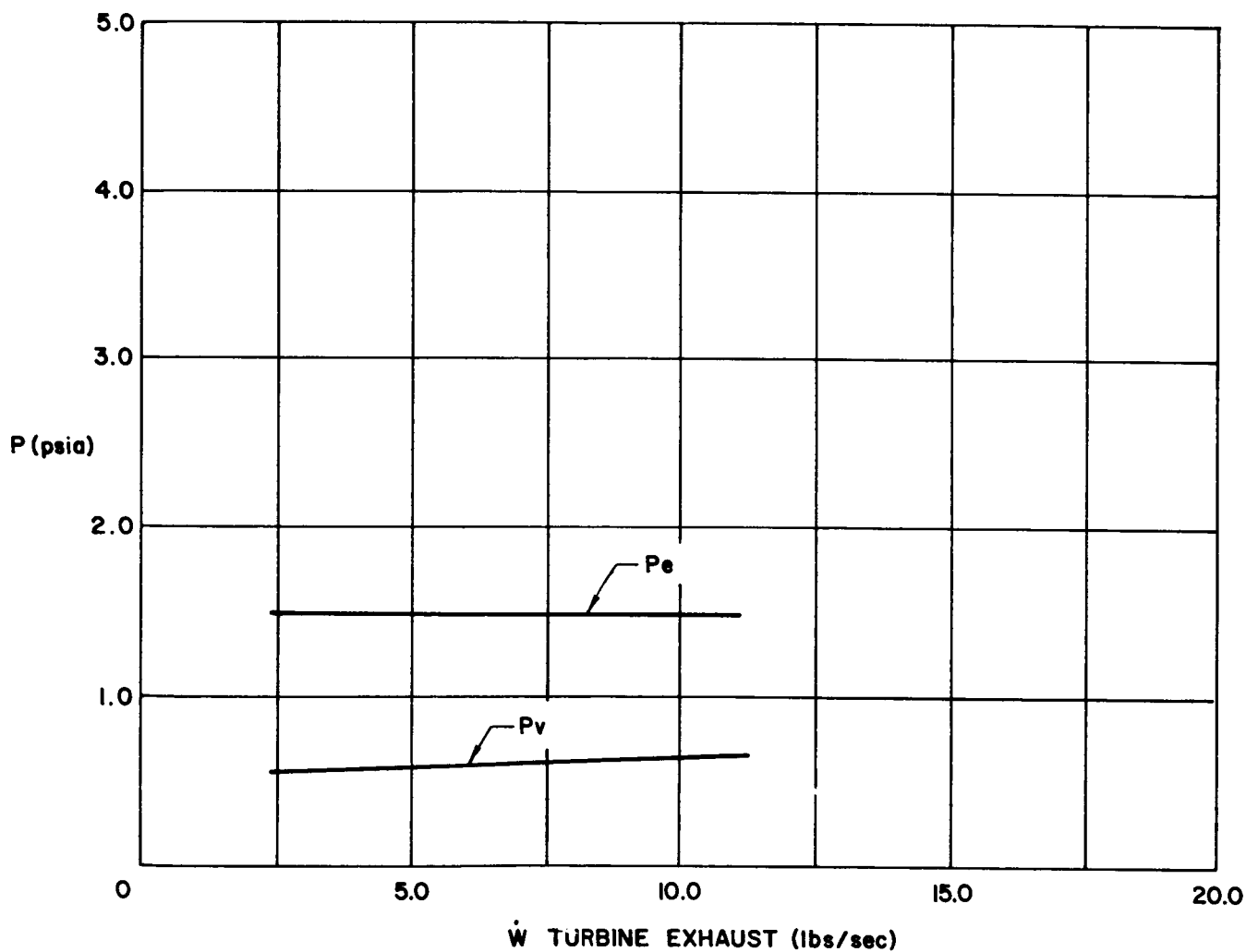


Figure I-11

Nozzle Exit and Engine Compartment  
Pressures vs Turbine Exhaust Flow Rate  
when Testing the 10:1 Nozzle, 40%  $P_c$

NOTES.

1.  $P_e$  = NOZZLE EXIT PRESSURE,  $P_v$  = ENGINE COMPARTMENT PRESSURE
2.  $N_2$  SEAL LEAKAGE = 1.50 lb/sec
3. SAFETY PURGE AT DESIGN VALUE
4.  $P_a$  = 12.8 psia

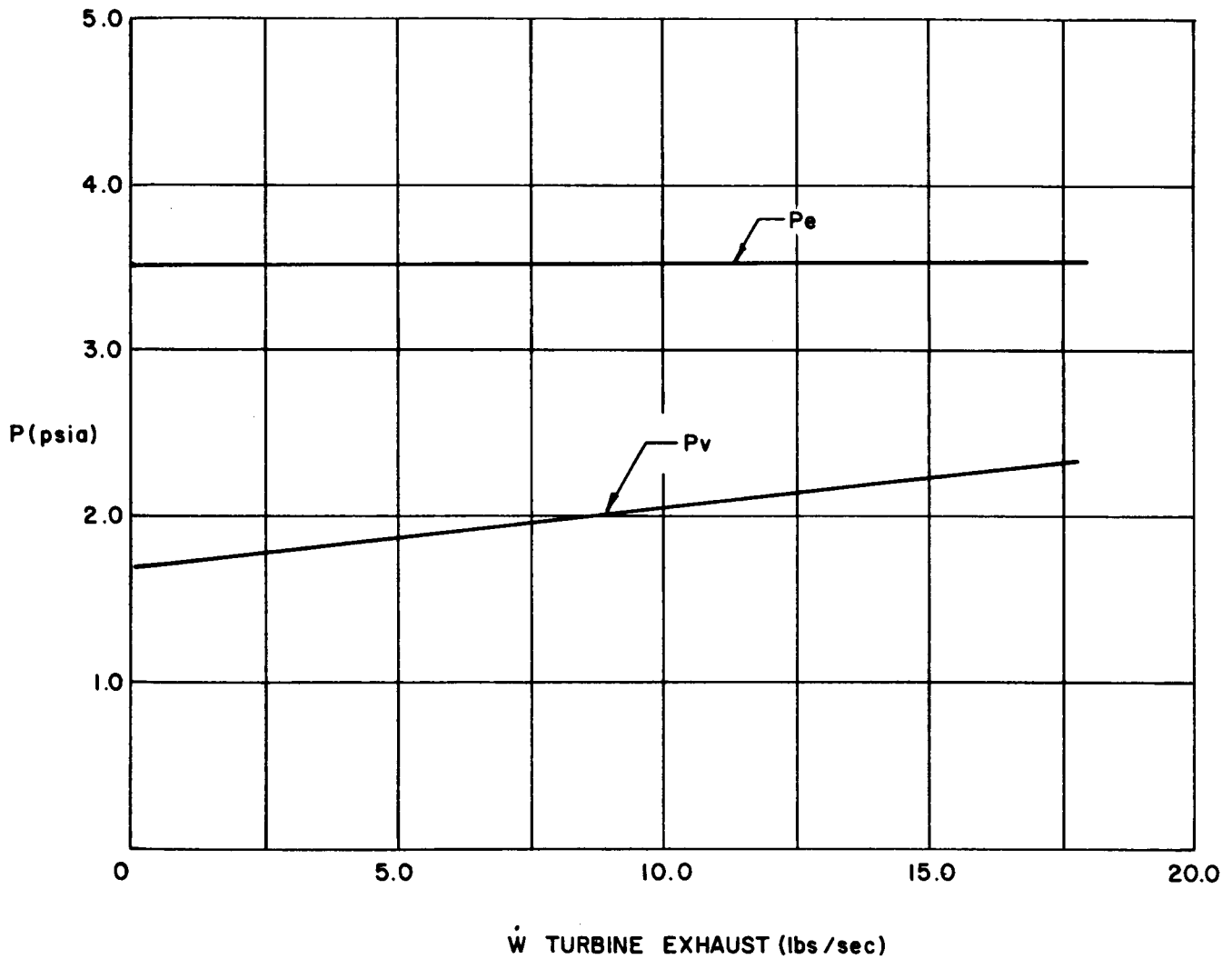


Figure I-12

Nozzle Exit and Engine Compartment  
Pressures vs Turbine Exhaust Flow Rate  
when Testing the 10:1 Nozzle, 100%  $P_c$

NOTES.

1.  $P_e$  = NOZZLE EXIT PRESSURE,  $P_v$  = ENGINE COMPARTMENT PRESSURE
2. TURBINE EXHAUST FLOW AT DESIGN VALUE
3. SAFETY PURGE AT DESIGN VALUE
4.  $P_a = 12.8$  psia

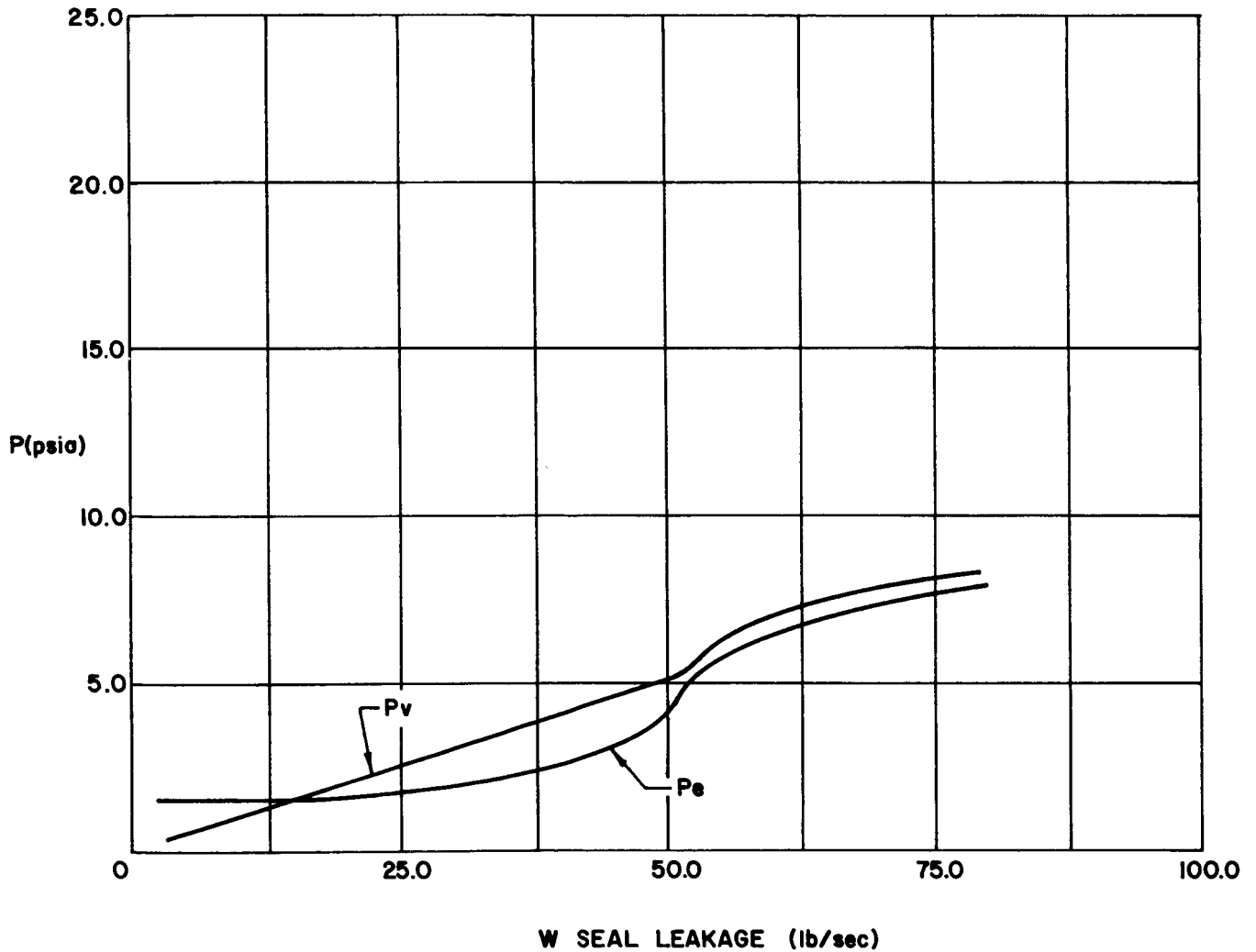


Figure I-13

Nozzle Exit and Engine Compartment  
Pressures vs Seal Leakage Flow Rate  
when Testing the 10:1 Nozzle, 40%  $P_c$

## NOTES.

1.  $P_e$  = NOZZLE EXIT PRESSURE,  $P_v$  = ENGINE COMPARTMENT PRESSURE
2. TURBINE EXHAUST FLOW AT DESIGN VALUE
3. SAFETY PURGE AT DESIGN VALUE
4.  $P_a = 12.8$  psia.

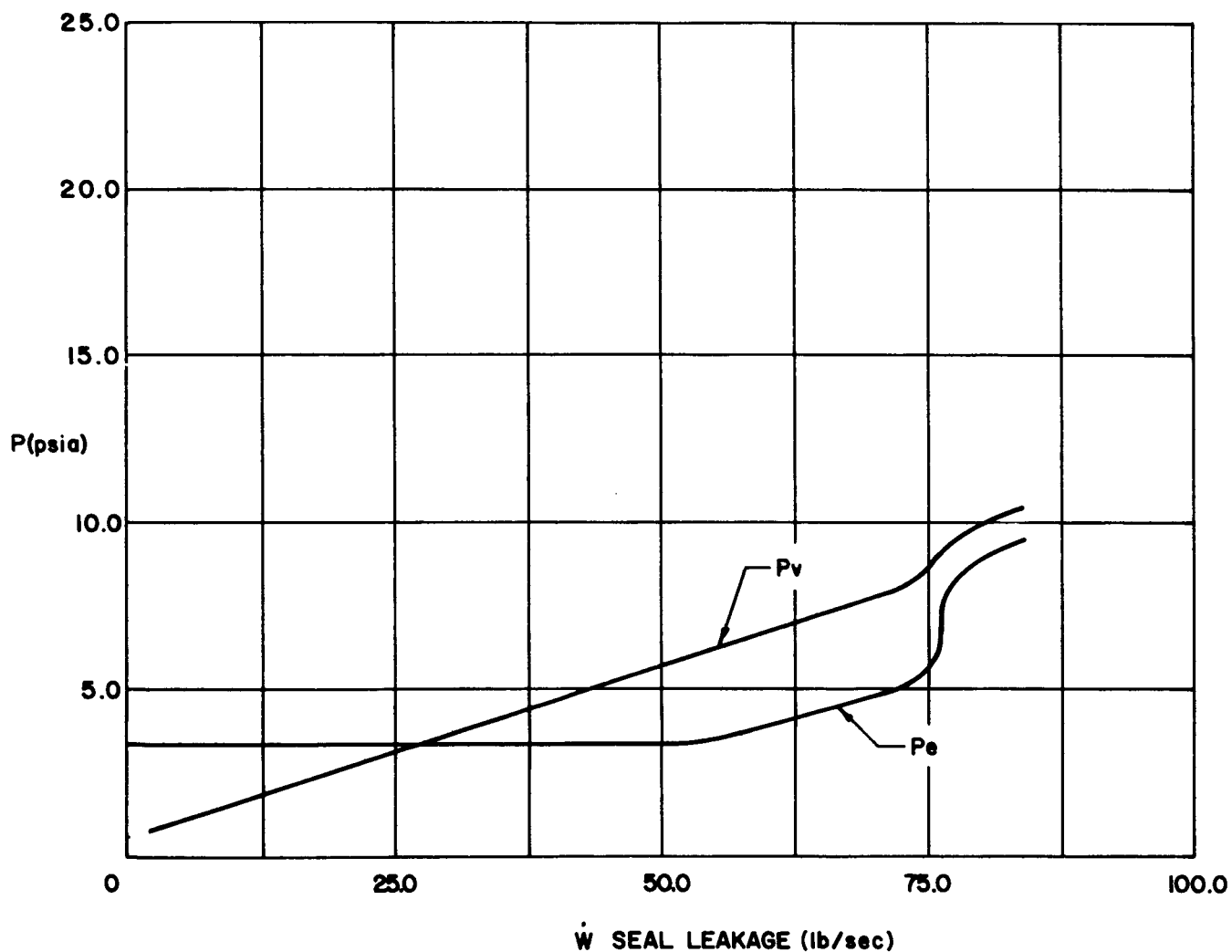


Figure I-14

Nozzle Exit and Engine Compartment  
Pressures vs Seal Leakage Flow Rate  
when Testing the 10:1 Nozzle, 100%  $P_c$

## NOTES.

1.  $P_e$  = NOZZLE EXIT PRESSURE,  $P_v$  = ENGINE COMPARTMENT PRESSURE
2.  $N_2$  SEAL LEAKAGE = 1.50 lbs/sec
3. SAFETY PURGE AT DESIGN VALUE
4.  $P_a = 12.8$  psia

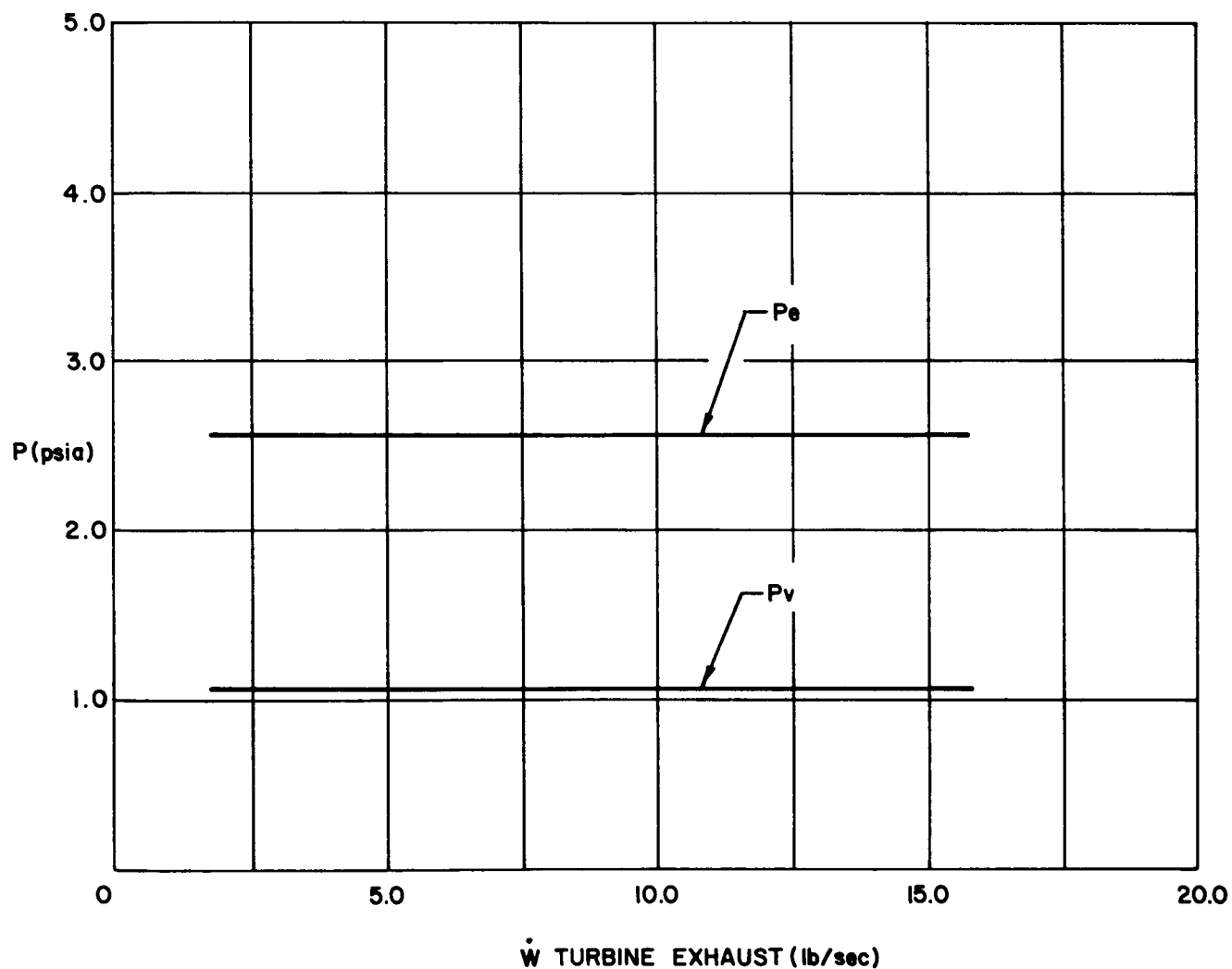


Figure I-15

Nozzle Exit and Engine Compartment  
 Pressures vs Turbine Exhaust Flow  
 Rate when Testing the 12:1 Nozzle, 40%  $P_c$



NOTES.

1.  $P_e$  = NOZZLE EXIT PRESSURE,  $P_v$  = ENGINE COMPARTMENT PRESSURE
2.  $N_2$  SEAL LEAKAGE = 1.50 lb/sec
3. SAFETY PURGE AT DESIGN VALUE
4.  $P_a$  = 12.8 psia

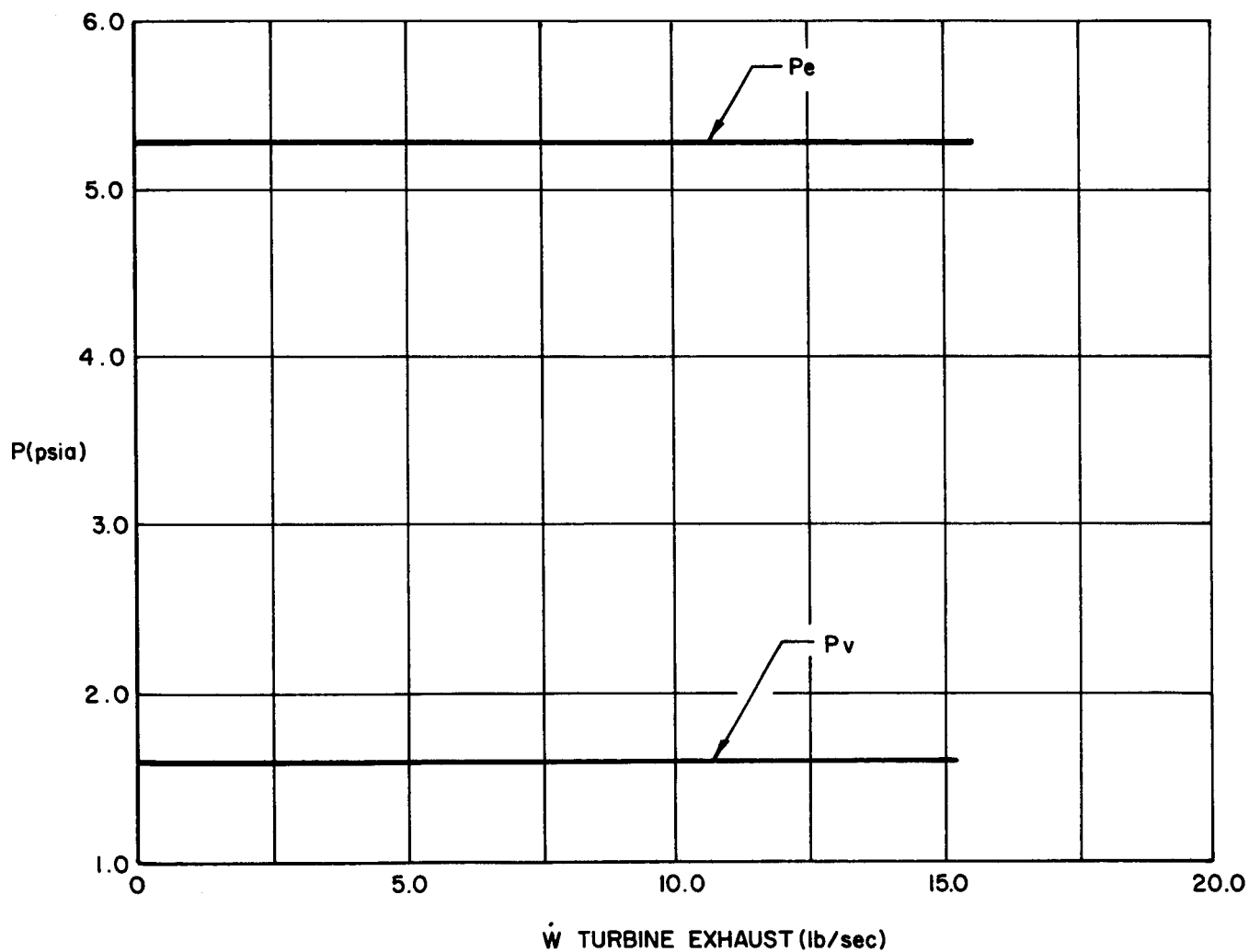


Figure I-16

Nozzle Exit and Engine Compartment  
Pressures vs Turbine Exhaust Flow  
Rate when Testing the 12:1 Nozzle, 100%  $P_c$

NOTES.

1.  $P_e$  = NOZZLE EXIT PRESSURE,  $P_v$  = ENGINE COMPARTMENT PRESSURE
2. TURBINE EXHAUST FLOW AT DESIGN VALUE
3. SAFETY PURGE AT DESIGN VALUE
4.  $P_a = 12.8$  psia

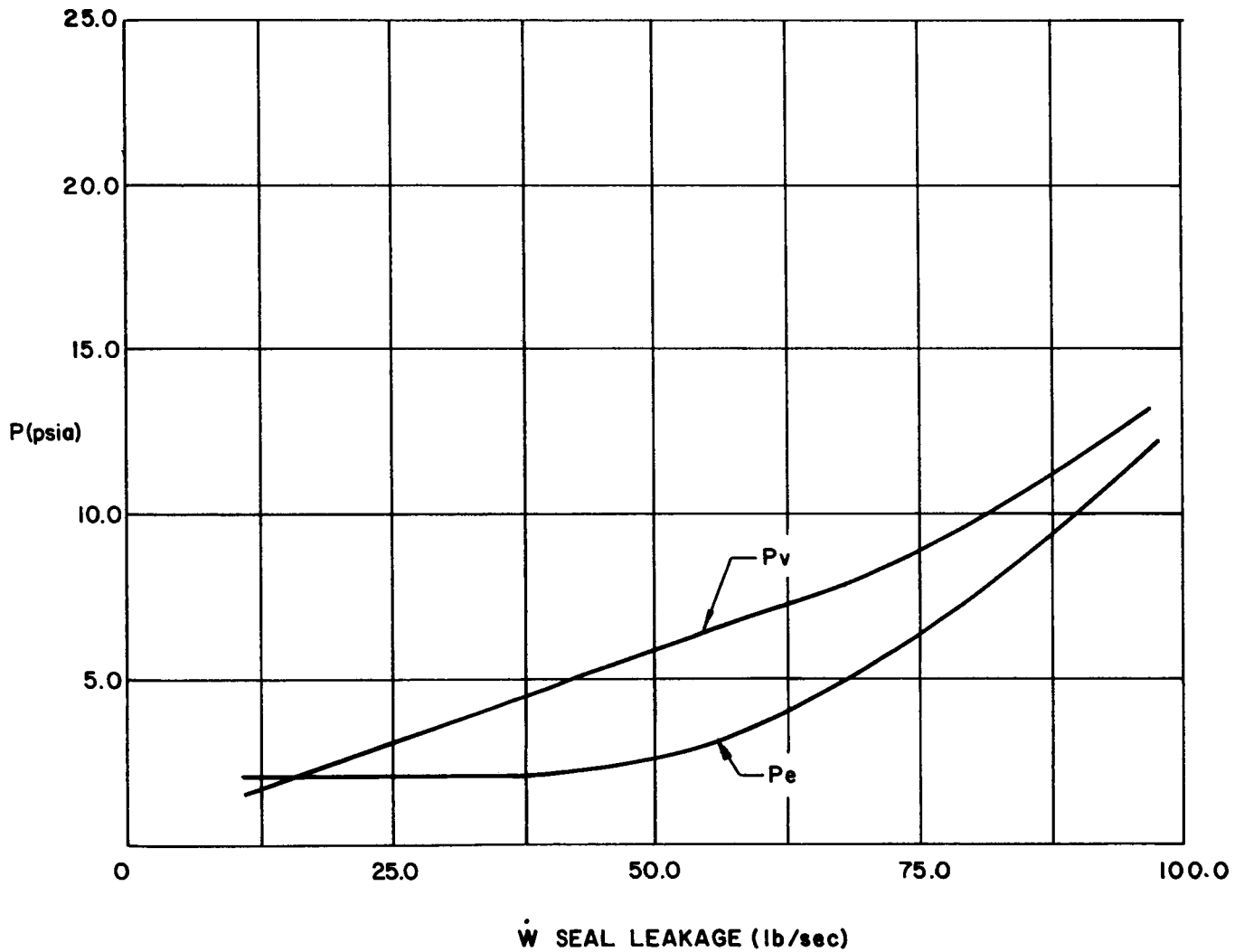


Figure I-17

Nozzle Exit and Engine Compartment  
Pressures vs Seal Leakage Flow Rate  
when Testing the 12:1 Nozzle, 40%  $P_c$

## NOTES.

1.  $P_e$  = NOZZLE EXIT PRESSURE,  $P_v$  = ENGINE COMPARTMENT PRESSURE
2. TURBINE EXHAUST FLOW AT DESIGN VALUE
3. SAFETY PURGE AT DESIGN VALUE
4.  $P_a = 12.8$  psia

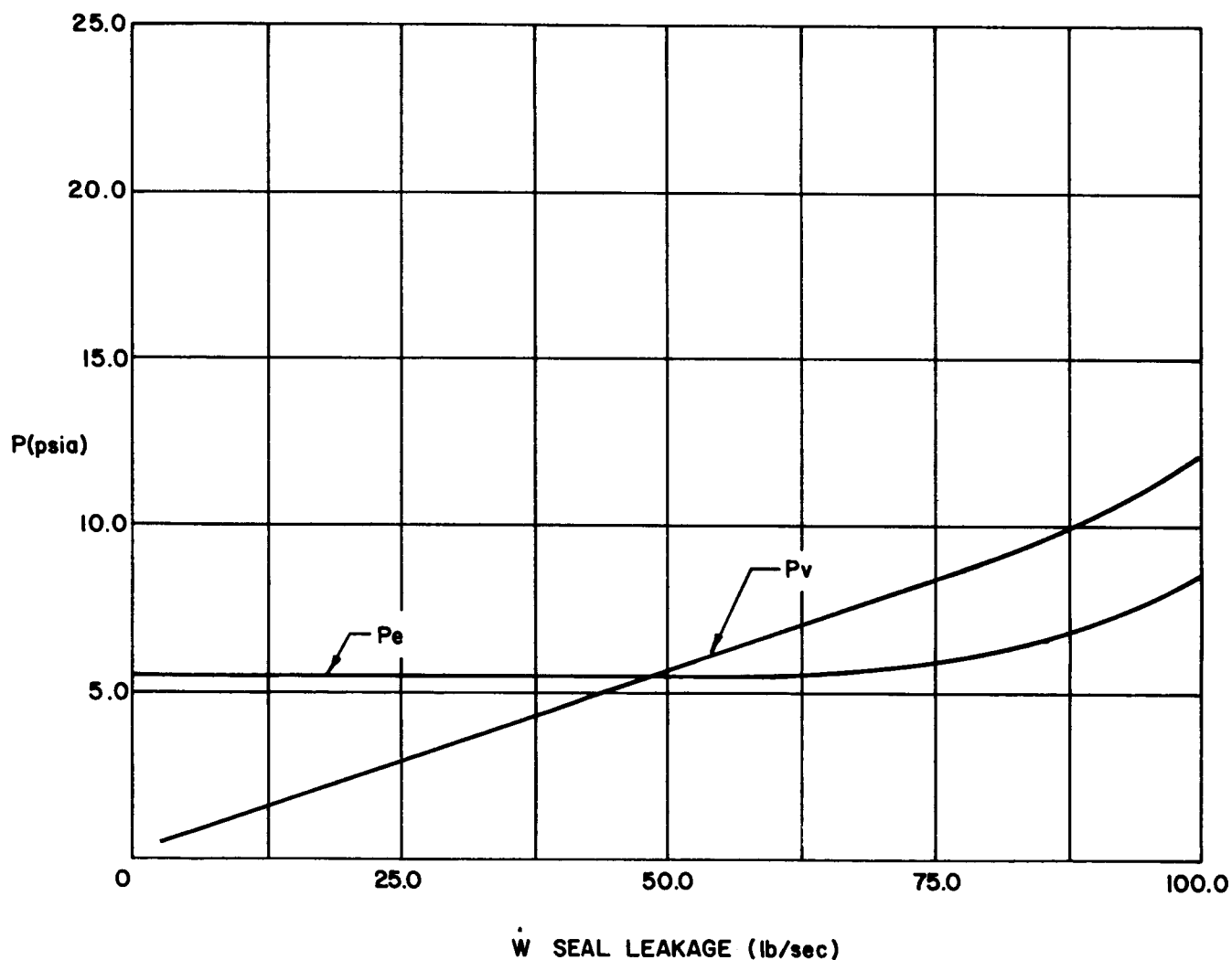


Figure I-18

Nozzle Exit and Engine Compartment  
Pressure vs Seal Leakage Flow Rate  
when Testing the 12:1 Nozzle, 100%  $P_c$

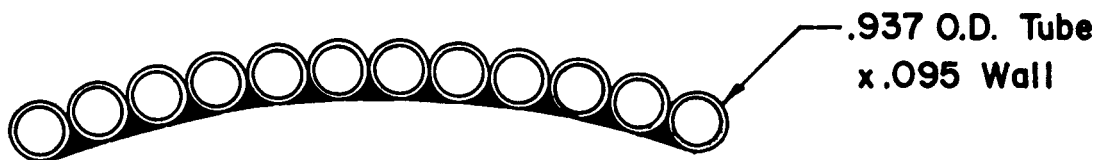
**FLOW CONDITIONS**

The following are the flow requirements for each section of the duct:

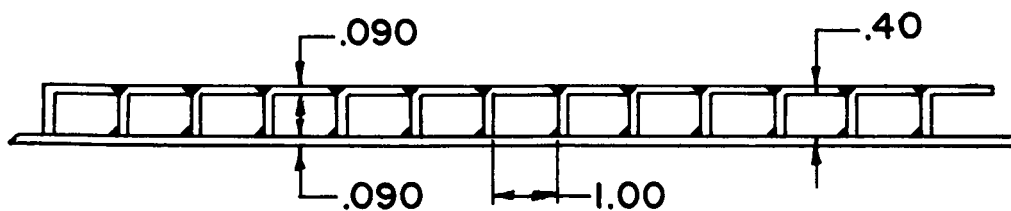
	GPM	Calculated Min. Press at Duct Inlet psig	Nom. Temp. at Duct Inlet °F	Overload Bulk °F	Operation Bulk Temp. °F	Max. ΔP Manif. to Manif. psi
Section I	8,650	193	85	180	140	62
Section II	11,600	190	85	180	140	139
Section III	10,500	192	85	180	140	68

**TOTAL FLOW = 30,750 GPM**

The above requirements are based on a minimum water head in the storage tank of 3.5 feet of water, with a total flow of 44,000 gpm in the 42 in. supply line and 30,750 gpm in the duct system.



**TYPICAL ELBOW (Section II)**



**TYPICAL STRAIGHT SECTION  
(Sections I & III)**

Figure I-19

Coolant Passage Configuration and Flow Conditions

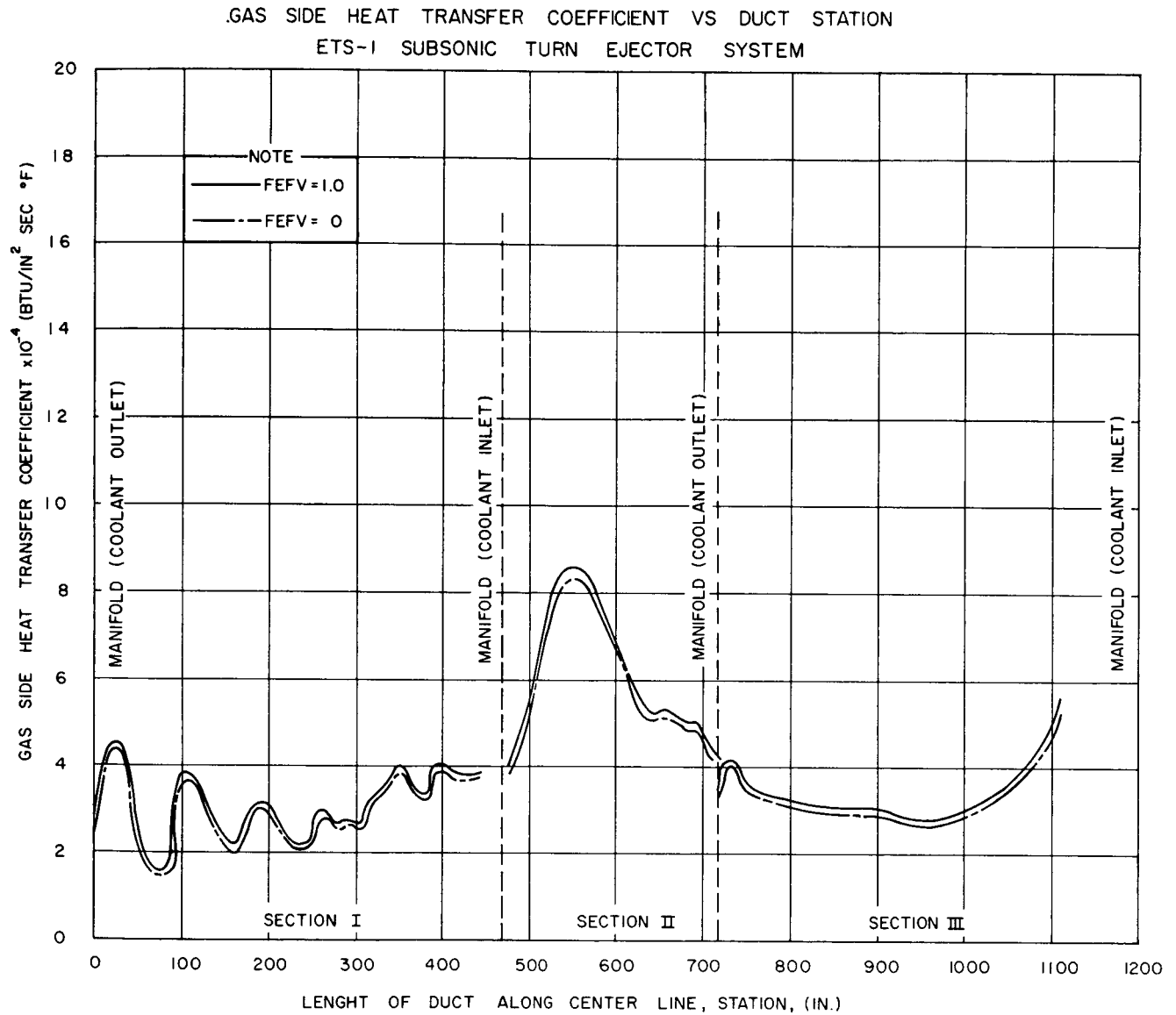


Figure I-20

Gas-Side Heat Transfer Coefficient vs Duct Station

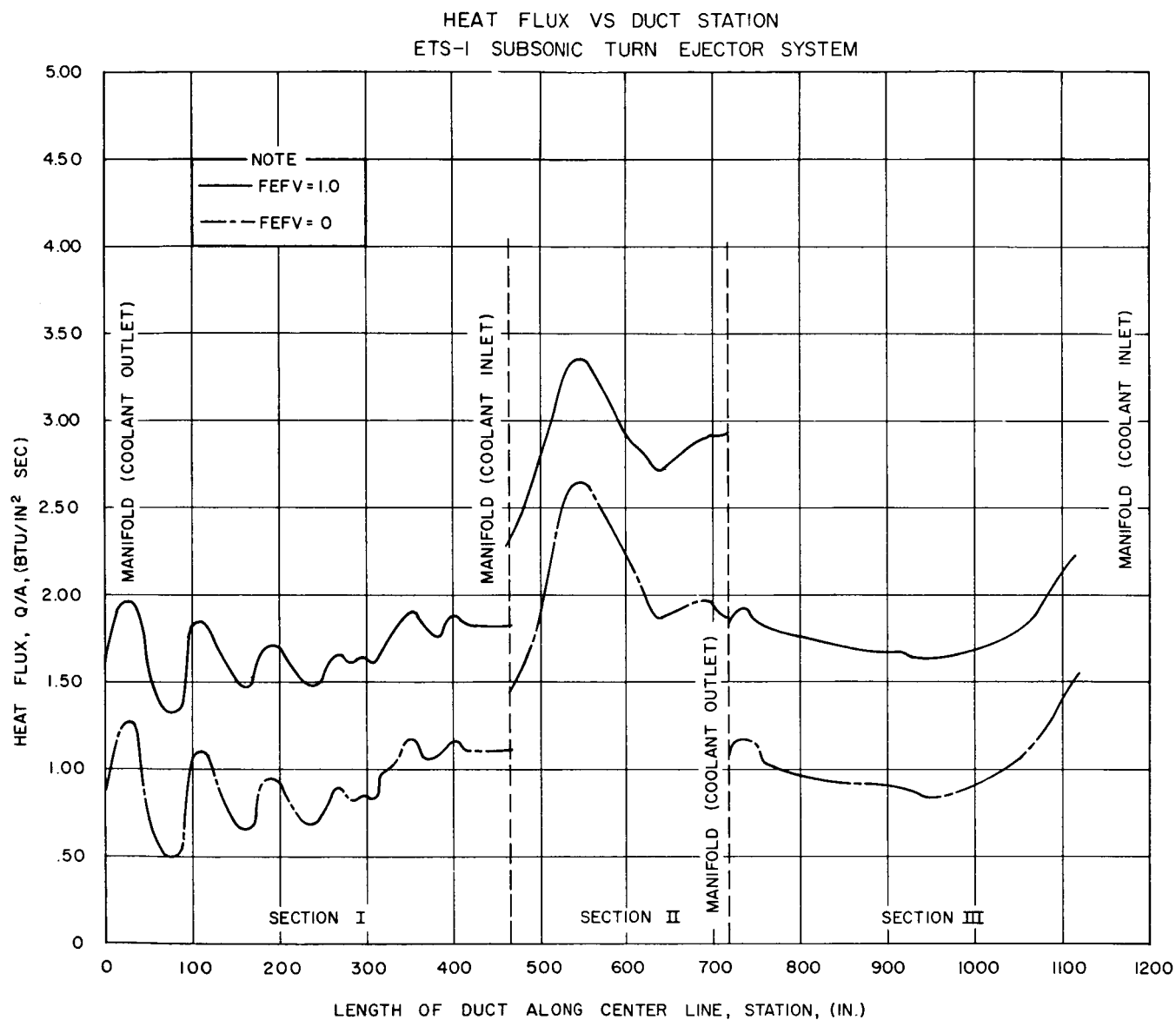


Figure I-21

Heat Flux vs Duct Station

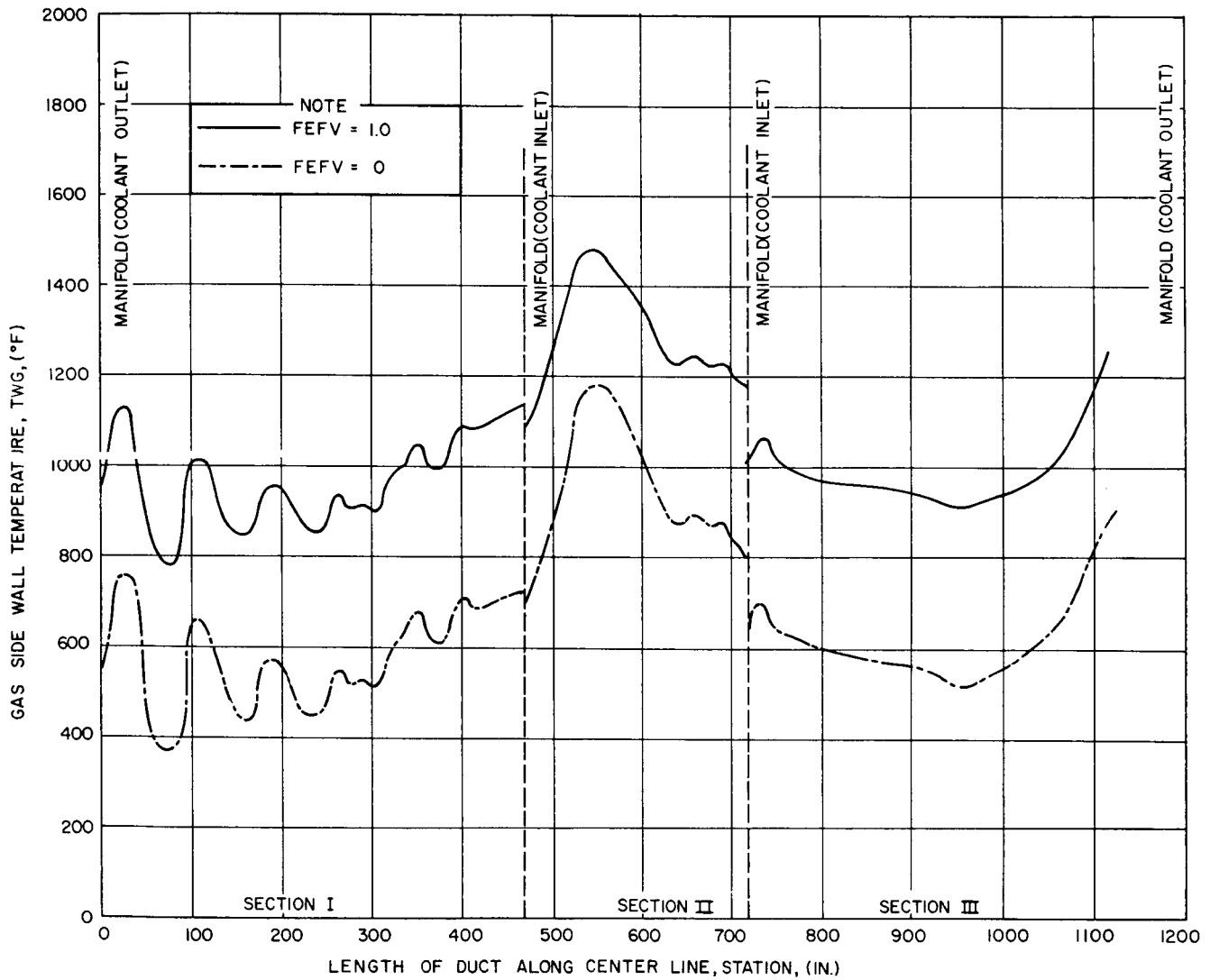
GAS-SIDE WALL TEMPERATURE VS. DUCT STATION  
ETS-1 SUBSONIC TURN EJECTOR SYSTEM

Figure I-22

Gas-Side Wall Temperature vs Duct Station

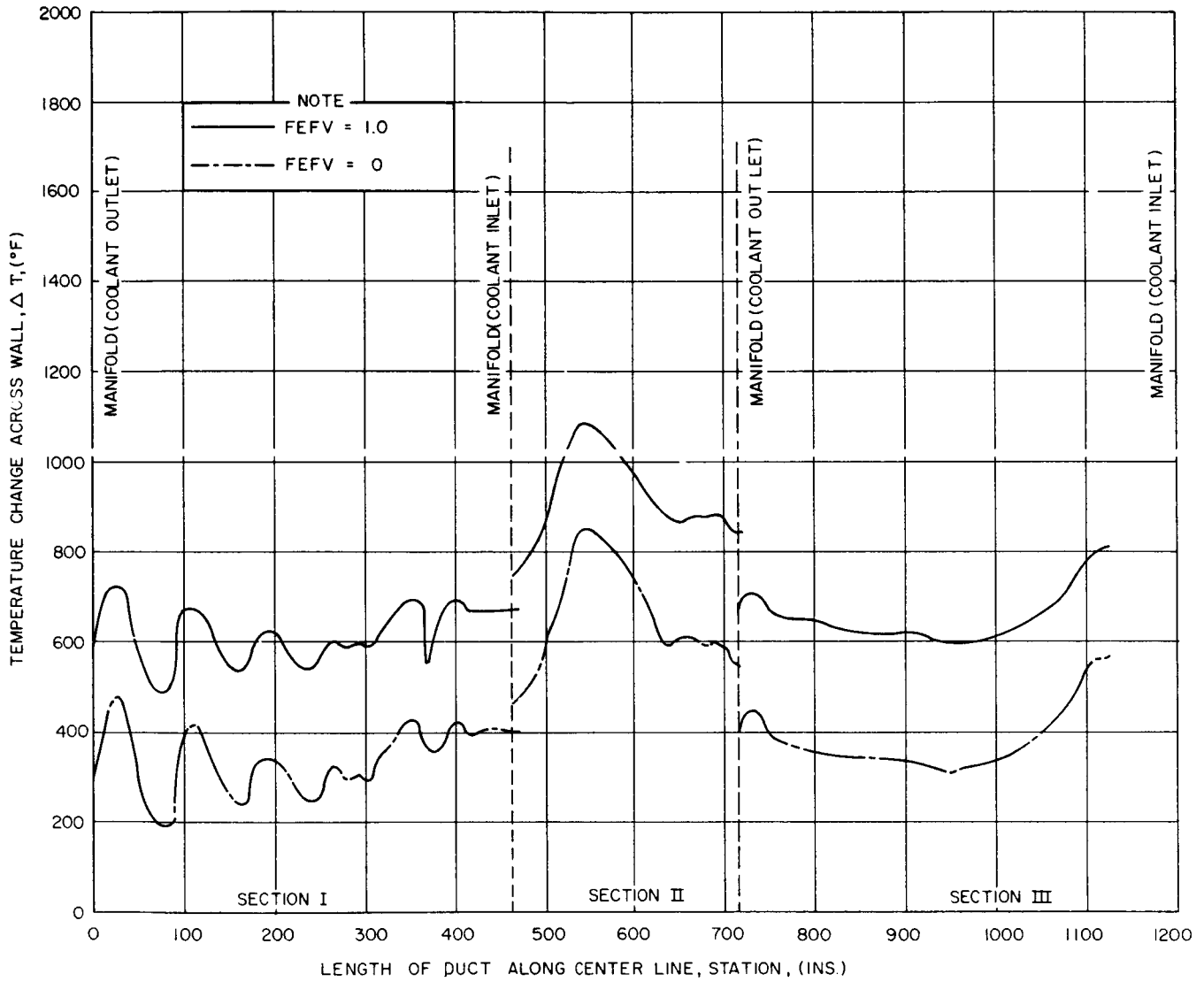


Figure I-23

Wall Temperature Change vs Duct Station



LIQUID SIDE HEAT TRANSFER COEFFICIENT VS DUCT STATION  
ETS-I SUBSONIC TURN INJECTOR SYSTEM

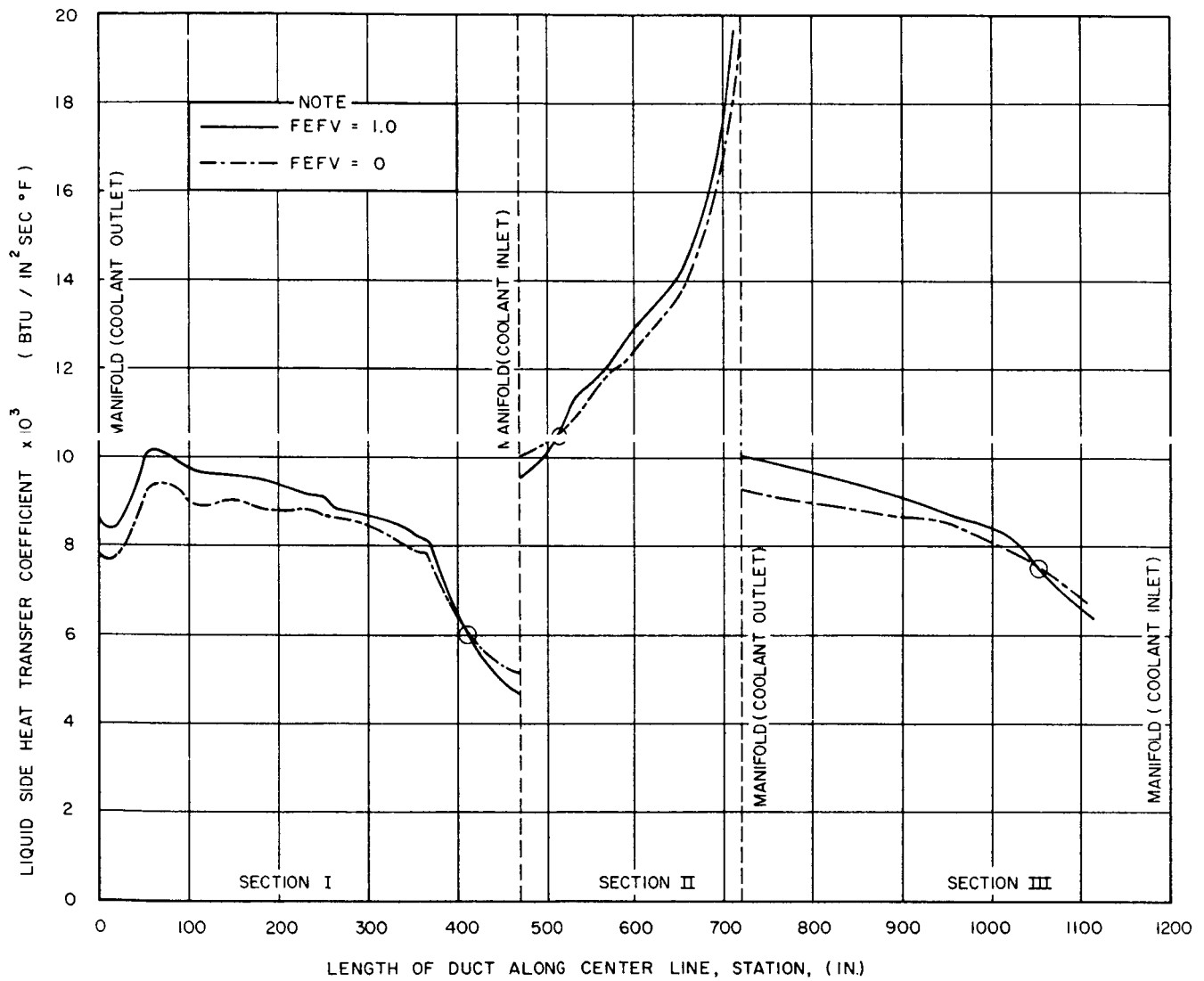


Figure I-24

Liquid-Side Heat Transfer Coefficient vs Duct Station

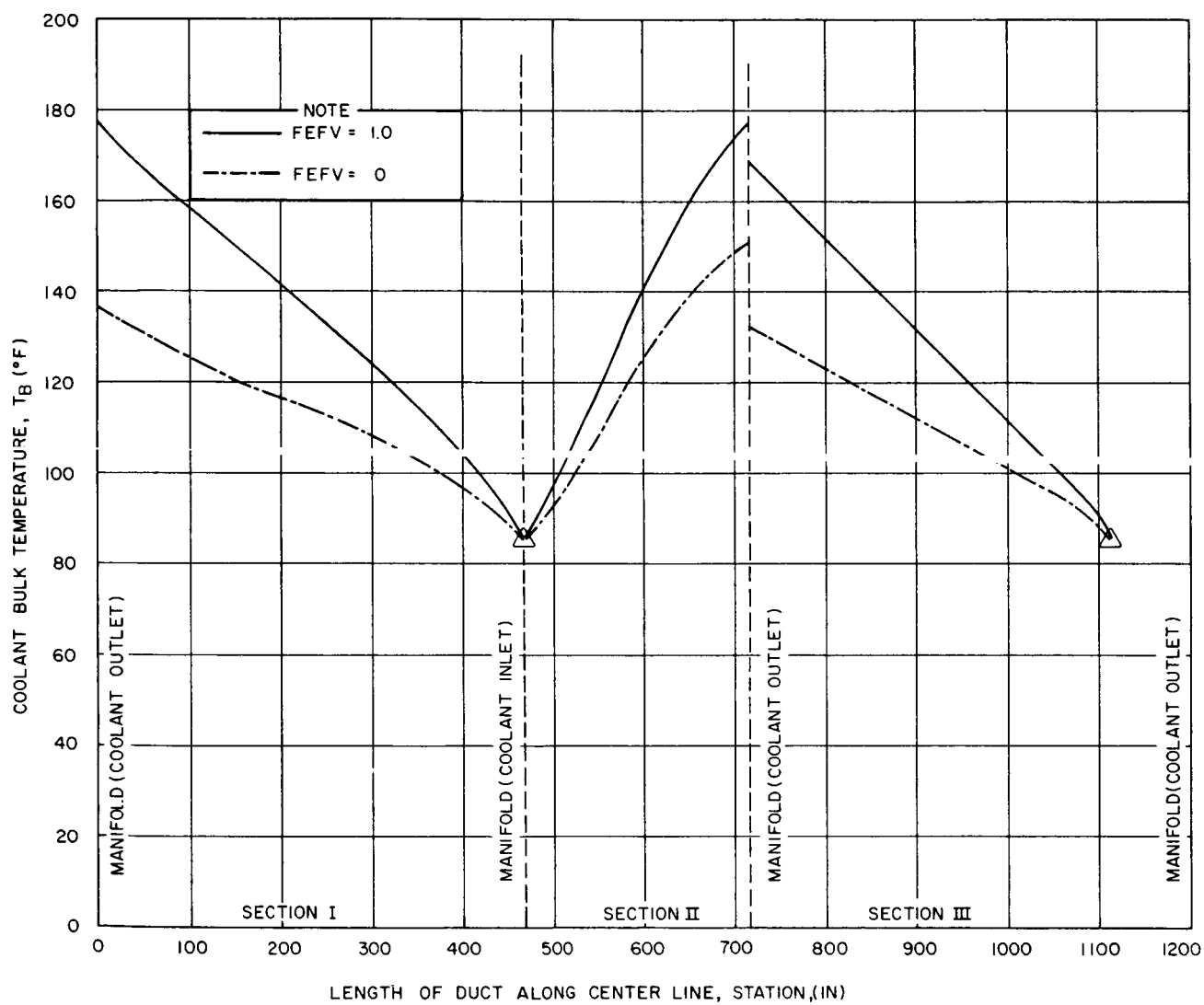
COOLANT BULK TEMPERATURE VS DUCT STATION  
ETS-I SUBSONIC TURN EJECTOR SYSTEM

Figure I-25

Coolant Bulk Temperature vs Duct Station

- NOTES. 1. TURBINE EXHAUST FLOW AT ENGINE DESIGN VALUE  
 2. SAFETY PURGE -  $P_{sc}=100-115$  psia ,  $T_{sc}=1600-1700$  °R ,  $\dot{W}_s=115-130$  lb/sec ,  $\dot{m}_s=18-21$   
 3. SEAL LEAKAGE FLOW = 0 - 2 lb/sec AMBIENT  $N_2$   
 4.  $P_a = 12.8$  psia

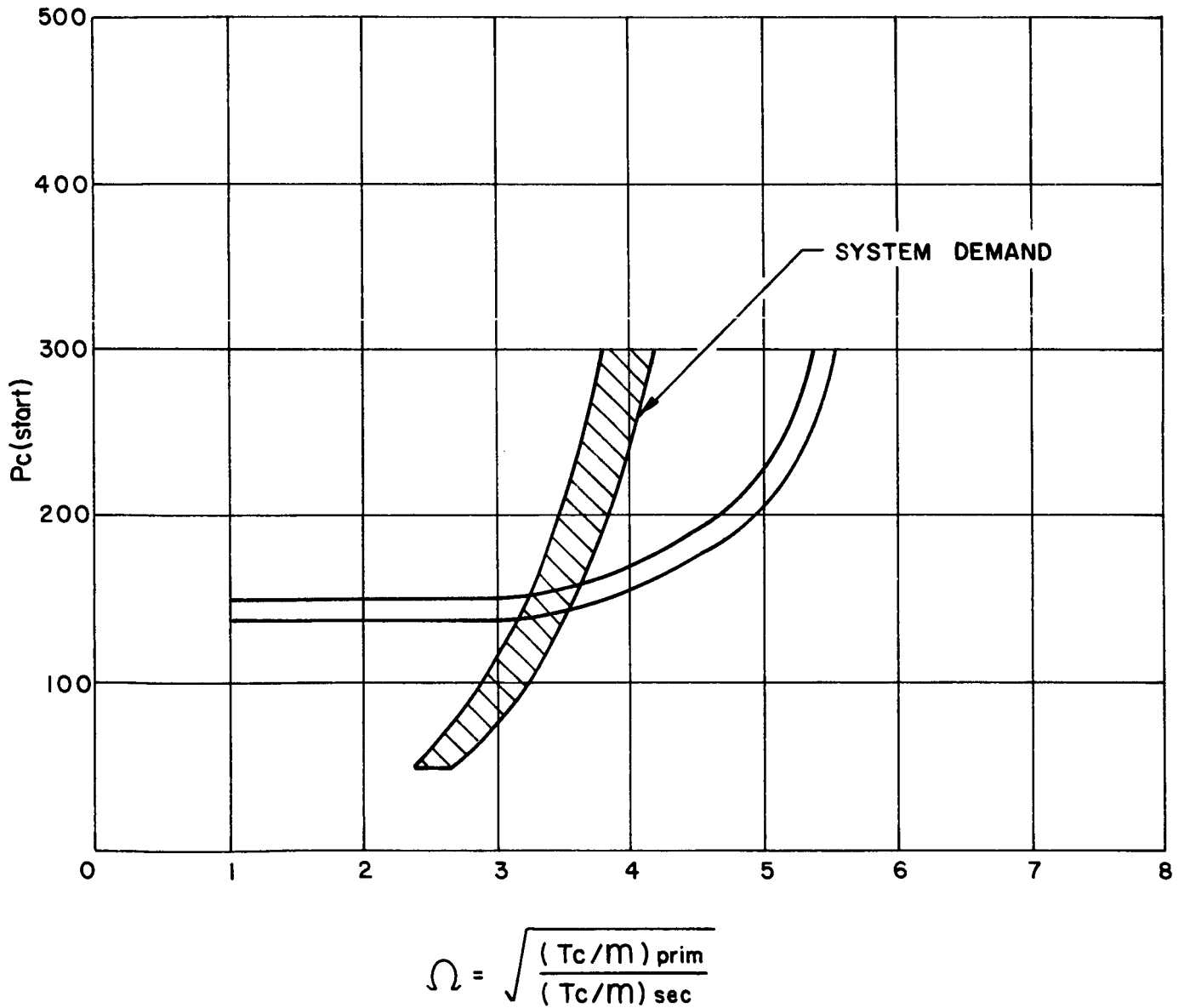


Figure I-26

Effect of Off-Design Safety Purge on Starting Pressure

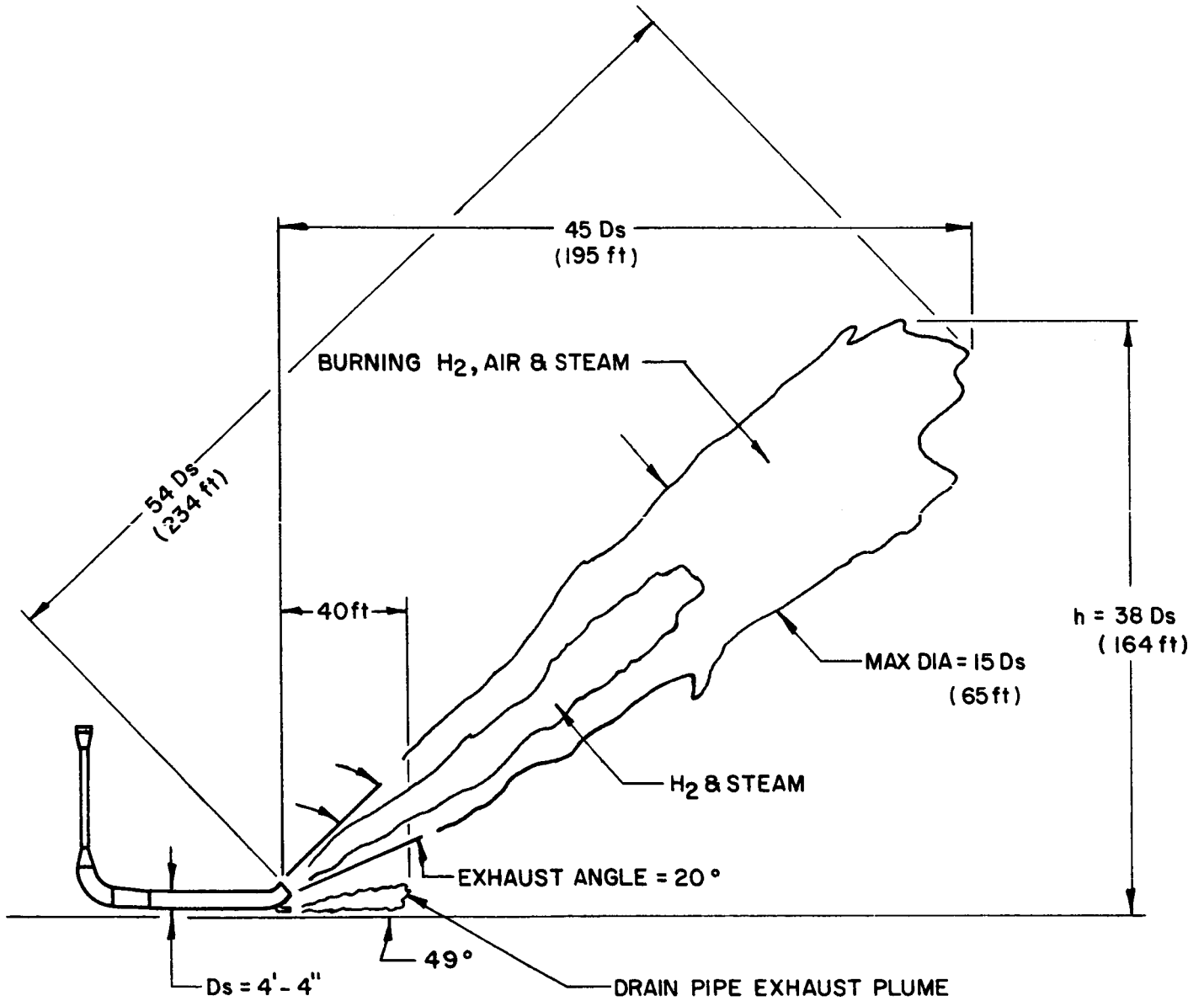


Figure I-27

Predicted Hydrogen Exhaust Plume Size and Shape

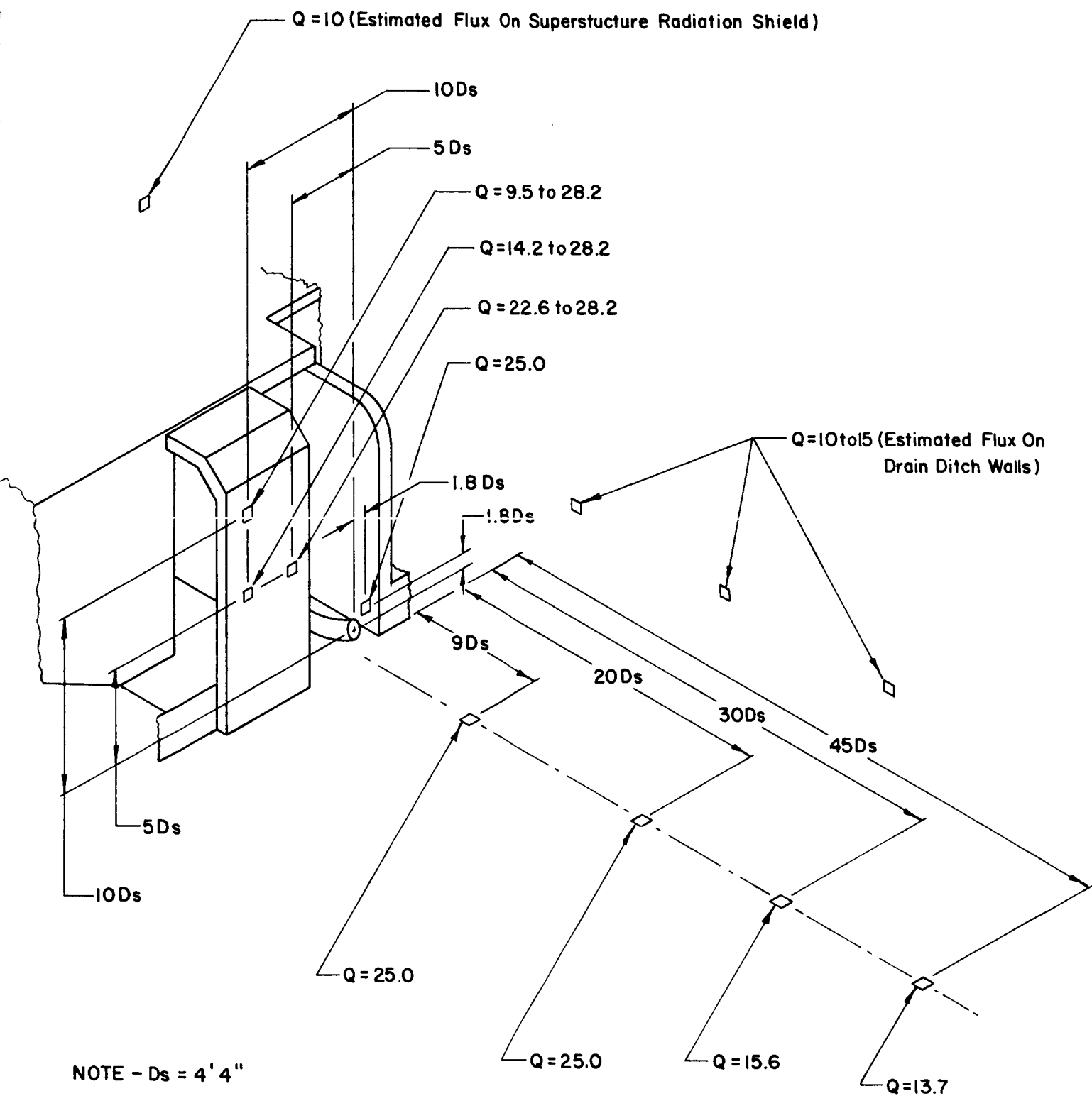


Figure I-28

Predicted Maximum Thermal Radiation Flux ( $Q$ , Btu/ft<sup>2</sup>)  
From Full-Scale NERVA Exhaust Plume  
at Selected Locations

## II. METHOD AND CONFIDENCE OF PREDICTIONS

### A. AERODYNAMICS

#### 1. Performance

The performance of the ETS-1 ejector system is influenced by two major factors; the mass flow of secondary purge fluid and the relative velocity of the primary and secondary fluids at the point of impingement of the two streams, commonly known as the  $\Omega$  factor.

The secondary safety purge system while acting to prevent air backflow into the ejector in case of sudden engine flow termination also acts to reduce the engine compartment pressure prior to and for the initial portion of engine start. The amount of pressure reduction in the engine compartment prior to engine start is a function of the secondary safety purge chamber pressure; the higher the chamber pressure, the lower the compartment pressure and vice versa. Figures I-1 and I-2 show that when the secondary safety purge system is operating at design conditions the engine compartment pressure is reduced from 12.8 psia (Nevada ambient) to 7.8 psia, a reduction of 5 psia. The performance of the ejector system during the initial period of engine startup is a direct function of the secondary purge system chamber pressure.

The other large influencing factor in the performance of the ejector system is  $\Omega$ . Figure I-25 shows the effect on the primary pull in pressure as  $\Omega$  is increased. Up to an  $\Omega$  of 3.5 there is no effect on  $P_c$  (start), from an  $\Omega$  of 3.5 to 5.5, there is an increasing  $P_c$  required to start the ejector and an  $\Omega$  over 5.5 will prevent the ejector from starting.

It is known that  $\Omega$  effects the  $P_c$  and  $P_v$  relationship during the initial startup period but the exact relationship is not known. It can be expected, however, that the higher the  $\Omega$  value, the higher will be the engine compartment pressure for a given value of  $P_c$ .

When comparing the 1/4-scale to the 1/8-scale performance curves for both the 10:1 and 12:1 nozzle, the above discussed performance influencing parameters ( $P_{sc}$  and  $\Omega$ ) can be utilized to account for differences in the 1/4- and 1/8-scale data. For the 10:1 nozzle (shown in Figure II-1), the

secondary chamber pressure was 25 psi higher during the 1/4-scale test, which would account for the majority of the difference in the two curves. However, at pull in, there was a difference of 0.4 in  $\Omega$  which would result in a difference of 6 psi in the starting chamber pressure.

In comparison of the 12:1 nozzle tests (Figure II-2), both  $P_{sc}$  and  $\Omega$  appear to have a large effect upon performance, especially during the initial period of engine startup. Up to 100 psi chamber pressure, there was approximately a 22-psi difference in  $P_{sc}$ , 1/4 scale having the lower value. Also, the value of  $\Omega$  for the 1/4 scale system ranged from 4.8 at start of run to 4.0 at pull in. This change in  $\Omega$  during start on the 1/4-scale test was caused by test stand limitations. The 1/8 scale test used nitrogen for both primary and secondary, and had an  $\Omega$  value of about 1 for the entire run.

Both the differences in  $P_{sc}$  and  $\Omega$  contribute to the differences between the 1/4 and 1/8 scale curves of Figures II-1 and II-2.

Other 1/4-scale tests have shown that when  $P_c = 0$  and  $P_{sc} = 100$  psia then  $P_v = 7.5$  psia. This would bring the initial portion of the 1/4-scale curve shown in Figure II-2 down to the 1/8-scale curve. Also at  $P_c = 100$  psia the value of  $P_v = 4.5$  psia when  $\Omega = 3$  instead of 6.5 for  $\Omega = 4.5$  as obtained during the 12:1 nozzle startup test. The third point of comparison is the start point. The value of  $\Omega$  at this chamber pressure during this test was 4.0. Figure I-28 shows that if  $\Omega$  was at or below the expected full scale value of 3.4 instead of 4.0 the starting pressure would have been decreased by about 15 psi. Correcting the 1/4-scale test data of Figure II-2 at the three values of  $P_c$  (0, 100 and 180) discussed above, the 1/4 scale corrected data follows the 1/8 scale test data very closely.

## 2. Wall Pressures and Mach Numbers

Comparison of the 1/4- to 1/8-scale pressure and Mach number data is shown in Figures II-3 through II-10. Figure II-11 shows the location of the pressure taps for these tests. The overall pressure level of the 1/4-scale system downstream of the second throat is slightly higher than that monitored during the 1/8-scale program. For convenience and ease of testing,

the 1/8-scale pressure profile tests were conducted with nitrogen for both primary and secondary fluid. As more knowledge was obtained from the 1/4-scale tests it was thought that perhaps  $\Omega$  could have some influence on the pressure distribution in the subsonic portion of the ejector system. This could be caused by the same aerodynamic blockage effect that causes a decrease in performance at higher  $\Omega$ 's. At a high value of  $\Omega$ , nitrogen from the safety purge nozzle has a lower velocity than the hydrogen primary gas. The hydrogen is decelerated through momentum transfer to the safety purge fluid, resulting in increased pressure of the hydrogen at the primary ejector exit. This higher pressure of the ejector means a lower Mach number in the subsonic portion of the primary ejector as well as a more uniform flow distribution in the elbow.

The supersonic region of the duct will not be affected by the flow interaction and is independent of the types of fluids ( $N_2$  or  $H_2$ ) used in the system. The, so called, turbulent mixing region which consists of a supersonic core and subsonic boundary will be slightly affected by the increase in pressure in the subsonic portion of the duct.

The use of hydrogen as the primary fluid and nitrogen as the secondary fluid simulates the conditions expected on full scale. The predicted pressure and Mach-number curves in Section I are based on this scale-model test condition.

### 3. Turbine Exhaust

The 1/8-scale data is inconsistent in that some cases the engine compartment pressure ( $P_v$ ) is higher than the nozzle exit pressure ( $P_e$ ). The reasons are the same as stated for the seal leakage tests. The comparison of the two programs is shown in Figures II-12 through II-15, and II-20, and II-21.

The 1/4-scale program was consistent and repeatable and pressure readings were verified by the mercury manometer.

Therefore, the 1/4-scale data is indicative of the performance expected from the full-scale duct.



#### 4. Seal Leakage

Refer to Figures II-16 through II-19 and II-22 through II-25, which compare the results of the 1/8-scale and 1/4-scale tests.

Tests conditions for all tests were nearly identical, secondary ejector and the turbine exhaust were at design values,  $N_2$  seal leakage was introduced at the top of the engine compartment and increased until the engine compartment pressure reached ambient.

The curves show the data points for both 1/8 and 1/4 scale and the line is faired through the 1/4-scale results.

During the 1/8-scale test program discrepancies were noted in both the nozzle exit pressure ( $P_e$ ) and engine compartment pressure ( $P_v$ ). Redundant gages were installed to monitor  $P_e$  and  $P_v$  but in most cases, the two readings did not agree. The two gages at each location were of two separate types. Type I gages, which are designated  $P_{e-1}$  and  $P_{v-1}$ , are absolute pressure gages calibrated from 0 to 5 psia, with a mechanical stop at approximately 7 psia. Type II gages, which are designated  $P_{e-2}$  and  $P_{v-2}$ , were calibrated from 0 psia to ambient. It was felt that the pressure region of concern would be in the range of the Type I gage and that this type of gage would yield data of greater accuracy. This was not the case, for (in some instances)  $P_{e-1}$  and  $P_{e-2}$  would differ by 2 psi.

Steps were taken to prove or disprove the validity of one of the gages. Some of the possible problem areas could be attributed to:

- a. Incorrect calibration procedures
- b. Malfunction of the gages
- c. Possible leak in instrumentation line.

Steps to rectify the problem consisted of:

- a. Pre- and post-calibration
- b. Close scrutiny of calibration procedure
- c. Leak check the system.

None of these checks proved fruitful.

Due to the problem areas encountered during the 1/8 scale program, emphasis was put on:

- a. Smoothness of nozzle walls after pressure taps were installed
- b. A mercury manometer was installed to verify the pressure readings obtained by the pressure transducers  $P_e$  and  $P_v$ .

Both of these measures proved quite successful; therefore, there is much greater confidence in the performance predicted by the 1/4-scale data.

#### 5. Required Flow into the Engine Compartment

During some of the initial 1/8 scale tests performed in the early part of CY '64, instability in the engine compartment pressure just prior to the pull in of the ejector was noticed. This instability was shown to be a result of the large difference in area between the nozzle exit (10:1 or 12:1 area ratio nozzle) and the ejector entrance. It should be mentioned that this large area difference cannot be reduced mechanically because of the necessity for 25:1 area ratio nozzle testing capability. It was also noticed that when there was flow from the turbine exhaust nozzles that this instability disappeared. The turbine flow essentially acted to reduce the entrance area and second throat area of the ejector which in turn reduced the ejector area ratio and enabled the overall starting pressure to be reduced as well as eliminating the instability.

The turbine exhaust nozzles for the above described tests were, however, located in the roll control position (above the engine). In this position, there would always be uniform flow surrounding the engine and nozzle to act as an instability eliminator.

When the turbine exhaust nozzles were relocated at the primary nozzle exit, this eliminated the source of flow into the engine compartment. There was, however, still the flow of nitrogen coming from the seals but it is possible that this seal leakage flow could be minimal leaving no extraneous flow entering the engine compartment.

A test, during the 1/4-scale program, in which there was no seal leakage confirmed that instability and an increase in primary pull in pressure would occur. Since the system can adequately handle 1 lb/sec plus the expected seal leakage, it is recommended that this 1 lb/sec ambient  $N_2$  gas flow be added.

The gas can be added through the pre-fire purge system modified with a low flow rate by-pass valve on the main system.

#### B. HEAT TRANSFER

Conversion of the scale model heat transfer coefficient data to the full-scale condition required that a correlation be developed to interpret the test data. Since the Mach number and mass flow rate vary along the wall in a manner not amenable to analysis, it was decided to convert the data to a turbulent pipe-flow correlation form, with the assumption that the axial location of the shock wall-attachment points and the variation of Mach number with axial distance will both be functions of ejector pressure ratio. Instrumentation location for the heat transfer tests is shown in Figure II-26.

Thus, from turbulent pipe flow correlation theory, the parameter  $h T_c^{.4} D^{.2} / P_c^{.8}$  for geometrically similar ejector systems should form a single curve when plotted versus distance along the ejector center line. Figure II-27 shows this plot at 100%  $P_c$  for the 1/8- and 1/4-scale test data for the selected ejector. The 1/8-scale line (used to design the full-scale ejector) is based on several runs and is the upper  $3\sigma$  limit of the data, while the 1/4 scale data is for one run only. The 1/4-scale data is interpreted by the dashed line. A difference between the 1/8- and 1/4-scale data is noted in the second throat-exit region ( $L \approx 400$  in.). This region is characterized by a supersonic core (with shocks) surrounded by a subsonic passage, with mass and momentum crossing the boundary of the core and subsonic region. As a function of distance downstream, the core diameter decreases (with shock "attached" to the boundary instead of the physical wall); thus, the subsonic region sees a diffusing passage and the overall effect of increasing static pressure is realized. However, this overall effect is three-dimensional in nature and apparently a function of duct

diameter that is not accounted for by the one-dimensional turbulent pipe-flow correlation. The coefficients used for the full scale duct design were scaled from the 1/8-scale data, thus allowing conservative estimates of thermal performance in this region.

Good agreement is noted in the initial shock region as to the form and location of the peaks and valleys, indicating that the shock structure is the same for both systems. Level wise, near the entrance, a 25% increase in heat-transfer coefficient is noted. This will cause an increase in the local wall temperature on the hot gas side of the ejector by approximately 12%. This will not affect the safe operation of the duct.

A divergence of the data is noted in the secondary ejector exit region ( $L \approx 1000$  in.). The 1/8-scale data was taken without a  $45^\circ$  exit elbow fitted to the exit. The curve shown is an estimate of the effect of a  $45^\circ$  elbow and was obtained by applying a correction<sup>1</sup> to the data acquired without the elbow. The 1/4-scale test data was taken with a  $45^\circ$  elbow attached to the exit of the secondary ejector, and the data shows no rise in heating rate due to the presence of the elbow. However, the 1/4-scale duct was fitted with a drainpipe while the 1/8-scale duct was not. Again, the full scale design was based on the 1/8-scale data which indicates that if the 1/4-scale data is correct, the full scale exit region temperatures are overstated.

Figure II-28 is presented to show the effects of chamber pressure (or ejector-pressure ratio) on heat-transfer coefficients. In general, as would be expected, the level is lower and lower temperatures will prevail. However, in the turbulent mixing region, the 40%- $P_c$  run shows the heat transfer coefficient values to be of the same order as the 100%  $P_c$  run.

The local temperatures will be slightly higher and the temperature distribution will be different from the 100%  $P_c$  condition; however, these differences are well within design limitations, thus assuring safe operation of the ejector. With the exception of this turbulent mixing region, the trend is as expected and agrees well with the turbulent pipe-flow correlation theory. It

<sup>1</sup>A. J. Ede, "The Effect of a Right Angled Bend on Heat Transfer in a Pipe," International Developments in Heat Transfer, Part III, ASME 1961.

should be noted that reduced chamber pressure reduces the number of shock waves but that the waves that are present occur at the same axial location in the duct as the 100%  $P_c$  run.

The method of conversion of scale model heat transfer coefficients to full scale values is the same as previously reported.<sup>1</sup>

One very important factor concerning the confidence level of scale data and predicted full-scale results can be found by comparing Figures II-4 and II-27. Figure II-4 is of course a pressure profile curve and Figure II-27 is a heat transfer curve but each curve has a series of peaks and valleys which designates the location at shock wave attachment points. Both temperature and pressure data indicate shock attachment points at exactly the same location. This verification of the shock structure provides a greater confidence level for the predicted full scale test results.

#### C. SAFETY PURGE

The effects of off design safety purge were discussed at some length in Section II,A,1 and will not be repeated here except to state that both safety purge chamber pressure and the  $\Omega$  factor effect overall system performance and operation.

Figure II-29 is a plot of all the data points taken for the 1/8- and 1/4-scale off-design safety purge tests. The trend of the data is in agreement with other 1/4-scale test data in that slightly better performance is exhibited with the 1/4-scale than with the 1/8-scale.

Figure II-29 shows only one point in the starting transient of the engine; namely, the ejector start point. It is known that  $\Omega$  and  $P_{sc}$  will influence the performance of the system throughout the engine start period but the exact magnitude of these effects is unknown.

---

<sup>1</sup>Evaluation Report, 90° Turn Ejectors for Engine Test Stand -1, Aerojet Report No. 2403, November 1962.

## D. PRE-FIRE PURGE

The scale-model experimental test results indicate that a safe oxygen content (a content of less than 4% by volume) is obtained by purging with approximately 1.5 ejector-system (including engine compartment) volumes of nitrogen. This amounts to approximately 1000 lb of nitrogen, if the ejector system volume pressure is 1 atmosphere. Because of the strong dependence of purge nozzle locations and orientations on reducing the oxygen content in semi-isolated areas, it is recommended that serious consideration be given to the location and orientation of these nozzles. A checkout run at NTS to determine the oxygen content in various locations in the engine compartment (corners, thrust structure, and other semi-isolated areas), as a function of pre-fire purge-flow duration, is required for safety considerations. Since safe operation of the ejector system must be assured, a safety factor of at least 2 is recommended in the amount of nitrogen used for purging.

## E. ENGINE COMPARTMENT TEMPERATURE SURVEY

Five thermocouples were installed in various locations of the engine compartment (Figure II-30) for the purpose of determining the effects of the nozzle on equipment located in the engine compartment. Based on the following model, the heating is one of radiation only. The following model employs:

1. Symbols
  - (a)  $T_v-1$  - Cell temperature (shown in Figure II-30)
  - (b)  $T_{cp}$  - Thrust Chamber Wall Temperature
  - (c)  $cp$  - Thrust Chamber
  - (d)  $v$  - Engine compartment
  - (e)  $Q$  - Heat Flux
2. Diameter of thermocouple = .06 in.
3.  $\epsilon$  = emissivity stainless steel = 0.2
4.  $\alpha$  = absorbtivity thermocouple = 1.0

5.  $F_{Tv-1 \rightarrow v}$  - Angle Factor Thermocouple  $\rightarrow$  Compartment = 1.0

6.  $F_{cp \rightarrow Tv-1}$  - Angle Factor Chamber  $\rightarrow$  Thermocouple

$$\frac{AREA_{Tv-1}}{AREA_v} = \frac{\pi D^2 / 4}{2\pi r_o h_o}$$

$$D = .06 \text{ in.}$$

$$r_o = 18 \text{ in.}$$

$$h_o = 107 \text{ in.}$$

$$= \frac{36 \times 10^{-4}}{8(18)(107)}$$

$$= .234 \times 10^{-6}$$

7. Area of Tv-1 = .785 (36 x 10<sup>-4</sup>) = 28.2 x 10<sup>-4</sup>

8. Surface area of thrust chamber = 2 $\pi$ rh = 6.28 (3.5)(104.7)

$$= 2.350 \times 10^3$$

9. Heat Balance

$$Q_{cp} = Q_{Tv-1}$$

$$\epsilon A_{cp} F_{cp \rightarrow Tv-1} T_{cp}^4 = \alpha A_{Tv-1 \rightarrow v} T_{Tv-1}^4$$

$$\left[ \frac{T_{cp}}{T_{Tv-1}} \right]^4 = \frac{\alpha A_{Tv-1} F_{Tv-1 \rightarrow v}}{\epsilon A_{cp} F_{cp \rightarrow Tv-1}}$$

$$= \frac{1.0(28.2 \times 10^{-4})(1.0)}{.2(2.350 \times 10^3)(.234 \times 10^{-6})}$$

$$= 25.6$$

$$\frac{T_{cp}}{T_{Tv-1}} = \underline{\underline{2.25}}$$

The following tabulation presents the results of Tv-1 and thrust chamber ( $T_{cp}$ ) for runs (D280LQ-30 and 34)

D280LQ-30	100% $P_c$
D280LQ-34	40% $P_c$

<u>Time</u>	<u>T<sub>V-1</sub>(°R)</u>	<u>T<sub>cp</sub>(°R)</u>	<u>T<sub>cp</sub>/T<sub>V-1</sub></u>	<u>Time</u>	<u>T<sub>V-1</sub>(°R)</u>	<u>T<sub>cp</sub>(°R)</u>	<u>(T<sub>cp</sub>/T<sub>V-1</sub>)</u>
Run 280 LQ - 30				Run 280 LQ - 34			
10.0	493	1291	2.619	8.0	552	1327	2.40
11.0	571	1327	2.324	8.3	540	1333	2.47
12.0	599	1340	2.25	9.0	552	1340	2.43
13.0	612	1365	2.23	10.0	575	1344	2.34
14.0	621	1386	2.23	11.0	590	1356	2.30
15.0	626	1390	2.22	12.0	600	1365	2.28
16.0	632	1407	2.23	13.0	604	1373	2.27
17.0	636	1418	2.23	14.0	612	1377	2.25
18.0	640	1428	2.23	16.0	6.9	1344	2.25
20.0	646	1439	2.23	18.0	625	1411	2.26
22.0	640	1449	2.24	20.0	625	1432	2.29
24.0	651	1449	2.23	22.3	633	1454	2.30
24.7	651	1454	2.23				

The actual temperature ratios of the test results shows good agreement with the analytical model. In order to predict full-scale temperatures, it will be necessary to know the properties of the materials being installed in the engine compartment.

The surface temperature of full scale engine is relatively low (order of ambient temperature); therefore, heating problems in the duct should be of little concern, due to radiation from the engine assembly.



○ — 1/8 SCALE  $T_{cp} = 955^{\circ}\text{R}, \text{H}_2$ ;  $T_{sc} = 1088^{\circ}\text{R}, \text{N}_2$ ;  $P_{sc} = 101 \text{ psia}$

□ — 1/4 SCALE  $T_{cp} = 1033^{\circ}\text{R}, \text{H}_2$ ;  $T_{sc} = 1500^{\circ}\text{R}, \text{N}_2$ ;  $P_{sc} = 126 \text{ psia}$

( VALUES ARE FOR EJECTOR STARTING POINT )

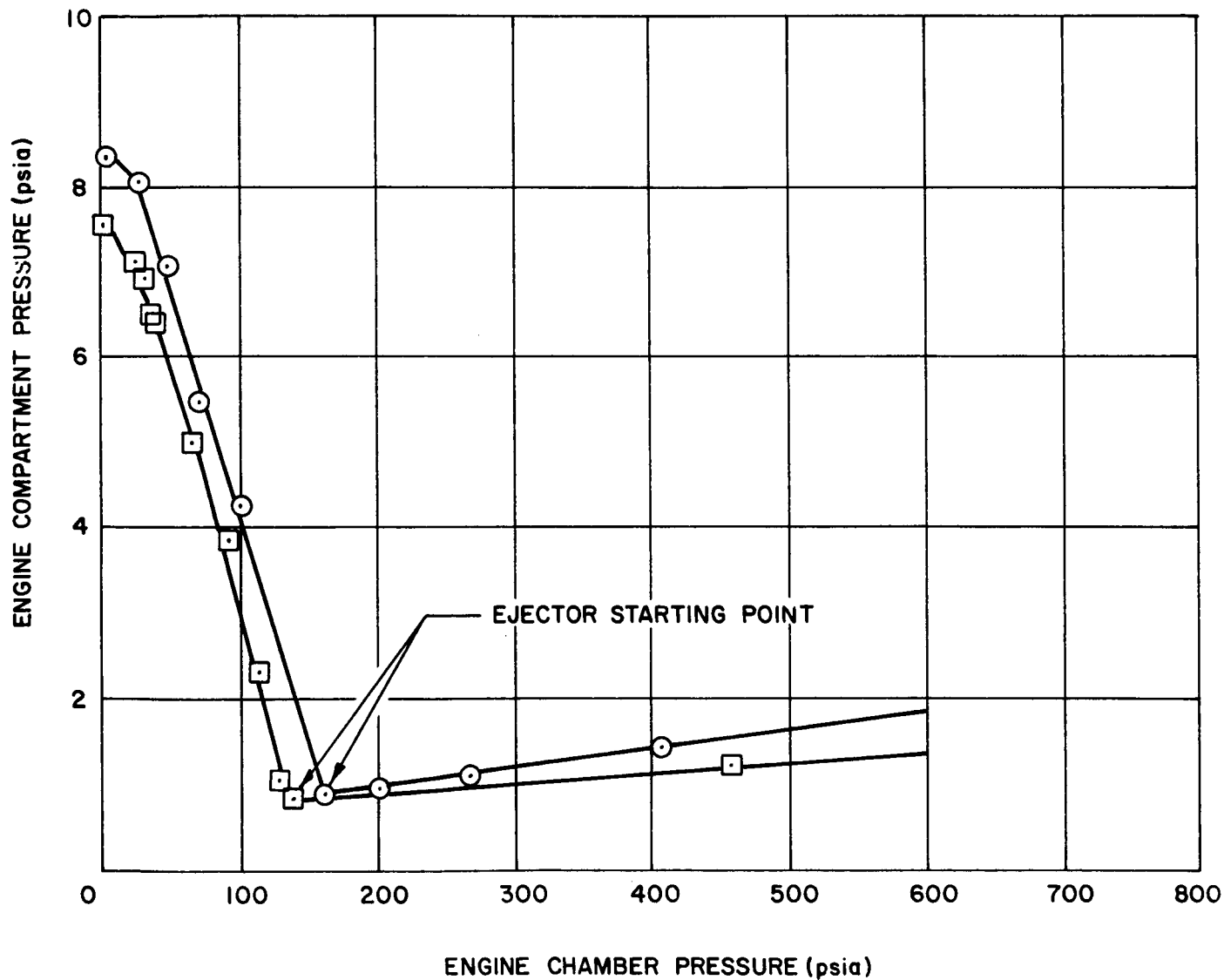


Figure II-1

Comparison of Performance Between  
1/8- and 1/4-Scale Ejector Systems (10:1 Nozzle)

- — 1/8 SCALE  $T_{cp} = 681^{\circ}\text{R}, \text{N}_2$ ;  $T_{sp} = 515^{\circ}\text{R}, \text{N}_2$ ;  $P_{sc} = 111 \text{ psia}$   
 □ — 1/4 SCALE  $T_{cp} = 1499^{\circ}\text{R}, \text{N}_2$ ;  $T_{sp} = 1308^{\circ}\text{R}, \text{N}_2$ ;  $P_{sc} = 102 \text{ psia}$   
 (VALUES ARE FOR EJECTOR STARTING POINTS)

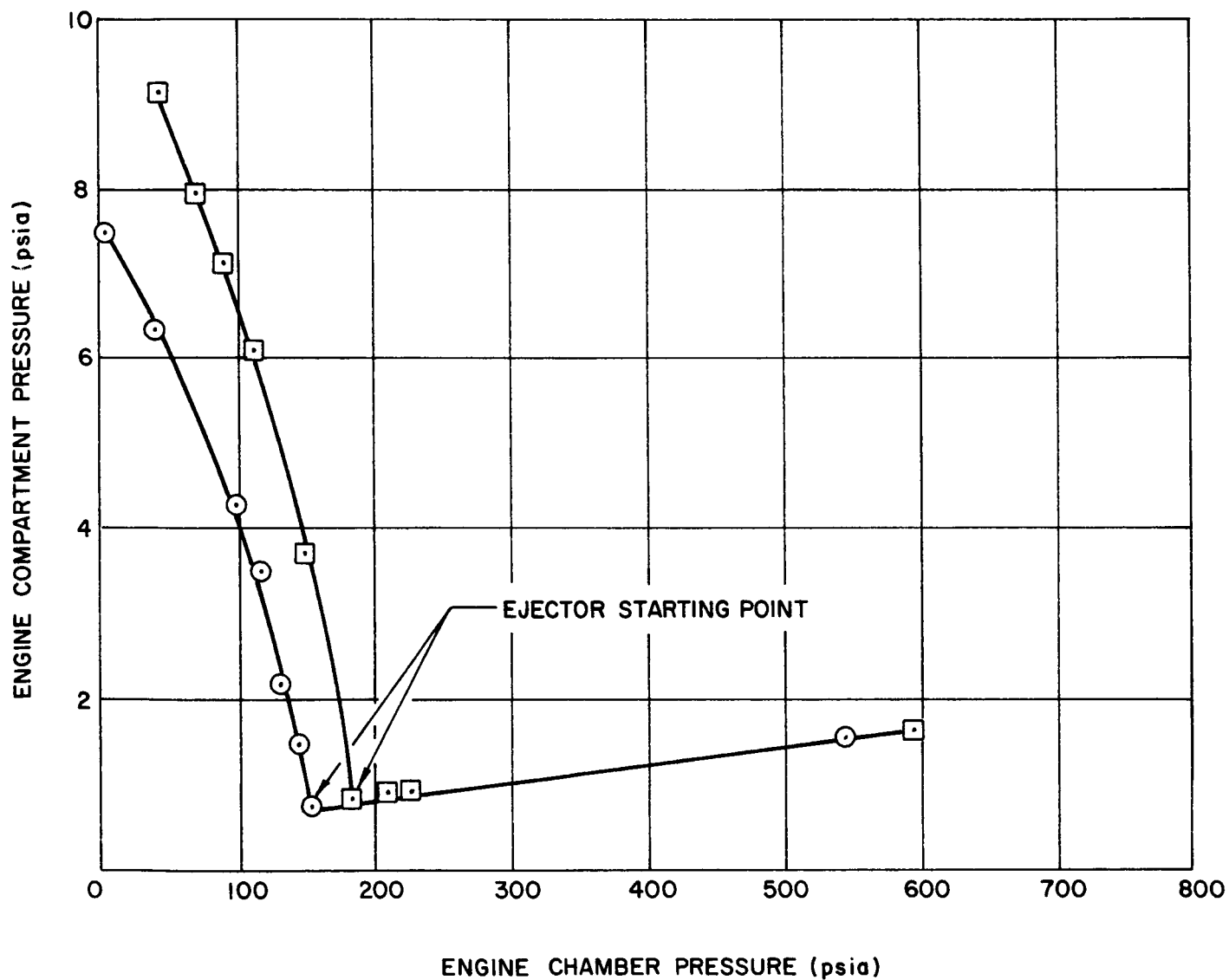


Figure II-2

Comparison of Performance Between  
1/8- and 1/4-Scale Ejector Systems (12:1 Nozzle)

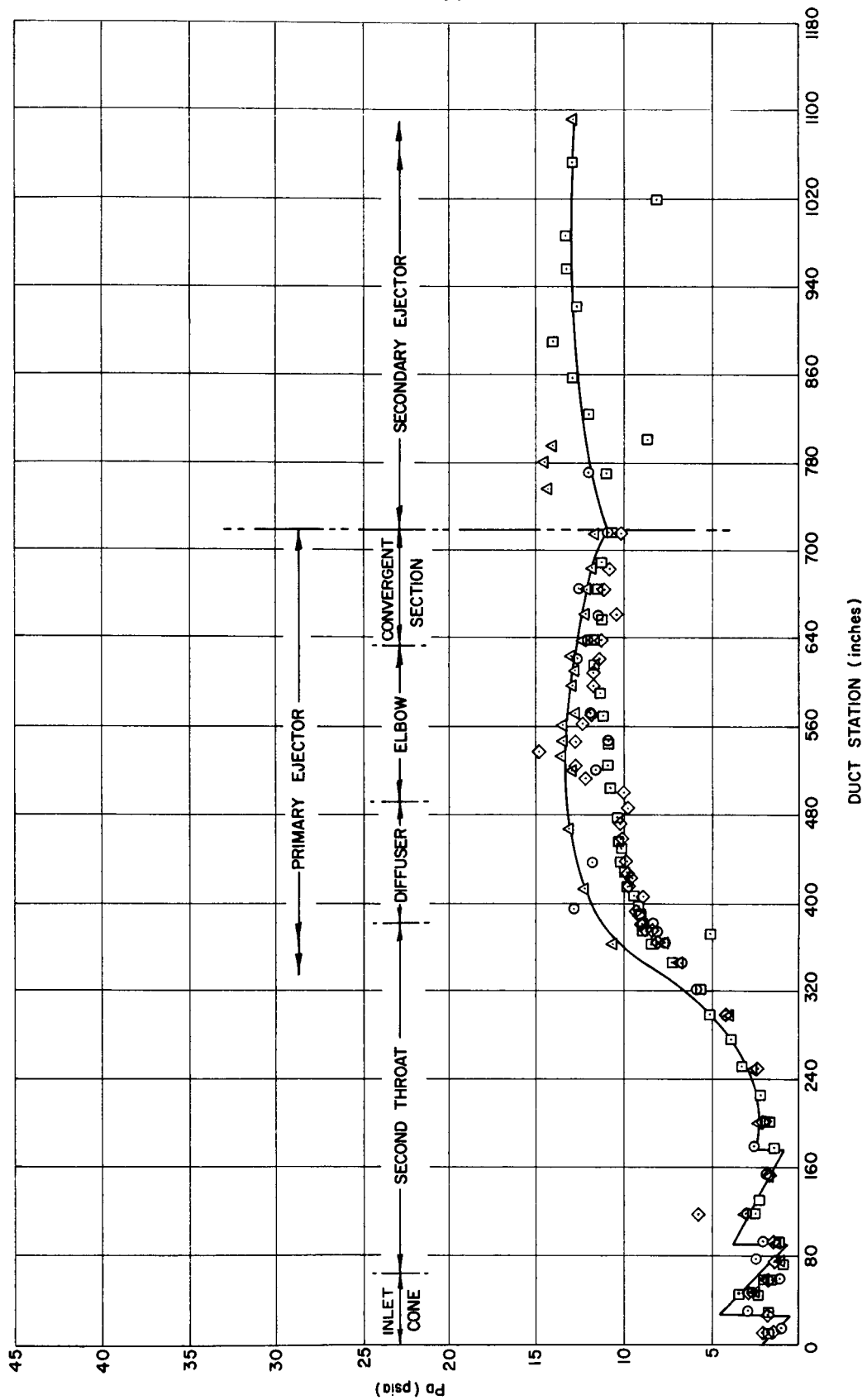


Figure II-3

Pressure Profile, Comparison of 1/8- and 1/4-Scale Data  
(10:1 Nozzle, 40%  $P_c$ )

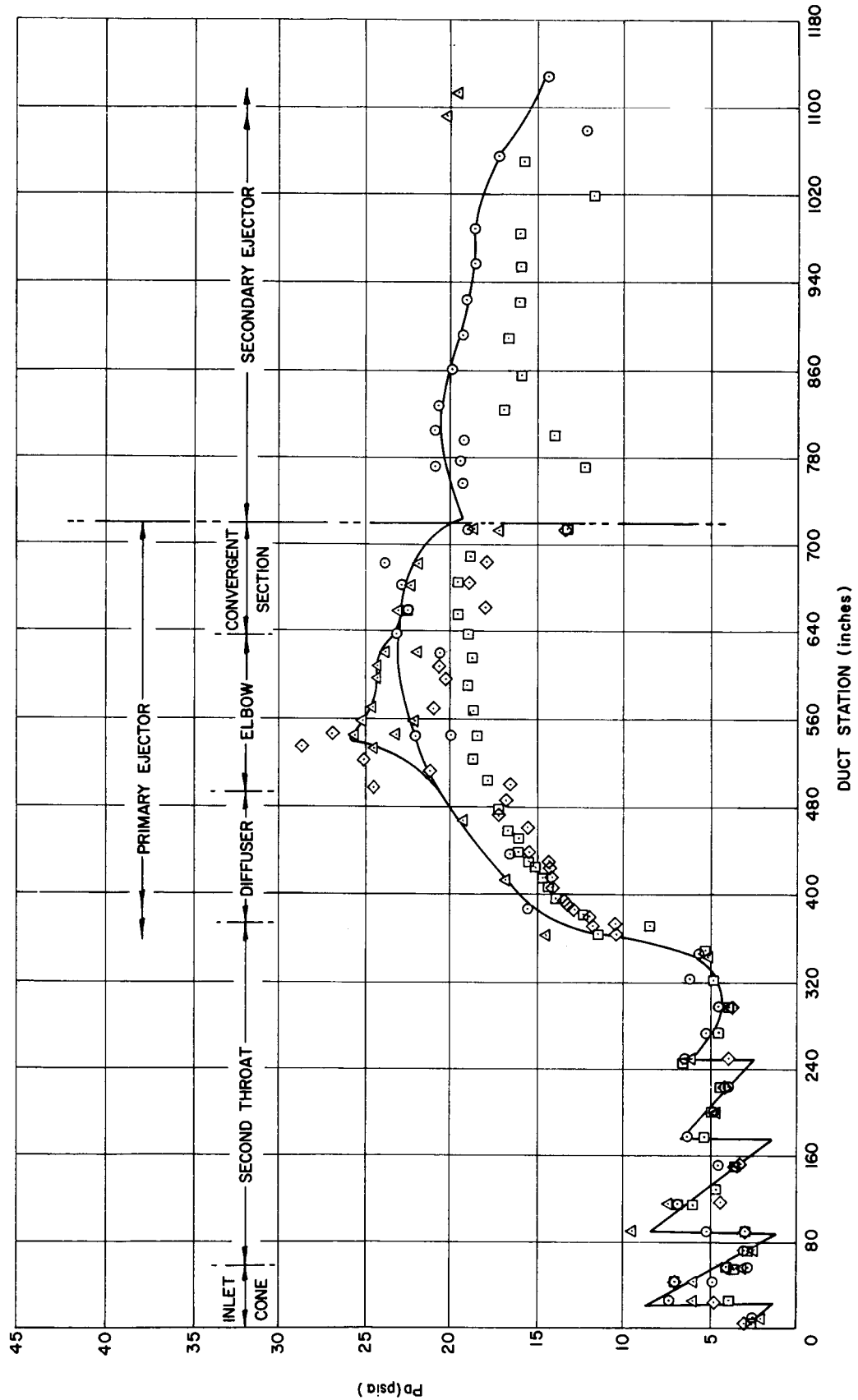


Figure II-4

Pressure Profile, Comparison of 1/8- and 1/4-Scale Data  
(10:1 Nozzle, 100%  $P_c$ )

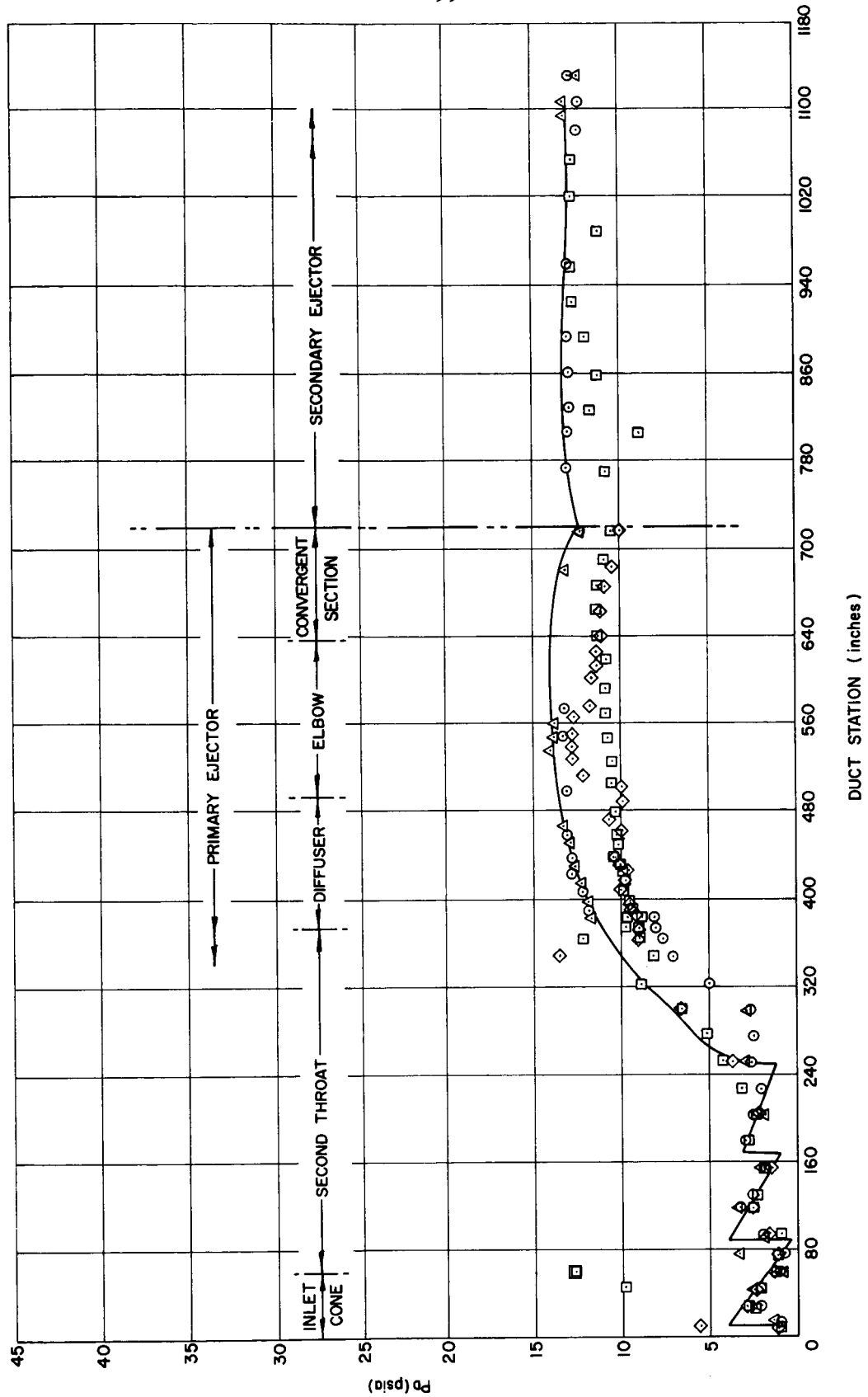


Figure II-5

Pressure Profile, Comparison of 1/8- and 1/4-Scale Data  
(12:1 Nozzle, 40%  $P_c$ )

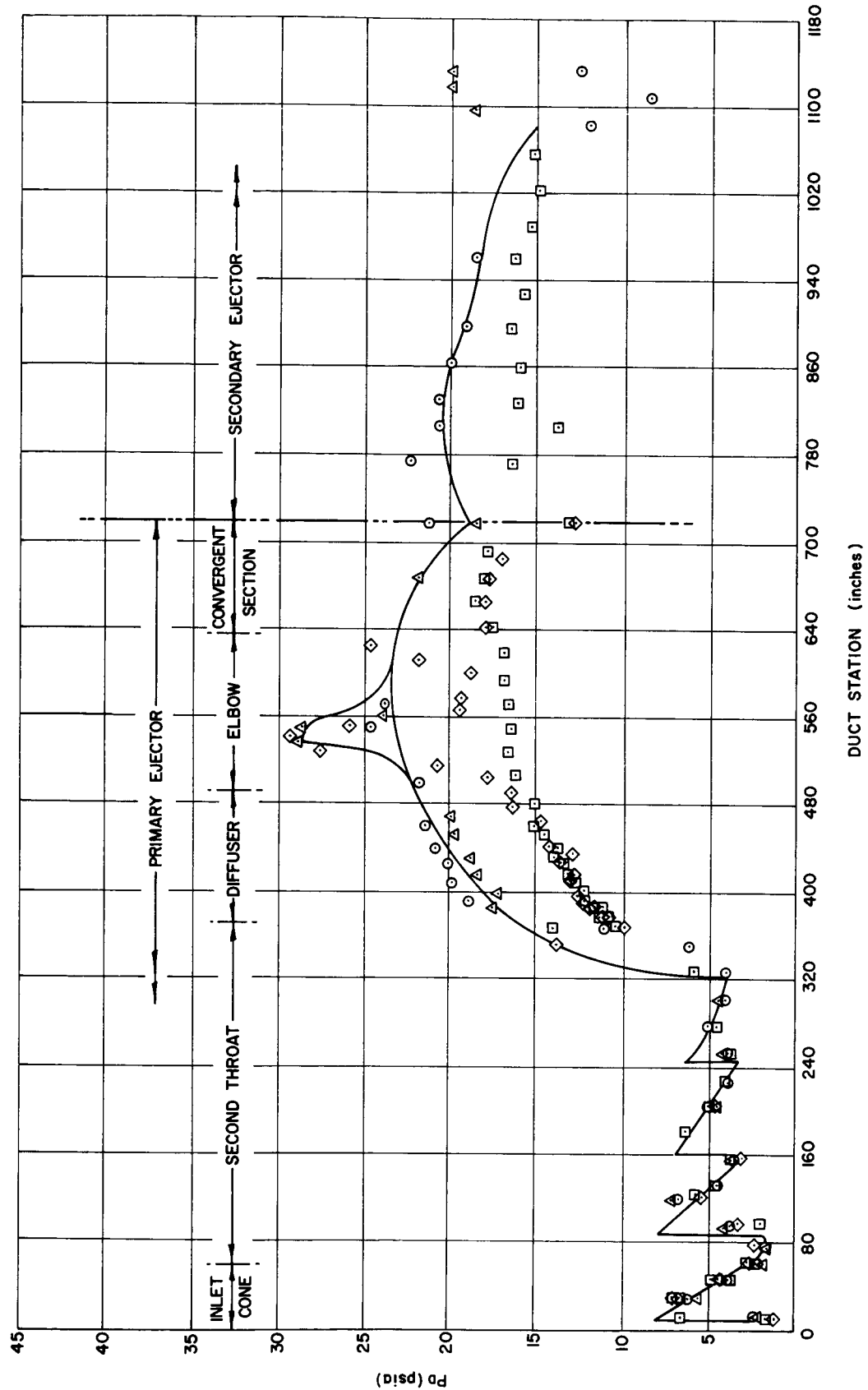


Figure II-6

Pressure Profile, Comparison of 1/8- and 1/4-Scale Data  
(12:1 Nozzle, 100%  $P_c$ )

## NOTES.

## 1. LEGEND

- PREDICTED FULL SCALE MACH NO. PROFILE  
 □ INSIDE DATA POINTS — 1/8 SCALE  
 ◇ OUTSIDE DATA POINTS — 1/8 SCALE  
 ○ INSIDE DATA POINTS — 1/4 SCALE  
 △ OUTSIDE DATA POINTS — 1/4 SCALE

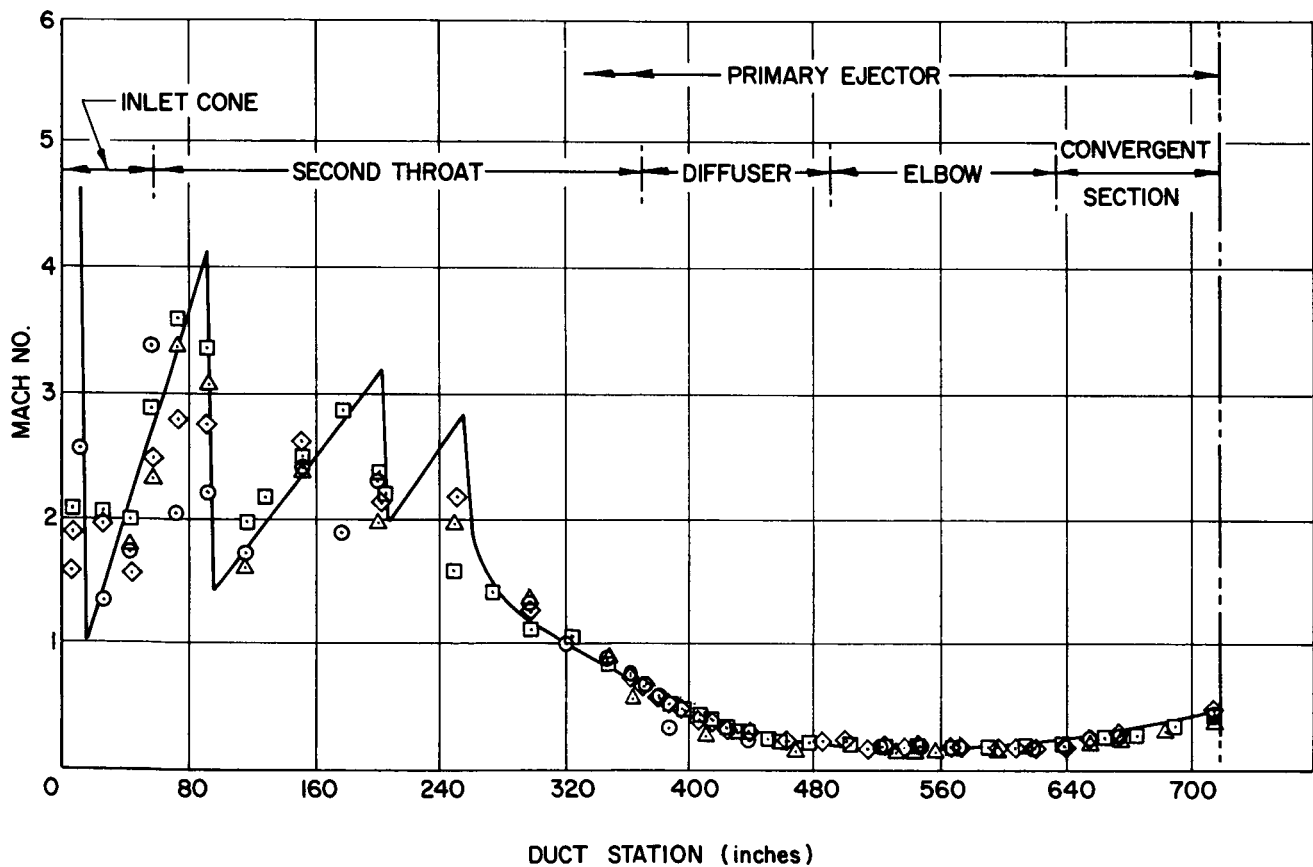


Figure II-7

Mach No. Profile, Comparison of 1/8- and 1/4-Scale Data  
 (10:1 Nozzle, 40%  $P_c$ )

## NOTES.

## 1. LEGEND

- PREDICTED FULL SCALE MACH NO. PROFILE  
 □ INSIDE DATA POINTS — 1/8 SCALE  
 ◇ OUTSIDE DATA POINTS — 1/8 SCALE  
 ○ INSIDE DATA POINTS — 1/4 SCALE  
 △ OUTSIDE DATA POINTS — 1/4 SCALE

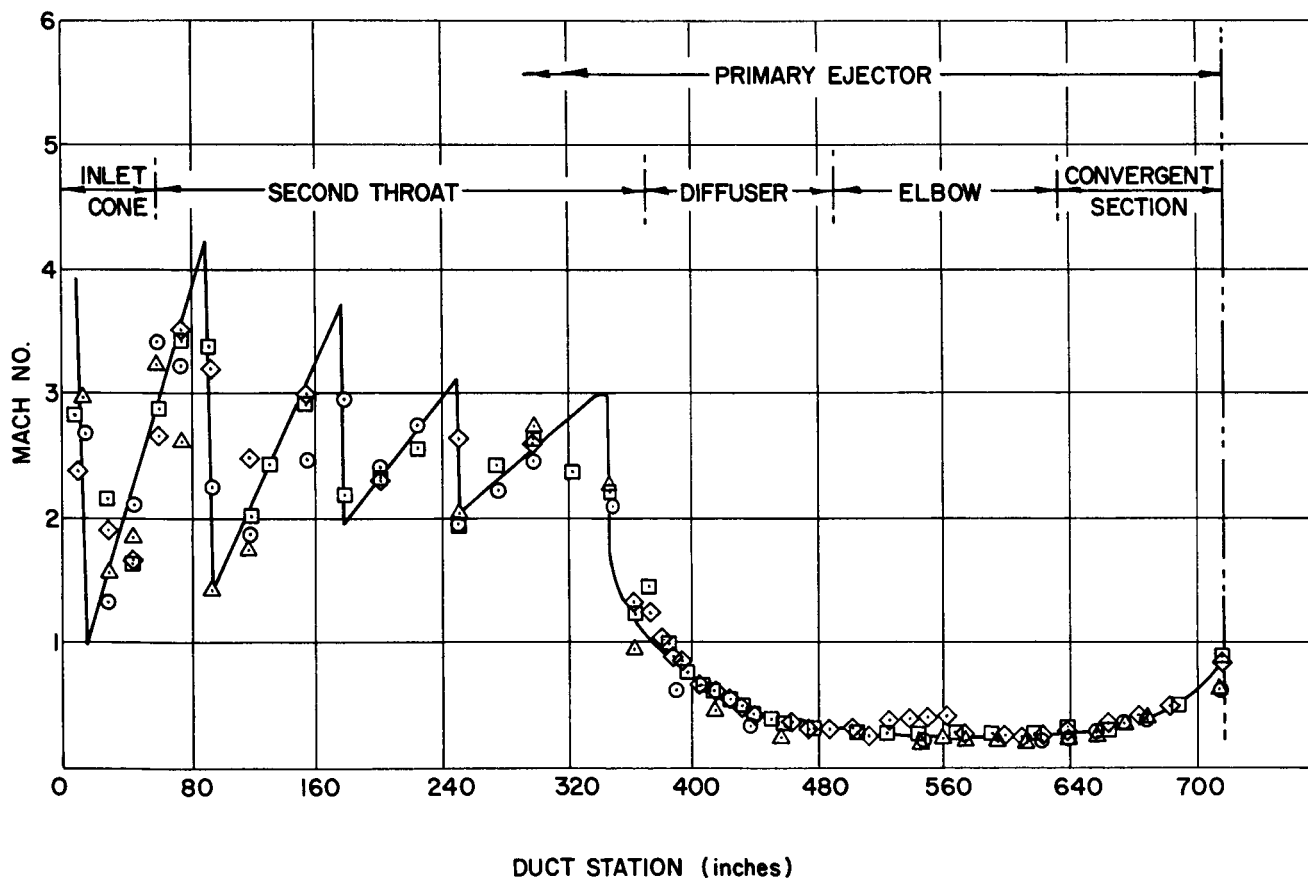


Figure II-8

Mach No. Profile, Comparison of 1/8- and 1/4-Scale Data  
 (10:1 Nozzle, 100%  $P_c$ )



## NOTES.

## I. LEGEND

- PREDICTED FULL SCALE MACH NO. PROFILE  
 □ INSIDE DATA POINTS — 1/8 SCALE  
 ◇ OUTSIDE DATA POINTS — 1/8 SCALE  
 ○ INSIDE DATA POINTS — 1/4 SCALE  
 △ OUTSIDE DATA POINTS — 1/4 SCALE

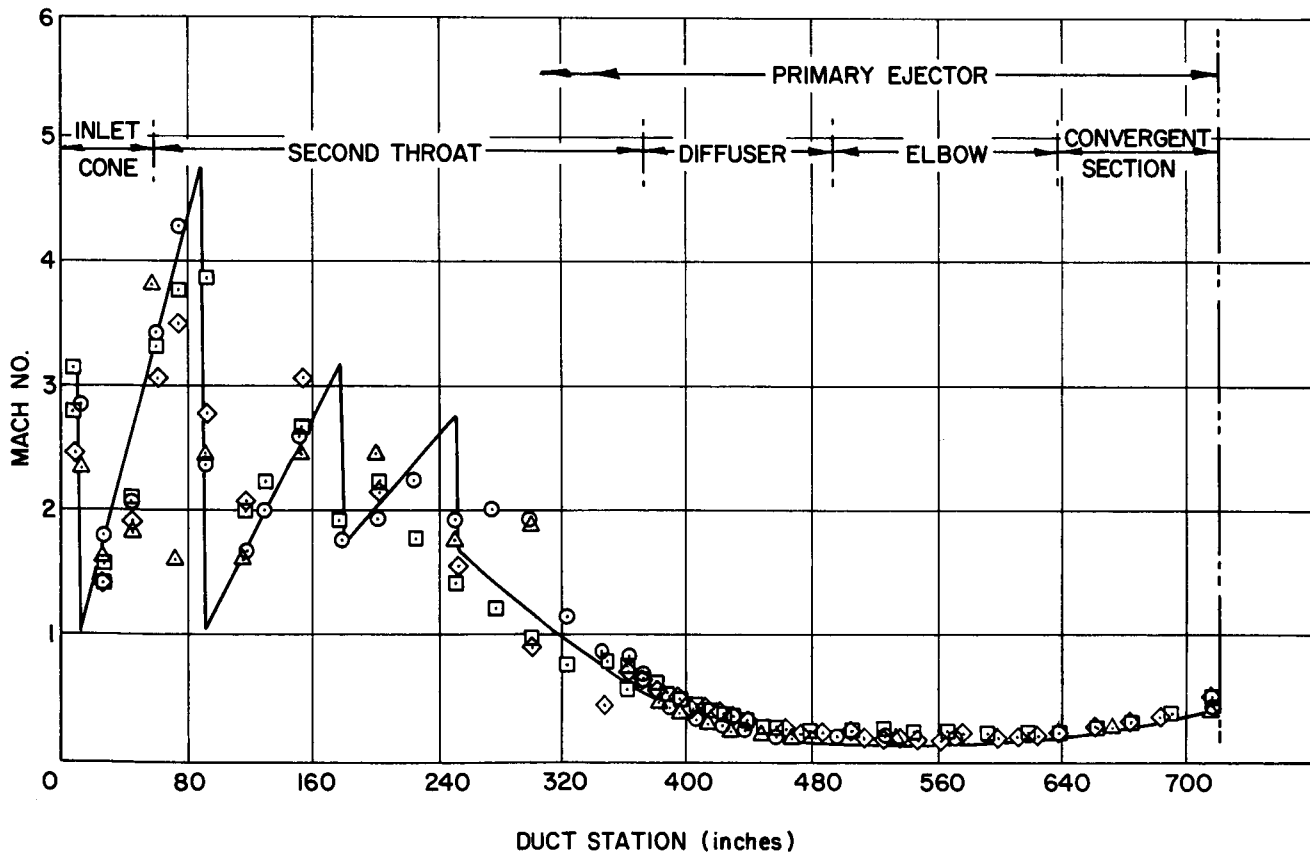


Figure II-9

Mach No. Profile, Comparison of 1/8- and 1/4-Scale Data  
 (12:1 Nozzle, 40%  $P_c$ )

## NOTES.

## I. LEGEND

- PREDICTED FULL SCALE MACH NO. PROFILE  
 □ INSIDE DATA POINTS — 1/8 SCALE  
 ◇ OUTSIDE DATA POINTS — 1/8 SCALE  
 ○ INSIDE DATA POINTS — 1/4 SCALE  
 △ OUTSIDE DATA POINTS — 1/4 SCALE

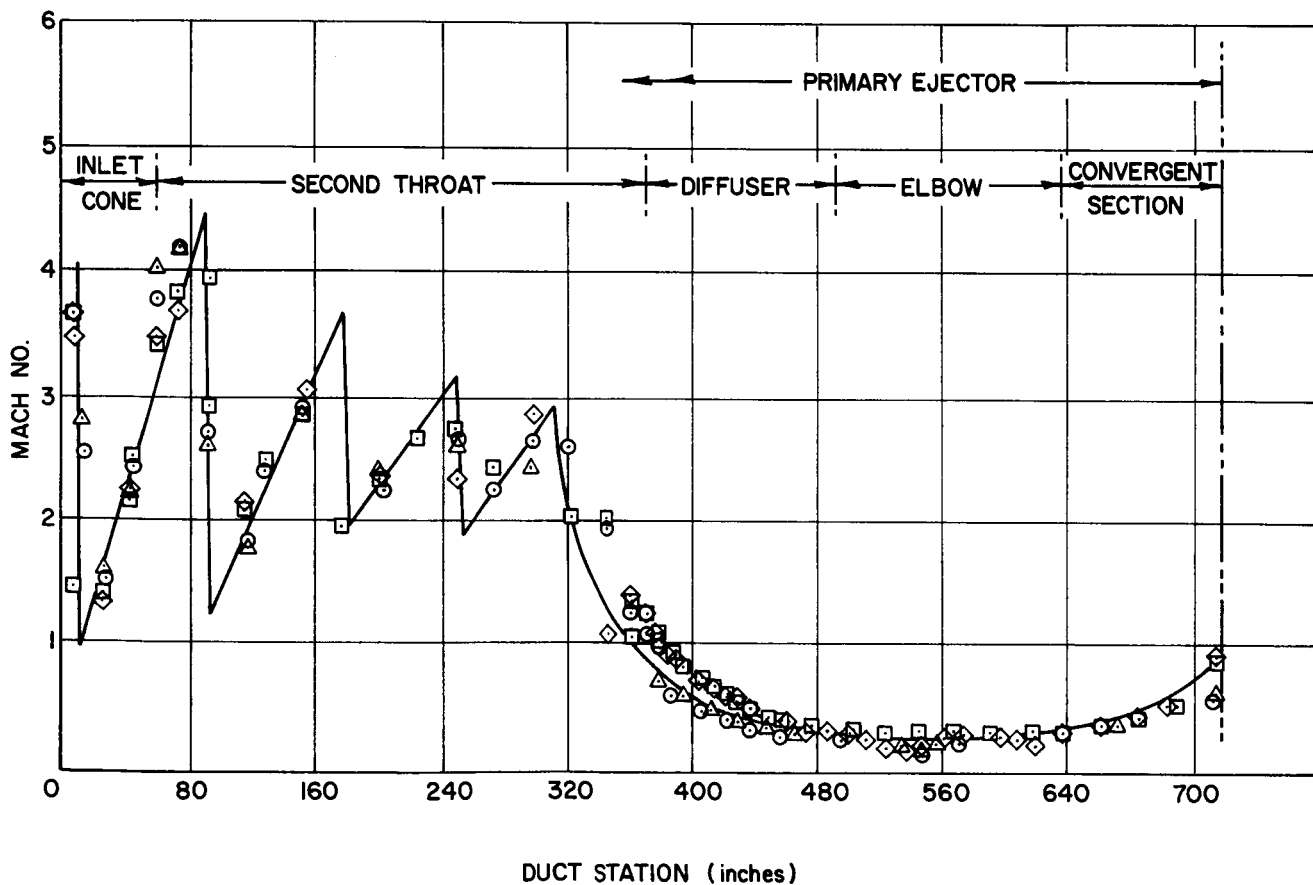


Figure II-10

Mach No. Profile, Comparison of 1/8- and 1/4-Scale Data  
 (12:1 Nozzle, 100%  $P_c$ )

## NOTES

- ① ORIGIN FOR "L" DIMENSIONS FOR PRIMARY EJCTOR  
 ② ORIGIN FOR "L" DIMENSIONS FOR SECONDARY EJCTOR.

## 3 JOINTS

- ①  $L/D_2 = 0.82$   
 ②  $L/D_2 = 1.35$   
 ③  $L/D_2 = 9.38$   
 ④  $L/D_2 = 12.02$   
 ⑤  $L/D_2 = 16.26$   
 ⑥  $L/D_2 = 18.20$   
 ⑦  $L/D_2 = 18.57$  PRIMARY EXIT  
 ⑧  $L/D_2 = 6.65$   
 ⑨  $L/D_2 = 8.07$  SECONDARY EXIT.

4. PSE-1, PSE-2, PSE-3 & PSE-4  $L/D_2 = 18.54$

5. TO OBTAIN FULL SCALE STATION NUMBERS  
 IN PRIMARY EJCTOR MULTIPLY  $L/D_2$   
 BY 38.6

6. TO OBTAIN FULL SCALE STATION  
 NUMBERS IN SECONDARY  
 EJCTOR MULTIPLY  $L/D_2$   
 BY 52.0

PRESSURE TAP	L D <sub>2</sub>	PRESSURE TAP	L D <sub>2</sub>	PRESSURE TAP	L D <sub>2</sub>
PD-1	0.29	PD-28	11.81	PD-56	12.81
PD-2	0.68	PD-29	12.03	PD-57	12.97
PD-3	1.10	PD-30	12.81	PD-58	12.03
PD-4	1.49	PD-31	15.46	PD-59	11.51
PD-5	1.89	PD-32	14.11	PD-60	11.50
PD-6A	2.54	PD-33	14.17	PD-61	11.30
PD-6	2.98	PD-34	15.41	PD-62	11.05
PD-7	3.30	PD-35	15.00	PD-63	10.89
PD-8	3.92	PD-36	12.50	PD-64	10.69
PD-9	4.66	PD-37	16.93	PD-65	10.45
PD-10	5.17	PD-38	17.38	PD-66	10.24
PD-11	5.80	PD-39	7.15	PD-67	10.02
PD-12	6.44	PD-40	18.51	PD-68	9.85
PD-13	7.05	PD-41	18.51	PD-69	9.60
PD-14	7.68	PD-42	17.15	PD-70	9.35
PD-15	8.30	PD-43	17.38	PD-71	8.95
PD-16	8.95	PD-44	2.45	PD-72	7.68
PD-17	9.35	PD-45	6.50	PD-73	6.44
PD-18	9.60	PD-46	16.06	PD-74	5.17
PD-19	9.84	PD-47	15.15	PD-75	5.92
PD-20	10.02	PD-48	15.41	PD-76	5.98
PD-21	10.25	PD-49	15.09	PD-77	2.54
PD-22	10.45	PD-50	14.17	PD-78	1.89
PD-23	10.66	PD-51	14.44	PD-79	1.49
PD-24	10.89	PD-52	14.11	PD-80	1.10
PD-25	11.05	PD-53	15.19	PD-81	0.68
PD-26	11.30	PD-54	15.46	PD-82	0.29
PD-27	11.80	PD-55	3.14		

## SECONDARY DUCT

PRESSURE TAP	L D <sub>2</sub>	PRESSURE TAP	L D <sub>2</sub>	PRESSURE TAP	L D <sub>2</sub>
PSD-2	1.04	PSD-8	4.42	PSD-14	7.95
PSD-3	1.67	PSD-9	5.24	PSD-15	7.93
PSD-4	2.11	PSD-10	5.82	PSD-16	7.69
PSD-5	2.73	PSD-11	6.50	PSD-17	7.24
PSD-6	3.36	PSD-12	6.98		
PSD-7	4.00	PSD-13	7.46		

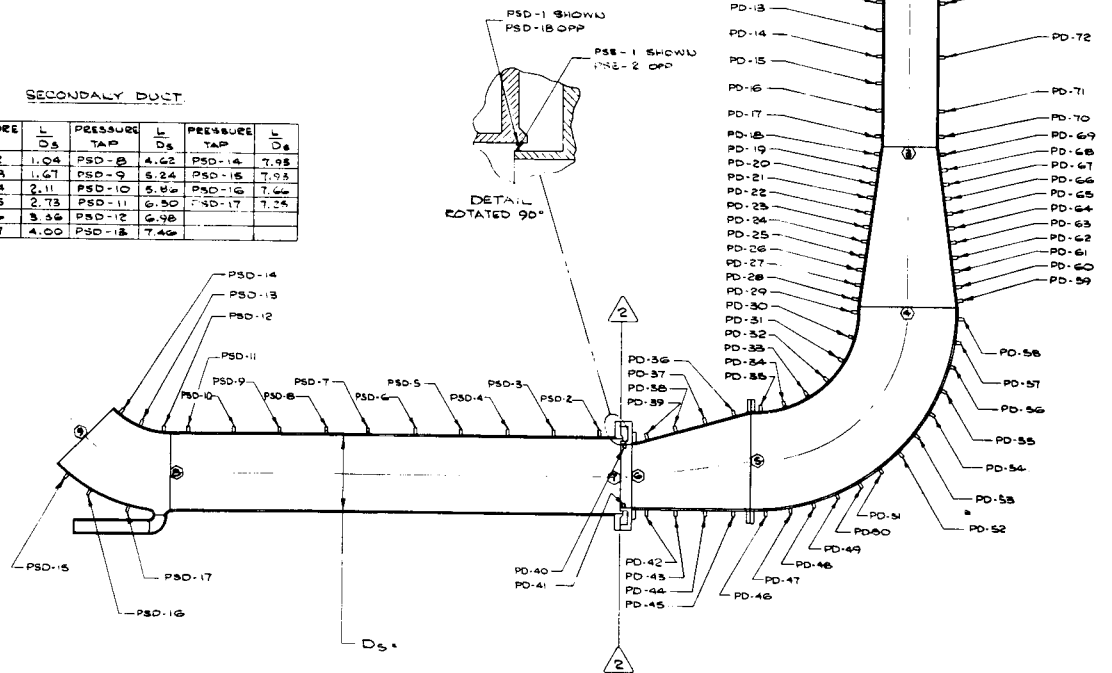


Figure II-11

Pressure Tap Locations

- NOTES. 1. COMPARISON OF 1/4 & 1/8 SCALE  
 2.  $P_{e-2}$  = NOZZLE EXIT PRESSURE  
 3. SEAL LEAKAGE FLOW = 1.50 lb/sec  
 4. SAFETY PURGE AT DESIGN VALUE  
 5.  $P_a$  = 12.8 psia  
 6 RUN NO.  
 280 - LQ - 12 (1/4 SCALE)  
 276 - LQ - 110 (1/8 SCALE)

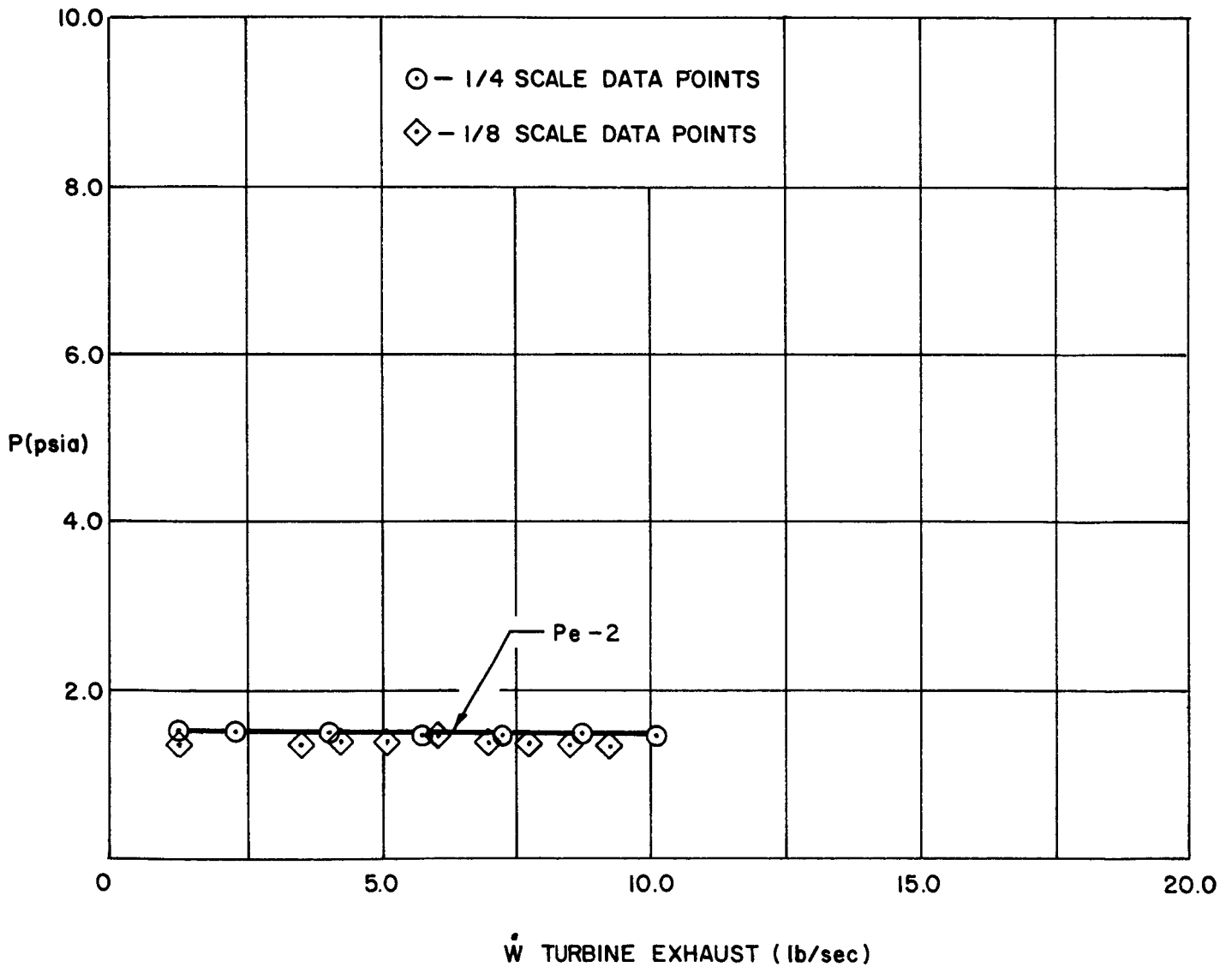


Figure II-12

Nozzle Exit Pressure vs Turbine Exhaust  
 Flow Rate when Testing the 10:1 Nozzle, 40%  $P_c$

- NOTES. 1. COMPARISON OF 1/4 & 1/8 SCALE  
 2.  $P_v-2$  = ENGINE COMPARTMENT PRESSURE  
 3. SEAL LEAKAGE FLOW = 1.50 lb/sec  
 4. SAFETY PURGE AT DESIGN VALUE  
 5.  $P_a = 12.8$  psia  
 6. RUN NO.  
 280-LQ-12 (1/4 SCALE)  
 276-LQ-110 (1/8 SCALE)

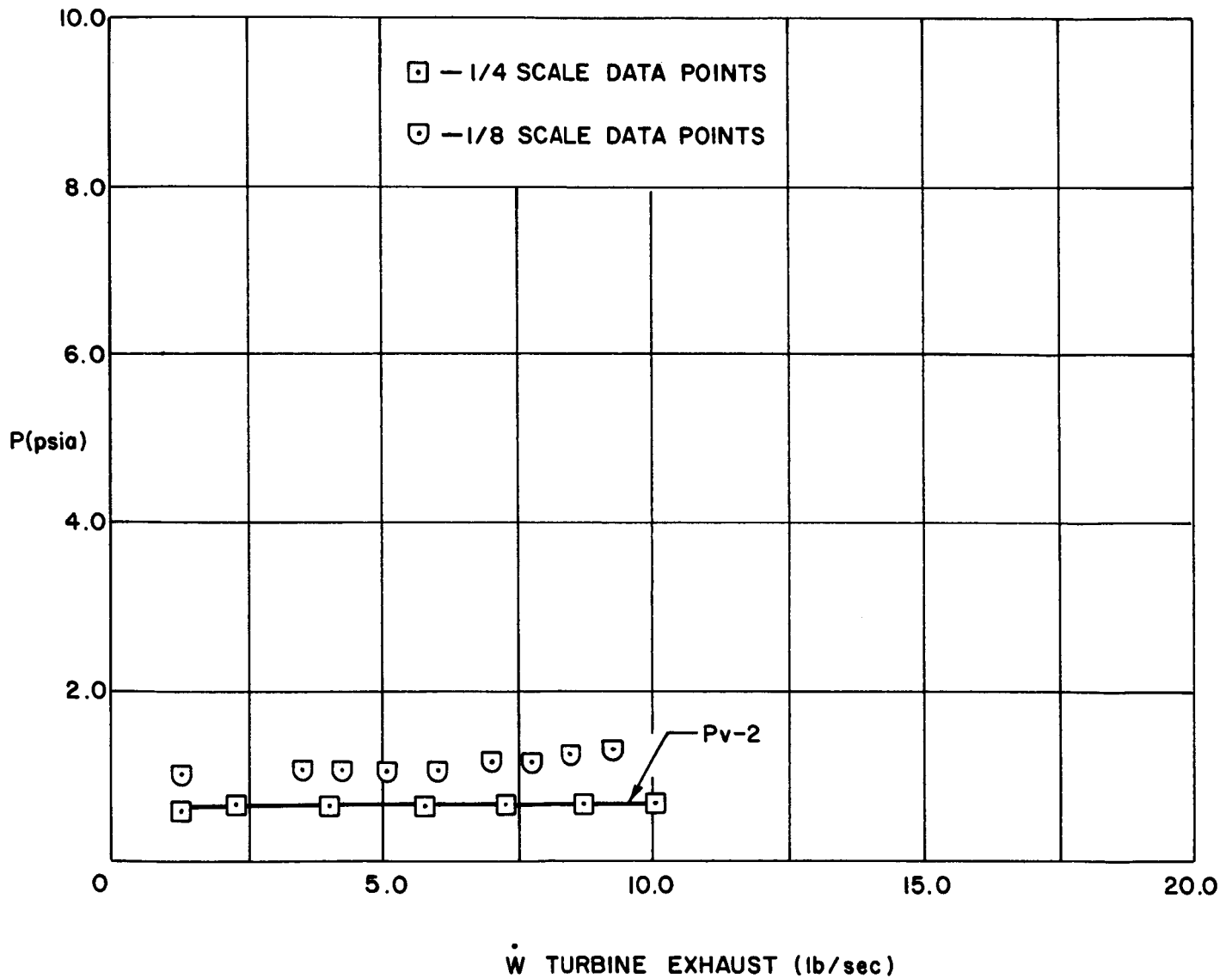


Figure II-13

Engine Compartment Pressure vs Turbine Exhaust  
 Flow Rate when Testing the 10:1 Nozzle, 40%  $P_c$

- NOTES 1. COMPARISON OF 1/4 & 1/8 SCALE  
 2.  $P_{e-2}$  = NOZZLE EXIT PRESSURE  
 3. SEAL LEAKAGE FLOW = 1.50 lb/sec  
 4. SAFETY PURGE AT DESIGN VALUE  
 5.  $P_a = 12.8$  psia  
 6. RUN NO.

280-LQ-42 (1/4 SCALE)

276-LQ-107 (1/8 SCALE)

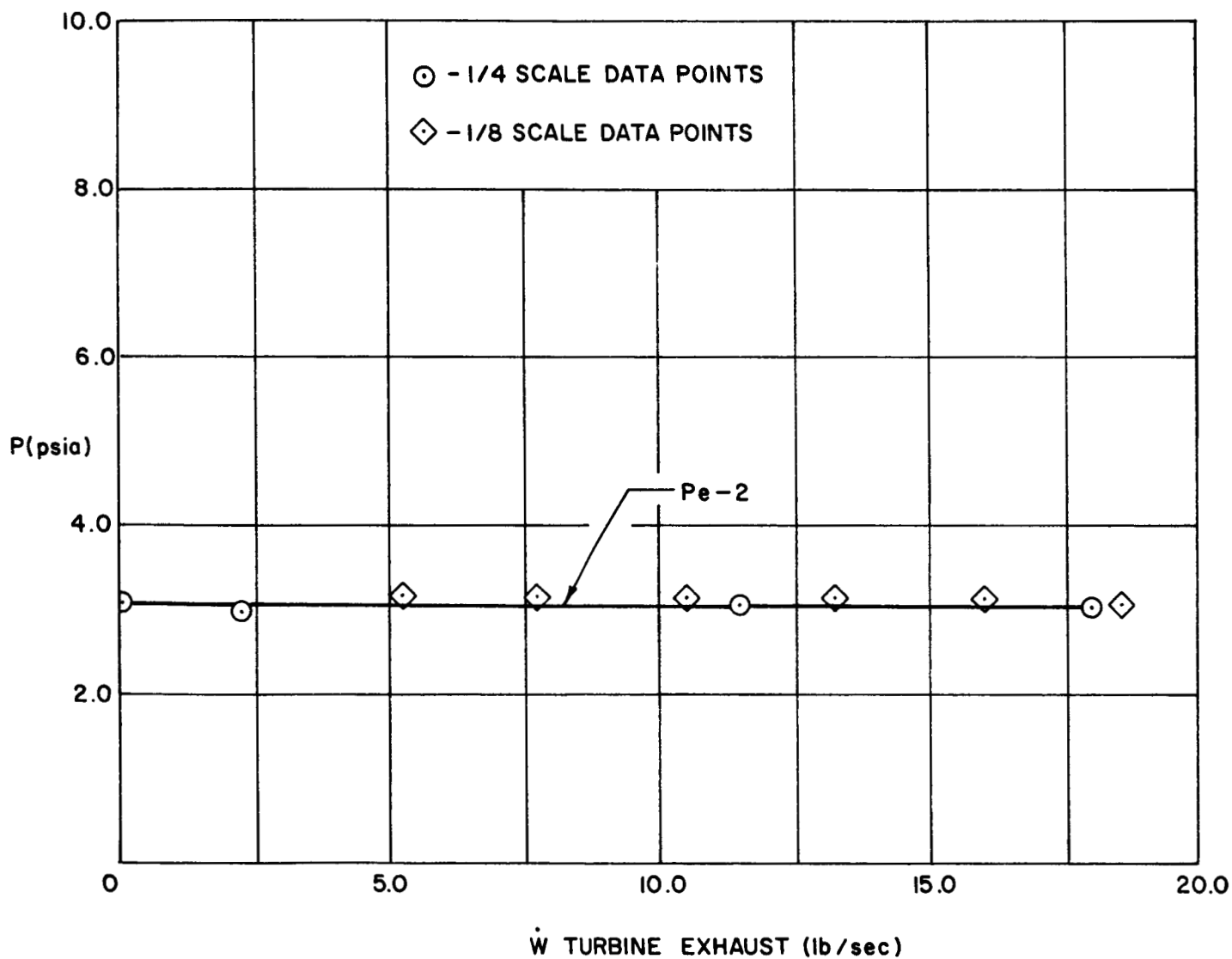


Figure II-14

Nozzle Exit Pressure vs Turbine Exhaust  
 Flow Rate when Testing the 10:1 Nozzle, 100%  $P_c$

- NOTES. 1. COMPARISON OF 1/4 & 1/8 SCALE
2.  $P_v-2$  = ENGINE COMPARTMENT PRESSURE
  3. SEAL LEAKAGE FLOW = 1.50 lb/sec
  4. SAFETY PURGE AT DESIGN VALUE
  5.  $P_a = 12.8$  psia
  6. RUN NO
    - 280 - LQ - 42 (1/4 SCALE)
    - 276 - LQ - 107 (1/8 SCALE)

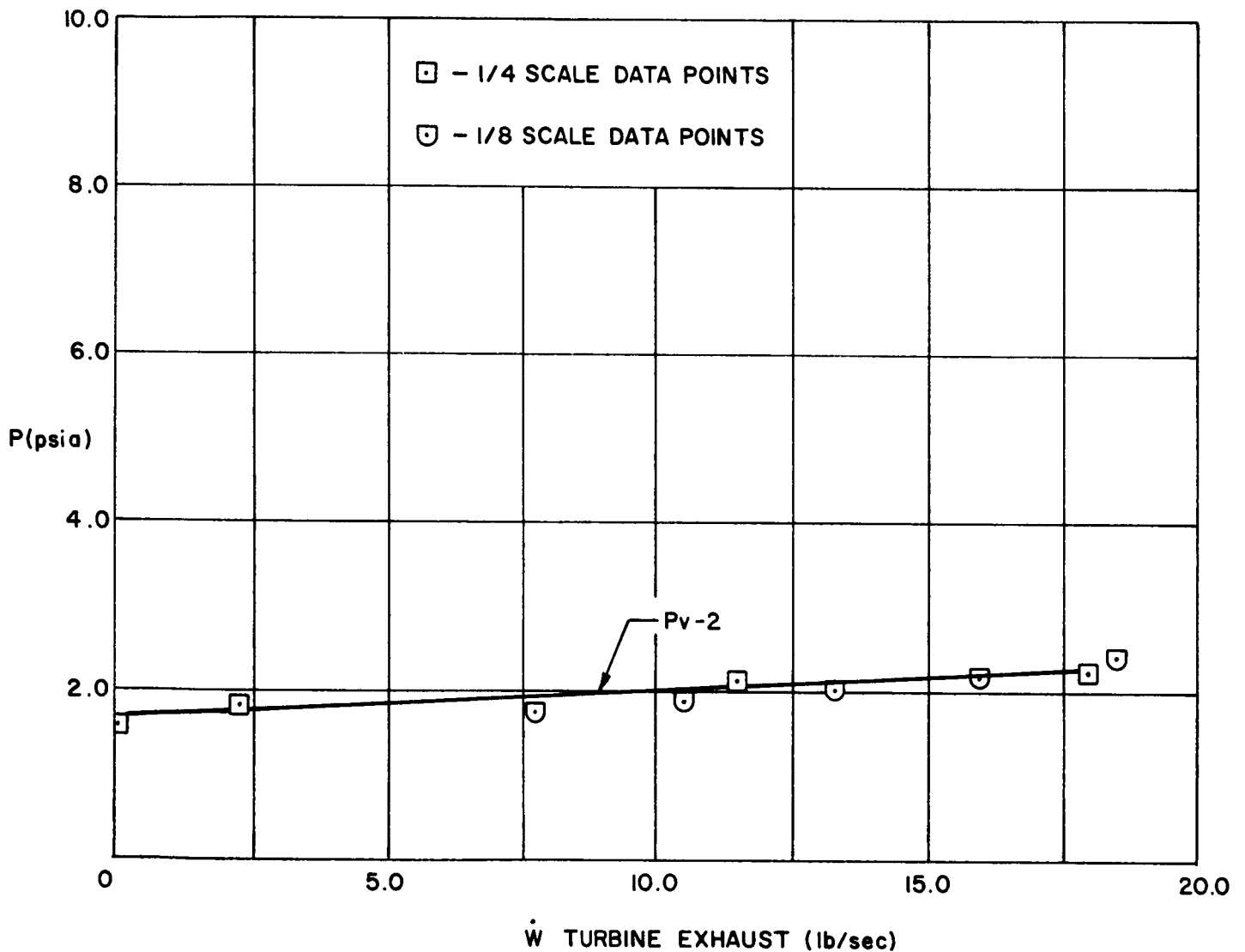


Figure II-15

Engine Compartment Pressure vs Turbine Exhaust  
Flow Rate when Testing the 10:1 Nozzle, 100%  $P_c$

- NOTES. 1. COMPARISON OF 1/4 & 1/8 SCALE  
 2.  $P_{e-2}$  = NOZZLE EXIT PRESSURE  
 3. TURBINE EXHAUST FLOW = 2.17 lb/sec  
 4. SAFETY PURGE AT DESIGN VALUE  
 5.  $P_a = 12.8$  psia  
 6. RUN NO.

280 - LQ - 17 (1/4 SCALE)

276 - LQ - 109 (1/8 SCALE)

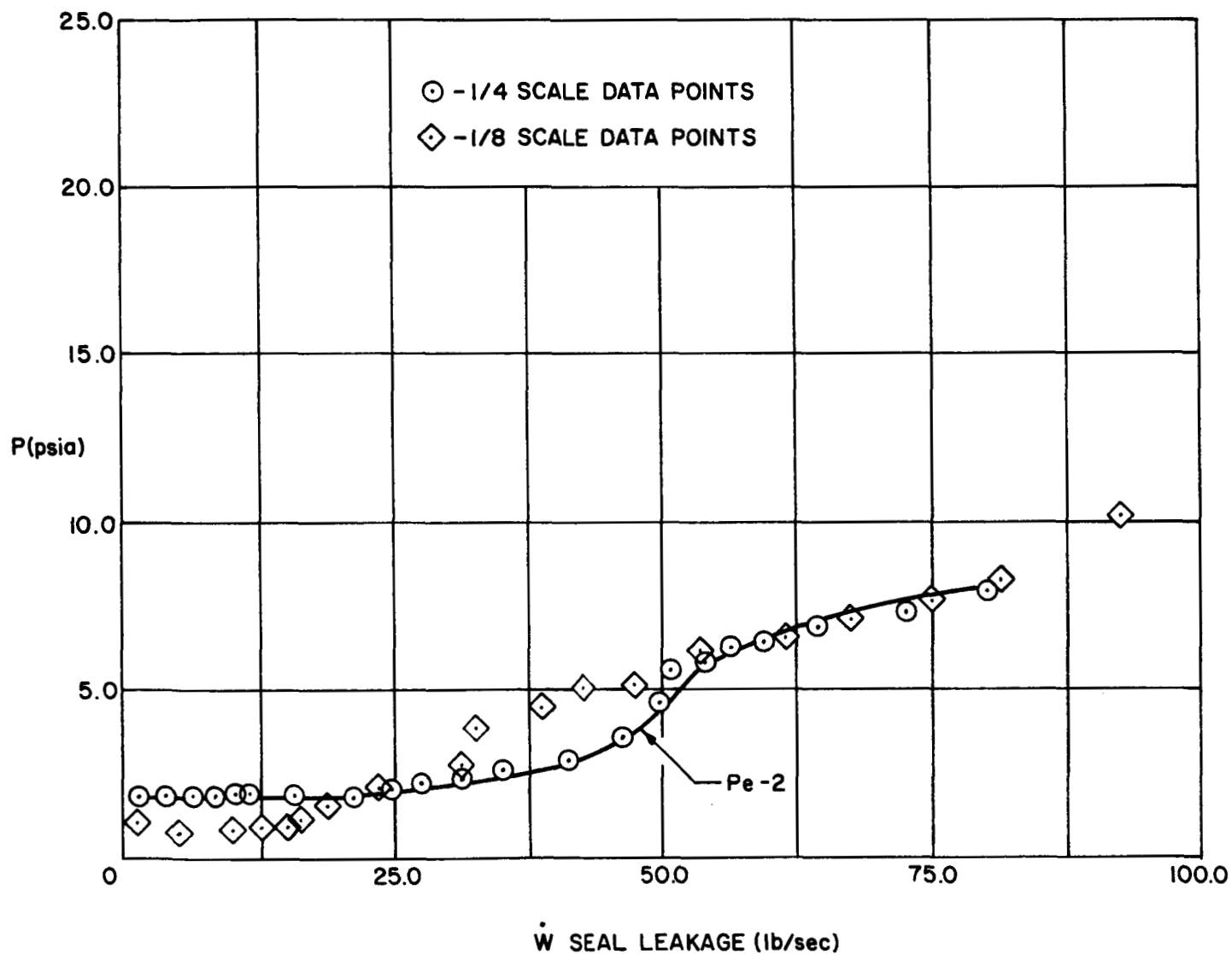


Figure II-16

Nozzle Exit Pressure vs Seal Leakage  
 Flow Rate when Testing the 10:1 Nozzle, 40%  $P_c$



- NOTES. 1. COMPARISON OF 1/4 & 1/8 SCALE  
 2.  $P_v-2$  = ENGINE COMPARTMENT PRESSURE  
 3. TURBINE EXHAUST FLOW = 2.17 lb/sec  
 4. SAFETY PURGE AT DESIGN VALUE  
 5.  $P_a = 12.8$  psia  
 6. RUN NO.  
 280-LQ-17 (1/4 SCALE)  
 276-LQ-109 (1/8 SCALE)

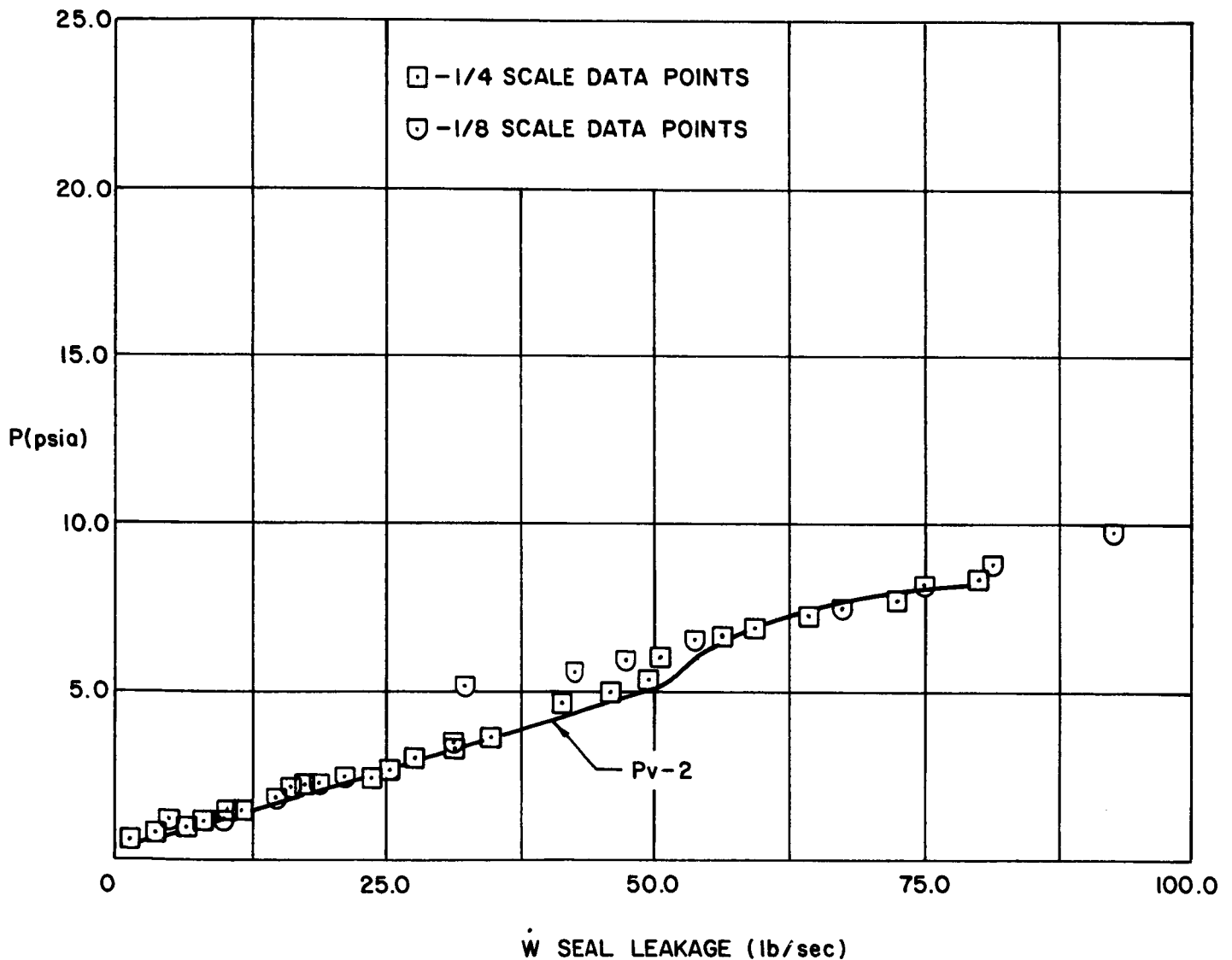


Figure II-17

Engine Compartment Pressure vs Seal Leakage  
 Flow Rate when Testing the 10:1 Nozzle, 40%  $P_c$

- NOTES. 1. COMPARISON OF 1/4 & 1/8 SCALE  
 2.  $P_{e-2}$  = NOZZLE EXIT PRESSURE  
 3. TURBINE EXHAUST FLOW = 5.6 lb/sec  
 4. SAFETY PURGE AT DESIGN VALUE  
 5.  $P_a$  = 12.8 psia  
 6. RUN NO.

280-LQ-24 (1/4 SCALE)

276-LQ-108 (1/8 SCALE)

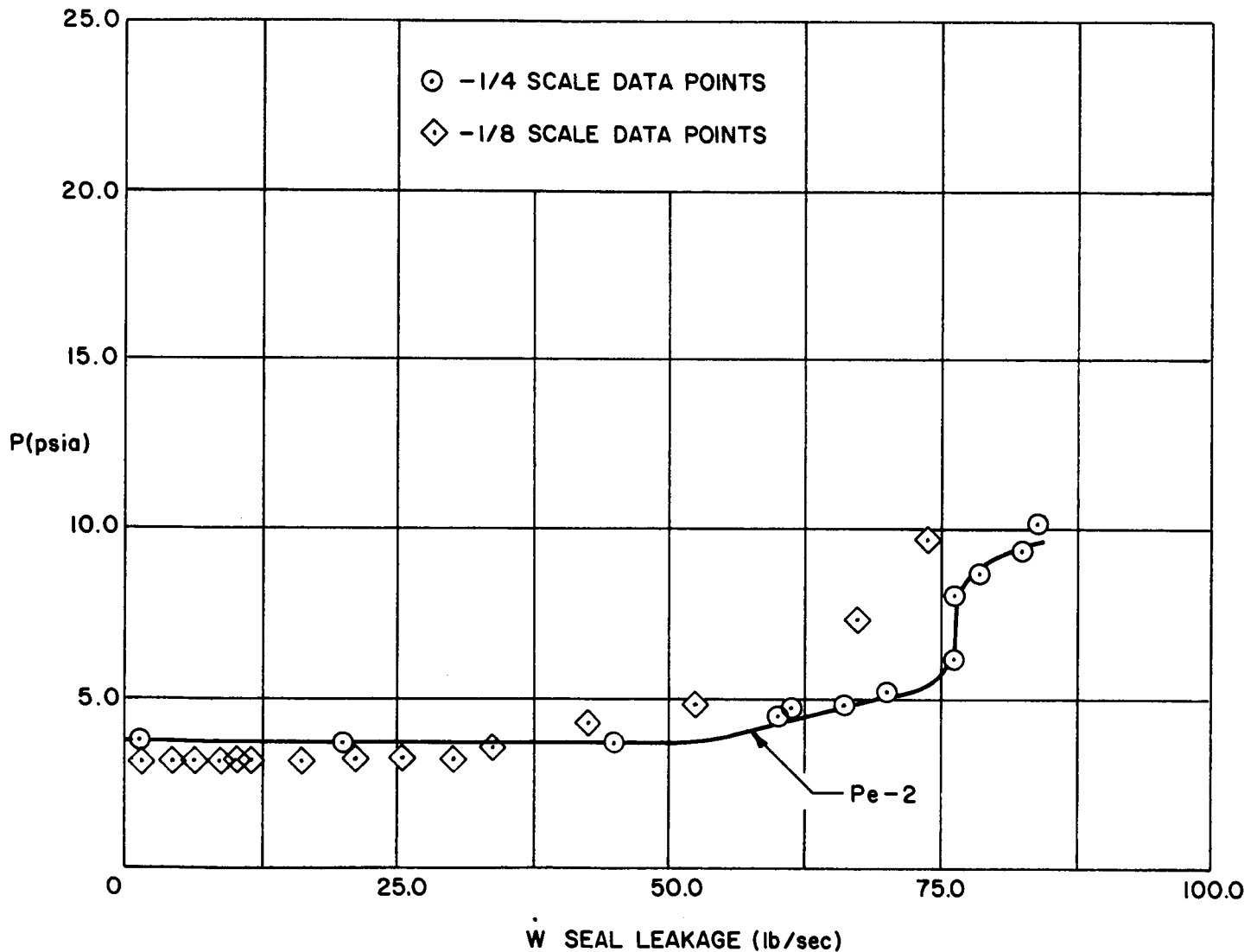


Figure II-18

Nozzle Exit Pressure vs Seal Leakage  
 Flow Rate when Testing the 10:1 Nozzle, 100%  $P_c$

- NOTES. 1. COMPARISON OF 1/4 & 1/8 SCALE  
 2. Pv-2 = ENGINE COMPARTMENT PRESSURE  
 3. TURBINE EXHAUST FLOW = 5.6 lb/sec  
 4. SAFETY PURGE AT DESIGN VALUE  
 5. Pa = 12.8 psia  
 6. RUN NO.

280-LQ-40 (1/4 SCALE)

276-LQ-108 (1/8 SCALE)

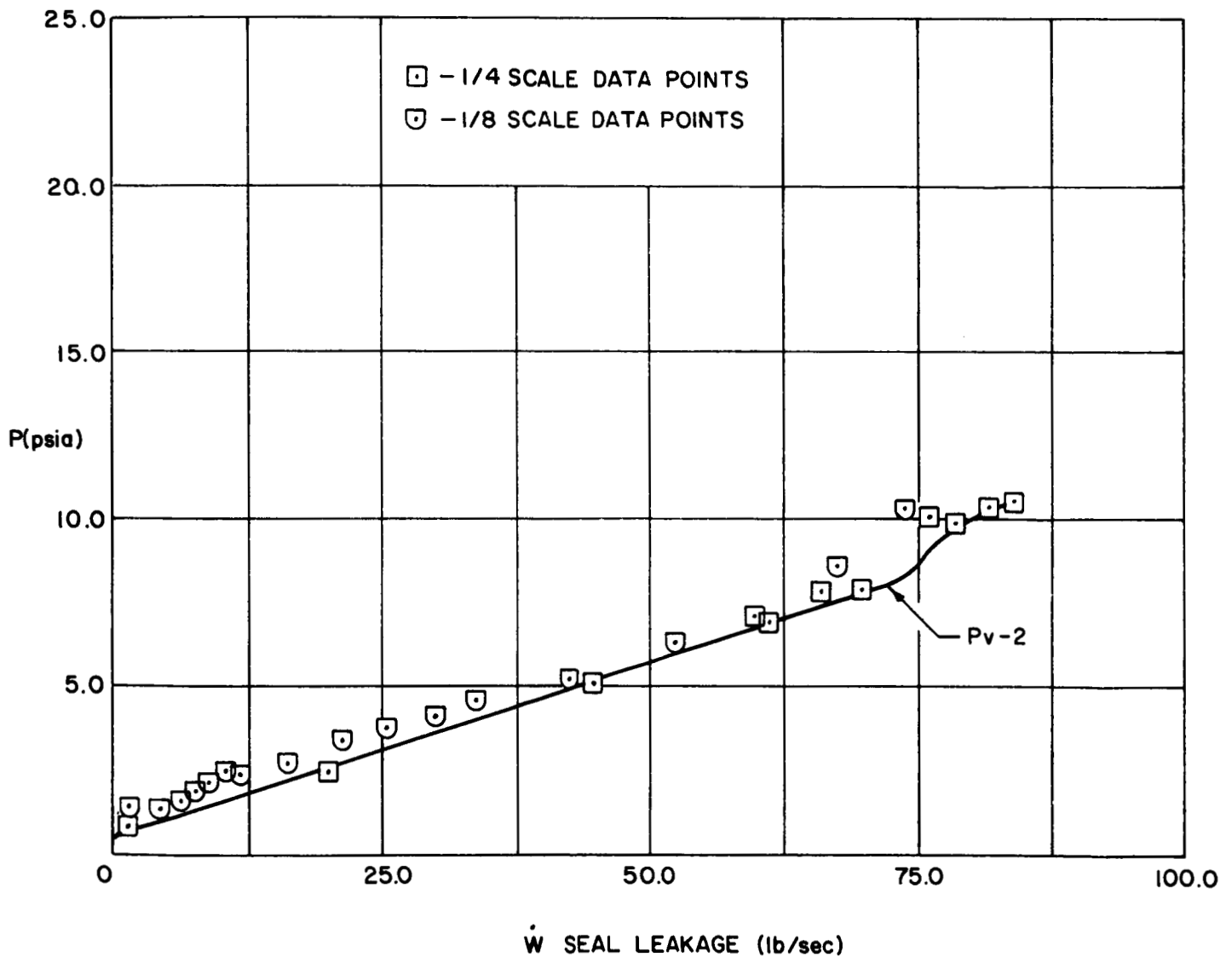


Figure II-19

Engine Compartment Pressure vs Seal Leakage  
 Flow Rate when Testing the 10:1 Nozzle, 100% P<sub>c</sub>

- NOTES. 1. COMPARISON OF 1/4 & 1/8 SCALE  
 2.  $P_{e-2}$  = NOZZLE EXIT PRESSURE  
 3. SEAL LEAKAGE FLOW = 1.50 lb/sec  
 4. SAFETY PURGE AT DESIGN VALUE  
 5.  $P_a$  = 12.8 psia  
 6. RUN NO.  
 280-LQ-39 (1/4 SCALE)  
 276-LQ-100 (1/8 SCALE)

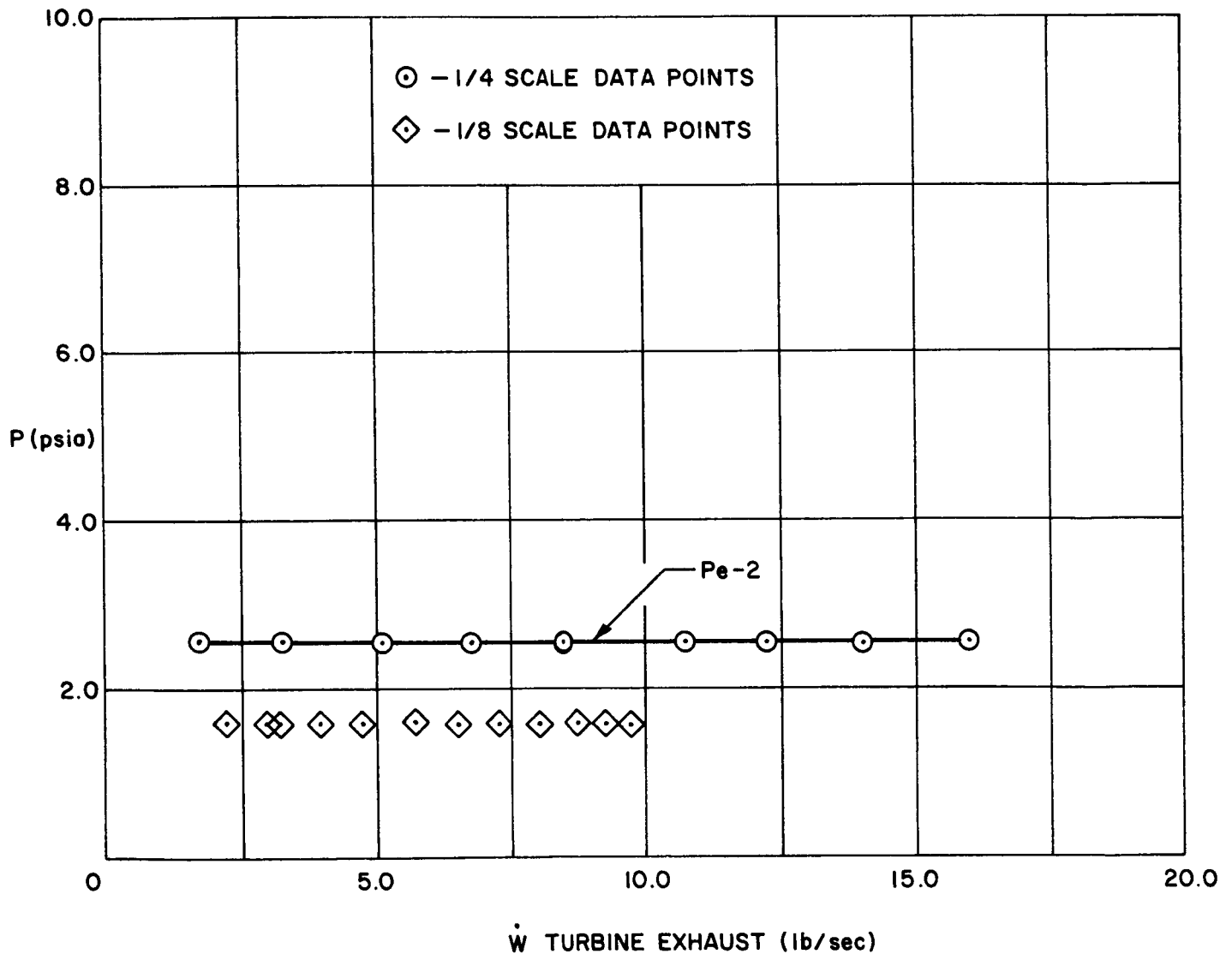


Figure II-20

Nozzle Exit Pressure vs Turbine Exhaust  
 Flow Rate when Testing the 12:1 Nozzle, 40%  $P_c$

- NOTES. 1. COMPARISON OF 1/4 & 1/8 SCALE  
 2.  $P_v - 2$  = ENGINE COMPARTMENT PRESSURE  
 3. SEAL LEAKAGE FLOW = 1.50 lb/sec  
 4. SAFETY PURGE AT DESIGN VALUE  
 5.  $P_a = 12.8$  psia  
 6. RUN NO.  
     280-LQ-39 (1/4 SCALE)  
     276-LQ-100 (1/8 SCALE)

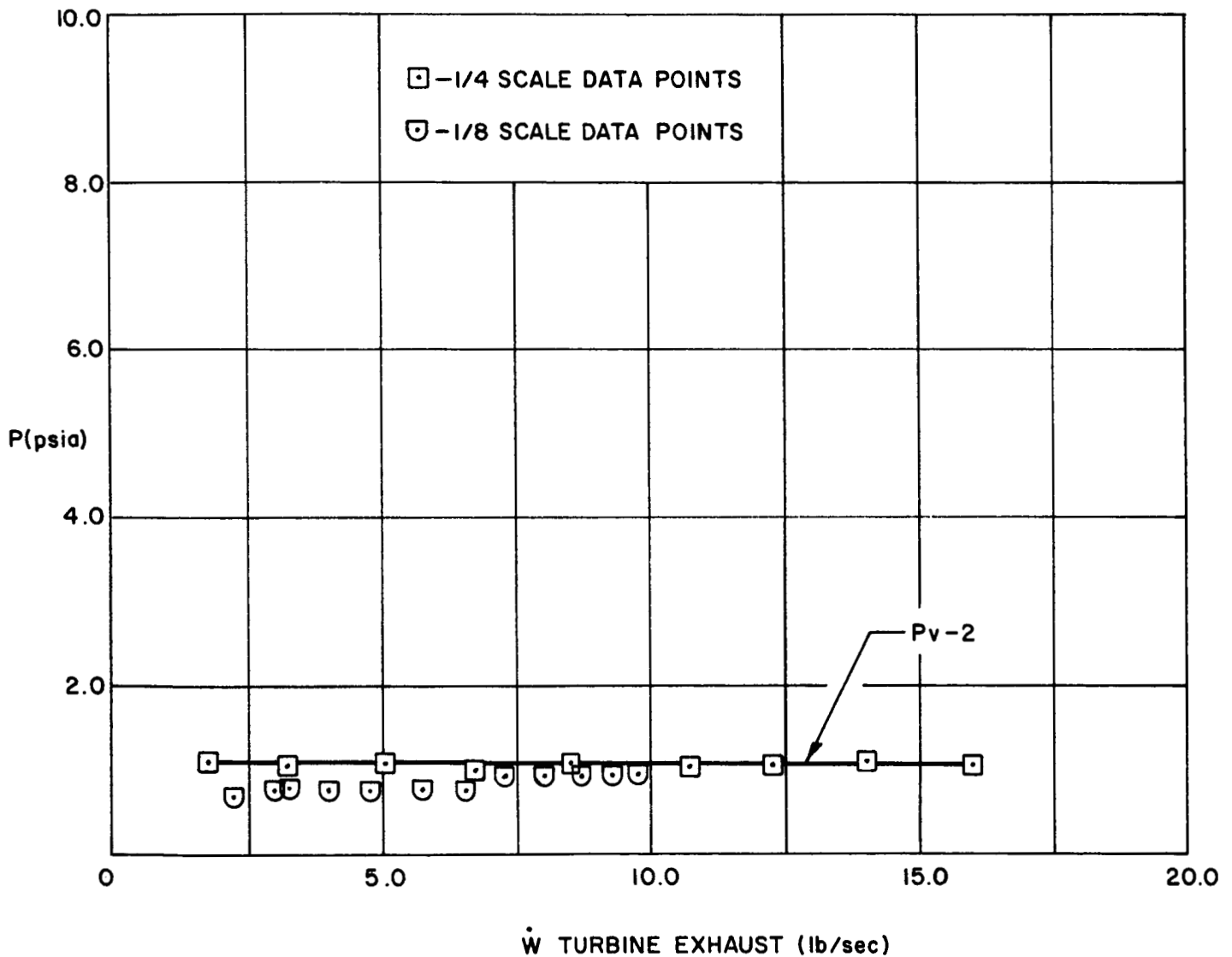


Figure II-21

Engine Compartment Pressure vs Turbine Exhaust  
 Flow Rate when Testing the 12:1 Nozzle, 40%  $P_c$

- NOTES. 1. COMPARISON OF 1/4 & 1/8 SCALE  
 2.  $P_{e-2}$  = NOZZLE EXIT PRESSURE  
 3. TURBINE EXHAUST FLOW = 2.4 lb/sec  
 4. SAFETY PURGE AT DESIGN VALUE  
 5.  $P_a = 12.8$  psia  
 6. RUN NO.

280-LQ-40 (1/4 SCALE)

276-LQ-99 (1/8 SCALE)

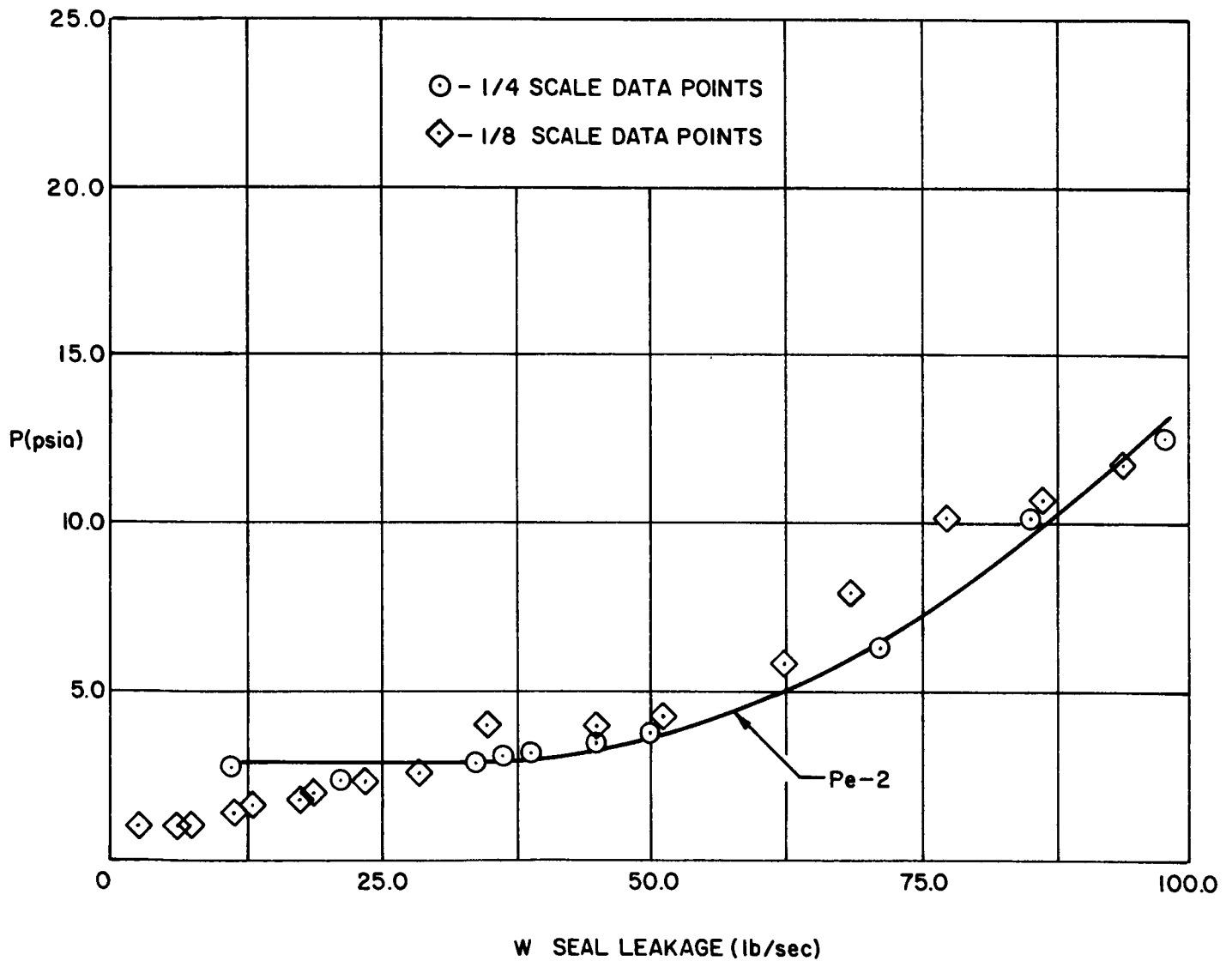


Figure II-22

Nozzle Exit Pressure vs Seal Leakage  
 Flow Rate when Testing the 12:1 Nozzle, 40%  $P_c$

- NOTES. 1. COMPARISON OF 1/4 & 1/8 SCALE  
 2.  $P_v-2$  = ENGINE COMPARTMENT PRESSURE  
 3. TURBINE EXHAUST FLOW = 2.4 lb/sec  
 4. SAFETY PURGE AT DESIGN VALUE  
 5.  $P_a = 12.8$  psia  
 6. RUN NO.

280-LQ-40 (1/4 SCALE)

276-LQ-99 (1/8 SCALE)

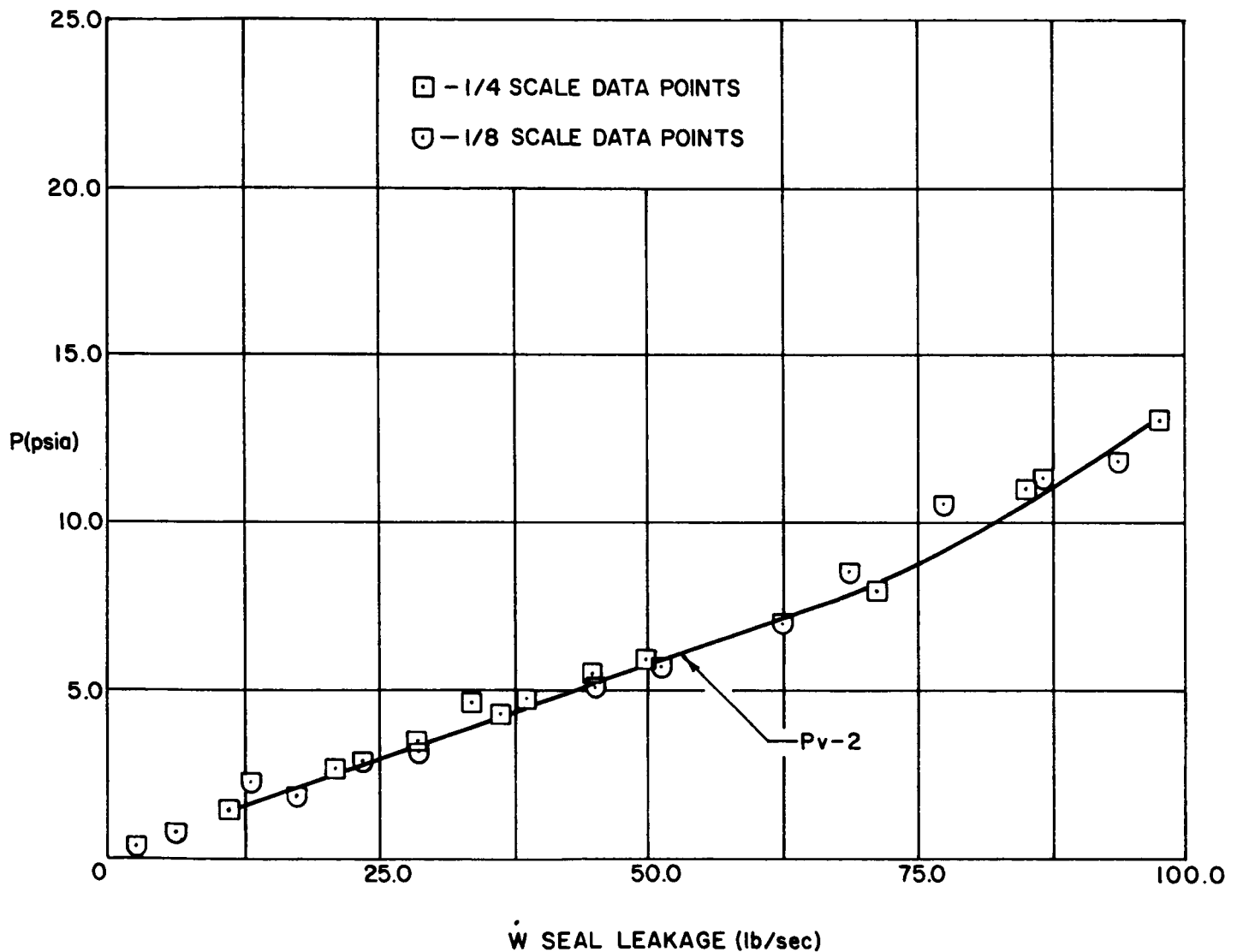


Figure II-23

Engine Compartment Pressure vs Seal Leakage  
 Flow Rate when Testing the 12:1 Nozzle, 40%  $P_c$

- NOTES. 1. COMPARISON OF 1/4 & 1/8 SCALE  
 2.  $P_{e-2}$  = NOZZLE EXIT PRESSURE  
 3. TURBINE EXHAUST FLOW = 5.59 lb/sec  
 4. SAFETY PURGE AT DESIGN VALUE  
 5.  $P_a = 12.8$  psia  
 6. RUN NO.

280 - LQ - 37 (1/4 SCALE)

276 - LQ - 98 (1/8 SCALE)

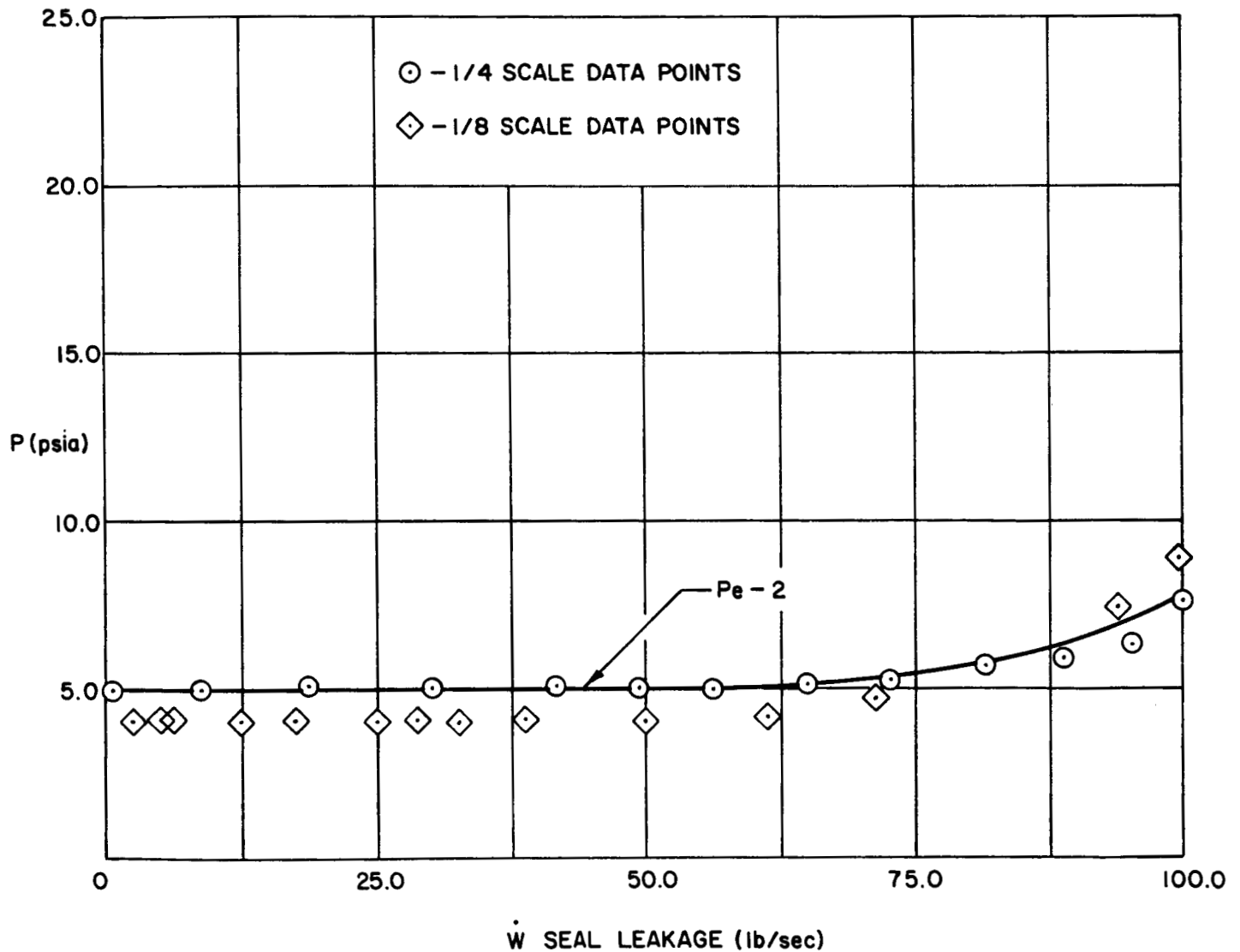


Figure II-24

Nozzle Exit Pressure vs Seal Leakage  
 Flow Rate when Testing the 12:1 Nozzle, 100%  $P_c$



- NOTES. 1. COMPARISON OF 1/4 & 1/8 SCALE  
 2. Pv-2 = ENGINE COMPARTMENT PRESSURE  
 3. TURBINE EXHAUST FLOW = 5.59 lb/sec  
 4. SAFETY PURGE AT DESIGN VALUE  
 5. Pa = 12.8 psia  
 6. RUN NO.  
 280-LQ-37 (1/4 SCALE)  
 276-LQ-98 (1/8 SCALE)

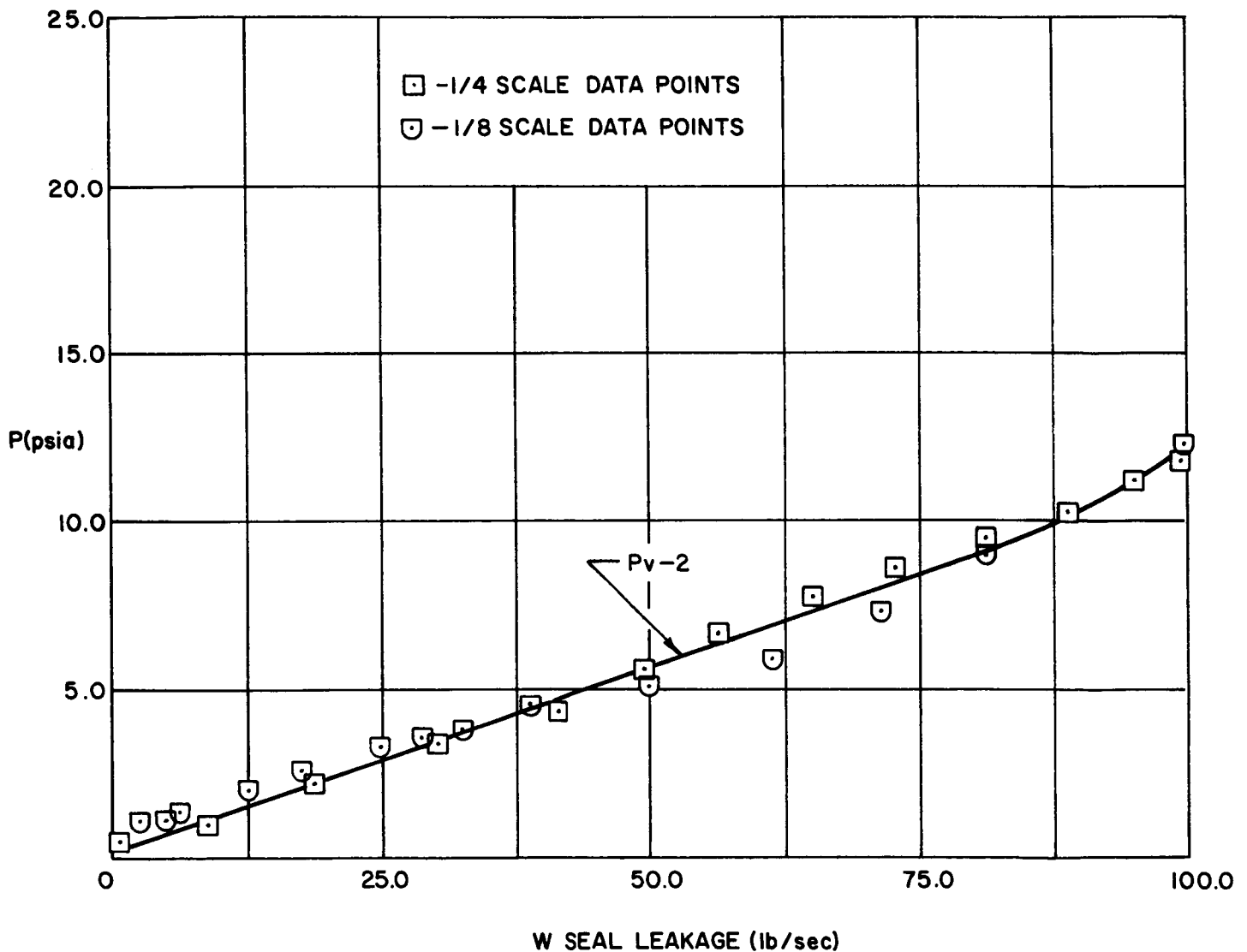


Figure II-25

Engine Compartment Pressure vs Seal Leakage  
 Flow Rate when Testing the 12:1 Nozzle, 100%  $P_c$

## NOTES

- △ ORIGIN FOR "L" DIMENSIONS FOR PRIMARY EJECTOR  
 △ ORIGIN FOR "L" DIMENSIONS FOR SECONDARY EJECTOR  
 3 JOINTS

- ①  $L/D_2 = 0.32$   
 ②  $L/D_2 = 1.35$   
 ③  $L/D_2 = 9.38$   
 ④  $L/D_2 = 12.02$   
 ⑤  $L/D_2 = 16.25$   
 ⑥  $L/D_2 = 18.20$   
 ⑦  $L/D_2 = 18.57$  PRIMARY EXIT  
 ⑧  $L/D_5 = 6.65$   
 ⑨  $L/D_5 = 8.07$  SECONDARY EXIT

4. TO OBTAIN FULL SCALE STATION NUMBERS  
 IN PRIMARY EJECTOR MULTIPLY  $L/D_2$   
 BY 50.0

5. TO OBTAIN FULL SCALE STATION  
 NUMBERS IN SECONDARY EJECTOR  
 MULTIPLY  $L/D_5$  BY 52.0

## PRIMARY EJECTOR

THERMO COUPLE	$L/D_2$	THERMO COUPLE	$L/D_2$	THERMO COUPLE	$L/D_2$
TW-1	0.29	TW-19	2.48	TW-37	9.31
TW-2	0.29	TW-20	2.82	TW-38	9.66
TW-3	12.95	TW-21	3.46	TW-39	9.91
TW-4	13.15	TW-22	3.89	TW-40	10.12
TW-5	13.62	TW-23	4.18	TW-41	10.52
TW-6	13.95	TW-24	4.65	TW-42	10.98
TW-7	14.27	TW-25	5.13	TW-43	11.40
TW-8	14.60	TW-26	5.48	TW-44	11.89
TW-9	14.93	TW-27	5.82	TW-45	12.33
TW-10	0.23	TW-28	6.17	TW-46	12.66
TW-11	0.45	TW-29	6.50	TW-47	13.28
TW-12	0.66	TW-30	6.86	TW-48	13.61
TW-13	0.86	TW-31	7.20	TW-49	13.94
TW-14	1.09	TW-32	7.55	TW-50	14.72
TW-15	1.24	TW-33	7.88	TW-51	17.16
TW-16	1.44	TW-34	8.24	TW-52	17.57
TW-17	1.79	TW-35	8.59	TW-53	18.10
TW-18	2.14	TW-36	8.97		

## SECONDARY EJECTOR

THERMO COUPLE	$L/D_5$	THERMO COUPLE	$L/D_5$	THERMO COUPLE	$L/D_5$
TSW-1	6.90	TSW-4	8.00	TSW-7	3.04
TSW-2	7.04	TSW-5	0.66	TSW-8	4.36
TSW-3	7.45	TSW-6	1.87	TSW-9	5.58

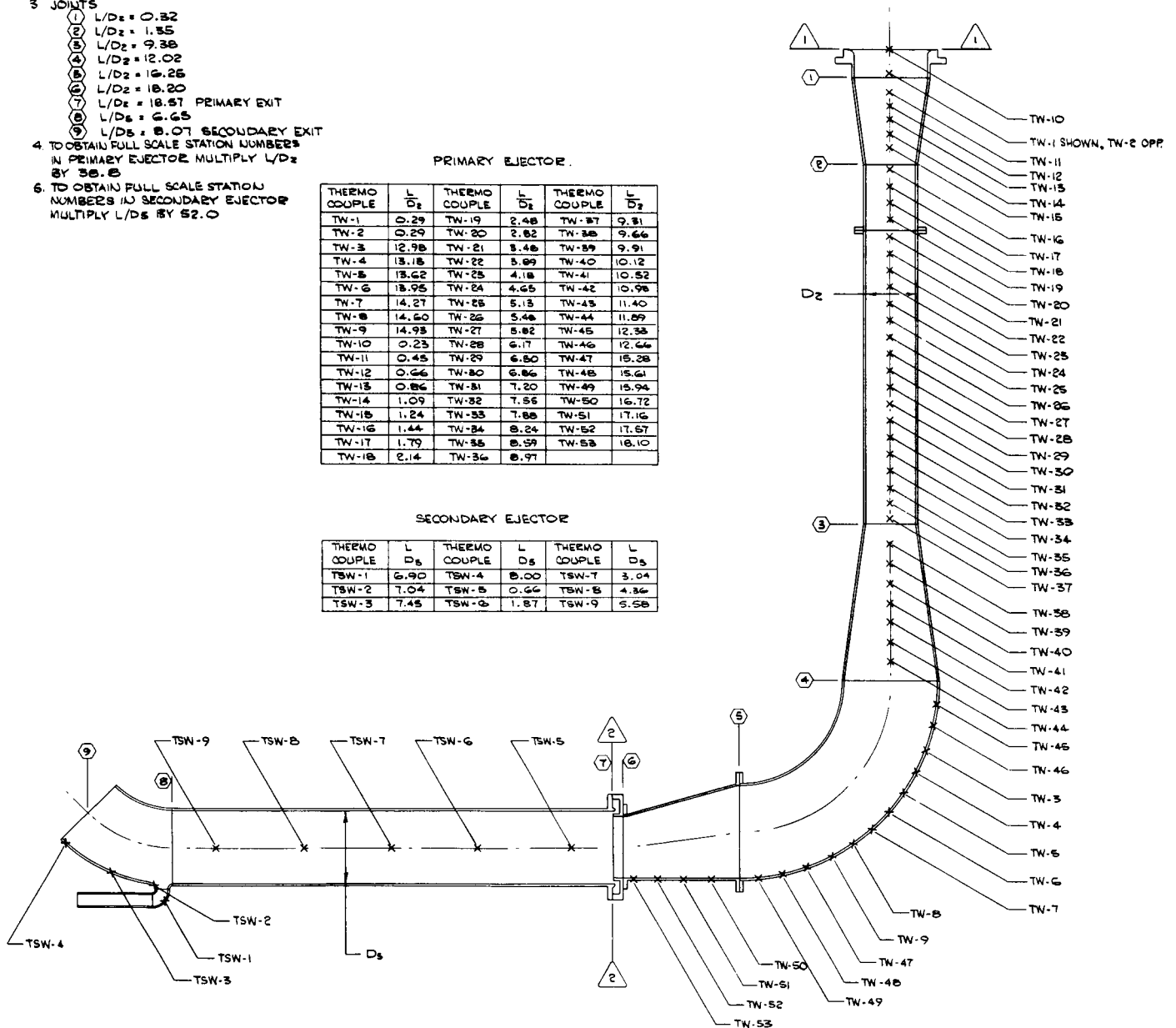
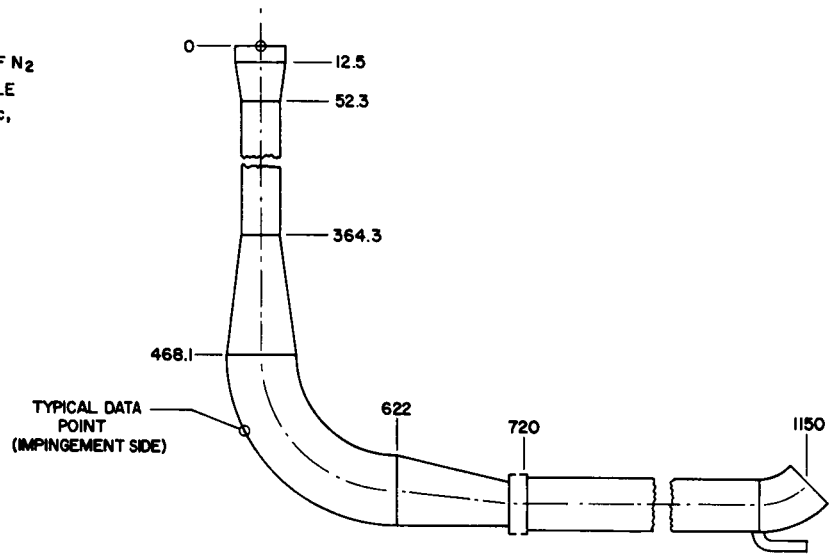


Figure II-26

Thermocouple Locations

## NOTES.

1. POINTS TAKEN ON IMPINGEMENT SIDE OF ELBOW
2. ——— DENOTES 1/8 SCALE, 3 σ UPPER LIMIT OF  $N_2$  TEST DATA, 100 %  $P_c$ , 25/1 CONICAL NOZZLE
3. ○---○ DENOTES 1/4 SCALE DATA,  $N_2$  AT 100%  $P_c$ , 10/1 CONICAL NOZZLE



AXIAL CENTERLINE LOCATIONS (INCHES)

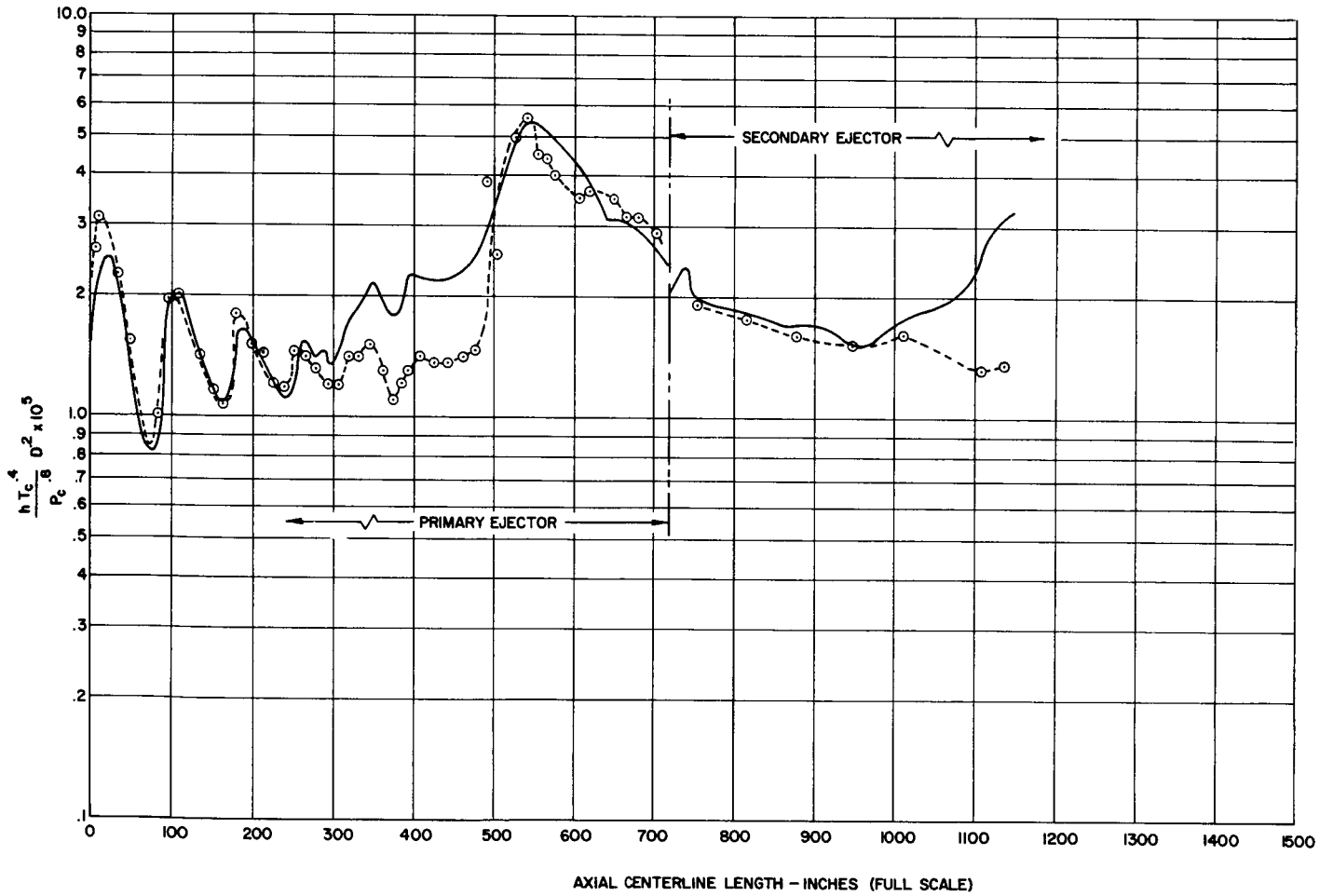


Figure II-27

Normalized Heat Transfer Coefficients,  
Comparison of 1/8- and 1/4-Scale Data

## NOTES.

1. POINTS TAKEN ON IMPINGEMENT SIDE OF ELBOW
2. ○---○ DENOTES 1/4 SCALE DATA,  $N_2$  AT 100%  $P_c$   
10/1 CONICAL NOZZLE
3. △---△ DENOTES 1/4 SCALE DATA, N AT 40%  $P_c$   
10/1 CONICAL NOZZLE

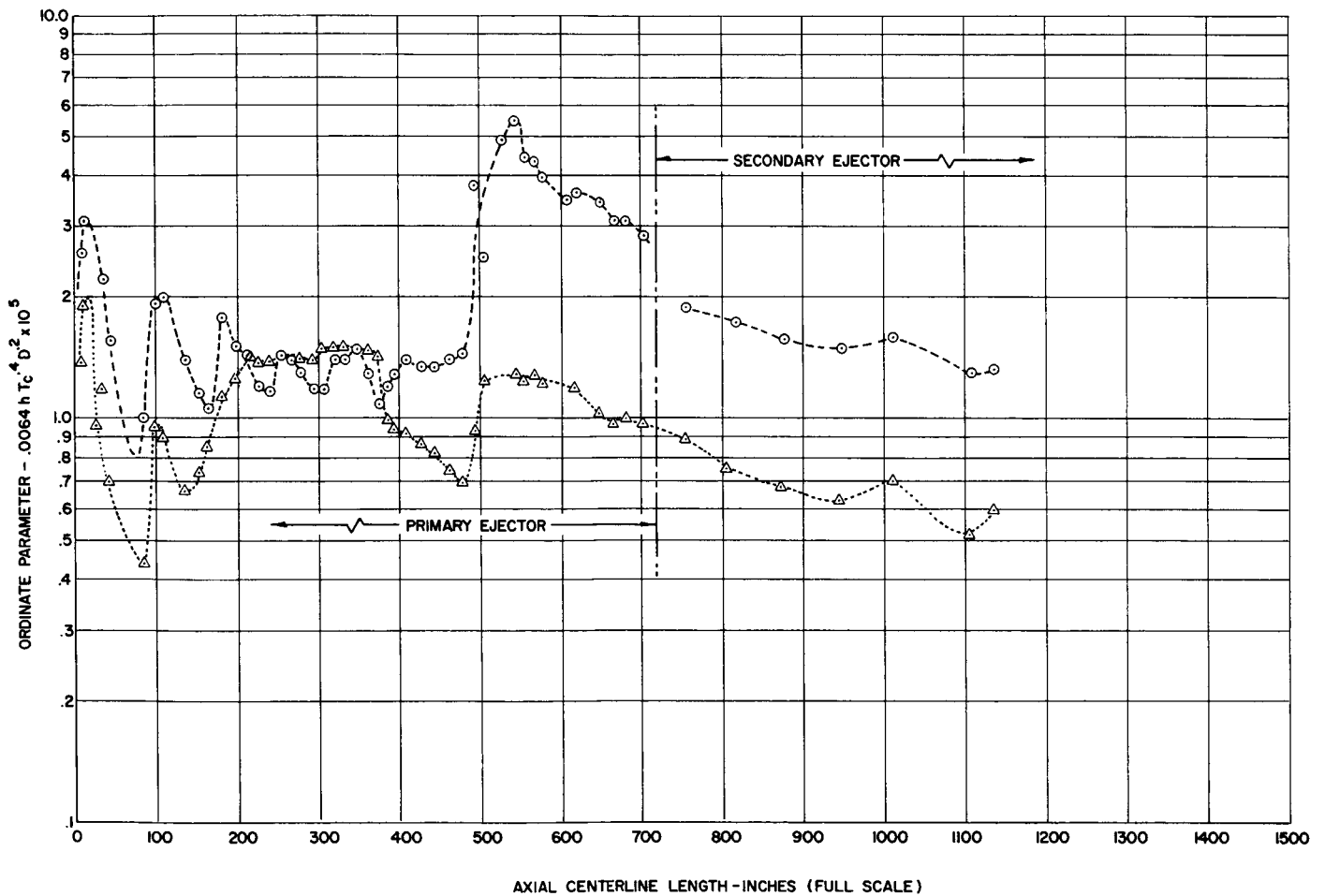
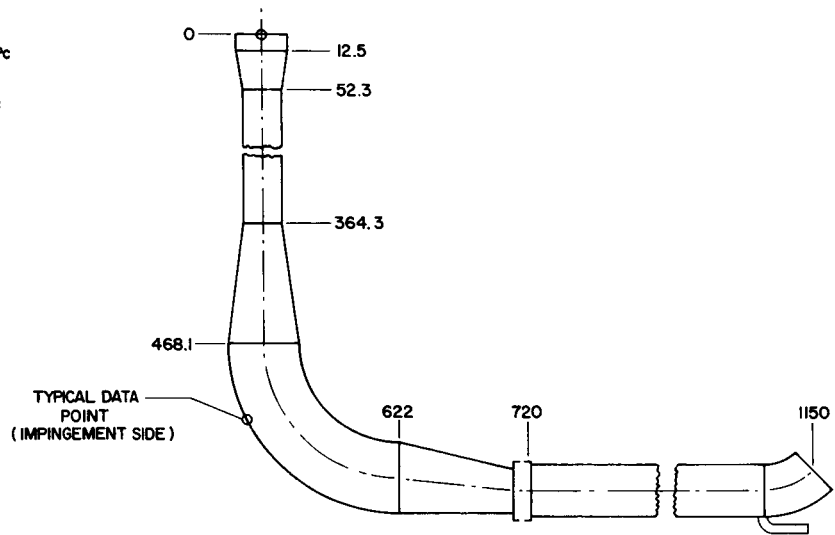
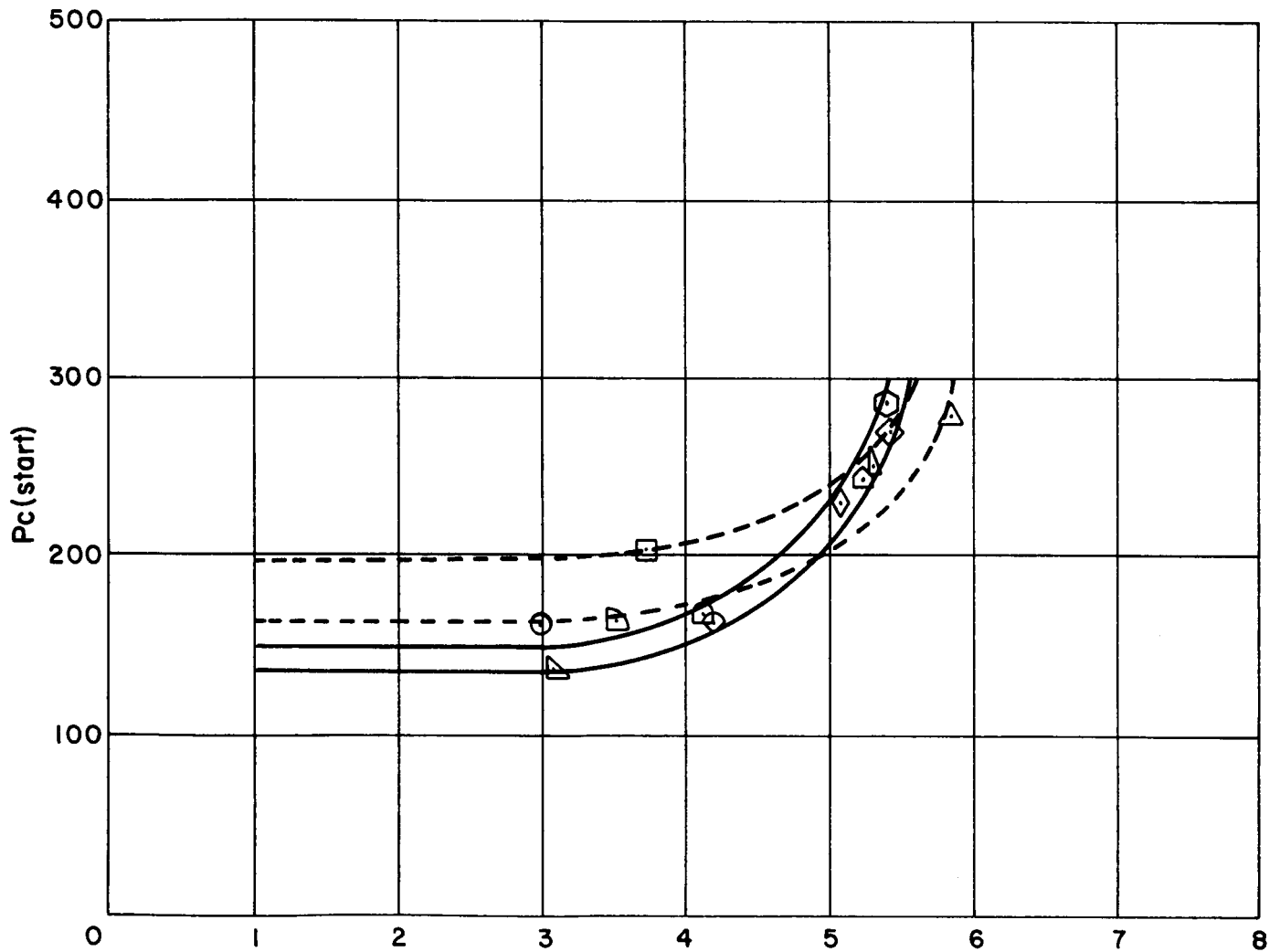


Figure II-28

Effect of Chamber Pressure  
on 1/4 Scale normalized Heat Transfer Coefficients

1/8 SCALE	
SYM.	Psc
○	101.0
□	144.0
◇	148.5
△	103.9

1/4 SCALE	
SYM.	Psc
▴	126.5
◀	163.3
◐	106.8
◑	111.8
◊	174.9
⬆	152.0
⬇	137.0
⬅	127.0



$$\Omega = \sqrt{\frac{(Tc/m)_{prim}}{(Tc/m)_{sec}}}$$

Figure II-29

Off-Design Safety Purge Scale-Model Test Data  
(1/8- and 1/4-Scale Comparison)

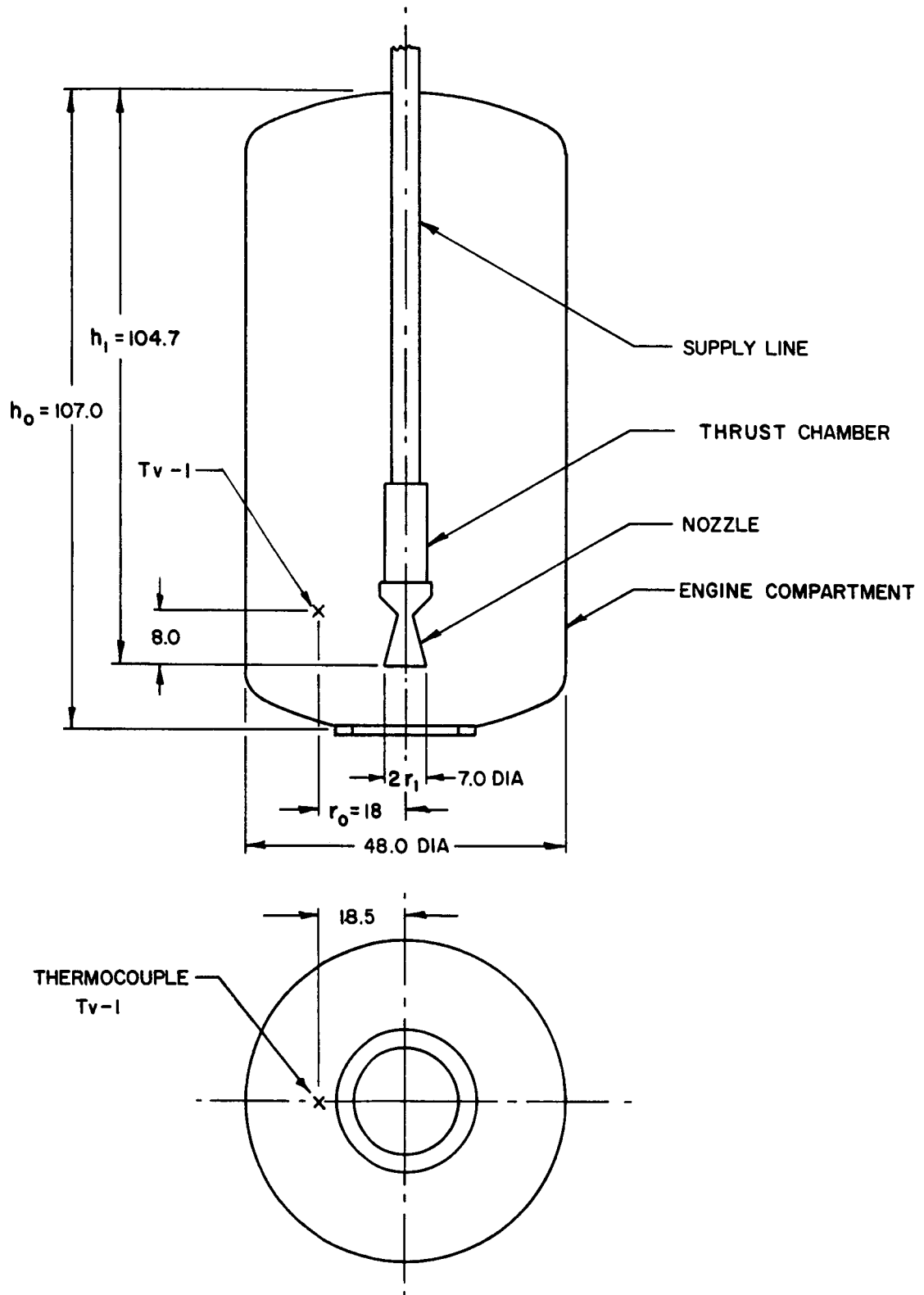


Figure II-30

Thermocouple Location and Dimensions  
of 1/4-Scale Engine Compartment